PERTURBATION SPECTROSCOPY IN CARBON DIOXIDE MOLECULAR GAS DISCHARGES

A THESIS PRESENTED BY M. BROOKS TO THE UNIVERSITY OF ST. ANDREWS IN APPLICATION FOR THE DEGREE OF DOCTOR OF PHILOSOPHY.

I hereby certify that this thesis has been composed by me, and is a record of work done by me, and has not previously been presented for a higher degree. This research was carried out in the Physical Sciences Laboratory of St. Salvator's College, in the University of St. Andrews under the supervision of Dr. A.L.S. Smith.

M. Brooks

I certify that M. Brooks, B.Sc., has spent nine terms at research work in the School of Physical Sciences in the University of St. Andrews under my direction, that he has fulfilled the conditions of the Resolution of the University Court, 1967, No. 1, and that he is qualified to submit the accompanying thesis in application for the degree of Doctor of Philosophy.

Michael Brooks was born in Newcastle-upon-Tyne on the 4th July, 1949. He was educated at the George Stephenson County Grammar School and entered the University of St. Andrews in 1967. In 1971 he graduated with an upper second class honours degree in Physics and subsequently completed three years research work under the supervision of Dr. A.L.S. Smith in the Physical Sciences Laboratory at St. Andrews. He is at present employed as a physicist by the National Health Service and works in the Medical Physics Department of Hull Royal Infirmary (Sutton).

I wish to gratefully acknowledge the enthusiasm and encouragement given to me by my supervisor Dr. A.L.S. Smith especially during the completion of this work. I would like to thank members of the glass-blowing and mechanical workshops and of the electronics department for their technical skills and assistance which made the work possible. Finally, I am indebted to Mrs. Janet Shipley and Mrs. Heather Rye for their patient efforts in typing the original manuscript.

Man tries to make for himself in the fashion that suits him best a simplified and intelligible picture of the world. He then tries to some extent to substitute this cosmos of his for the world of experience, and thus to overcome it. He makes this cosmos and its construction the pivot of his emotional life in order to find in this way the peace and serenity which he cannot find in the narrow whirlpool of personal experience. The supreme task is to arrive at those universal elementary laws from which the cosmos can be built up by pure deduction. There is no logical path to these laws; only intuition, resting on sympathetic understanding of experience, can reach them.

A.Einstein

ABSTRACT

An absorption cell containing dc excited active media consisting of CO_2 or mixtures of CO_2 with N_2, He, H_2 and Xe is irradiated by a modulated 10.6μm CO_2 laser field. Phase sensitive detection techniques are employed to measure perturbations induced in the macroscopic parameters of these molecular gas systems. A stabilised power supply enables the discharges to be excited in two modes:

(a) with the current free to change according to the influence of the laser field induced discharge impedance (cv mode),

(b) with current changes reduced to below 0.05% (cc mode).

Perturbations to the gas pressure (dp), and to the spontaneous sidelight emission (dS), at 4.3μm and between 2800 and 9000 Å, are measured in both discharge modes, and discharge current changes (di) are determined in the cv mode. It is established that parameters measured in the cc mode are primarily dependent upon gain conditions in the active medium and that at least two mechanisms are responsible for the observed high values of di. Consideration of electron impact excitation from the perturbed ground electronic $X^1\Sigma_g^+$ vibrational states allows interpretation of sidelight changes in the spontaneous emission from the $C^3\Pi_u - B^3\Pi_g$ and $B^3\Pi_g - A^3\Sigma_u^+$ systems of N_2 and, the $B^1\Sigma^+ - A^1\Pi$ system of CO. The anomalous perturbation effects seen in specific electronic-vibrational transitions in the $N_2$2+ system are explained in terms of vibrational temperature changes in the $X^1\Sigma_g^+$ state using a simple model. A semi-quantitative interpretation of band head intensities in the $C^3\Pi_u - B^3\Pi_g$

system is given. Perturbations to Xe I atomic transitions $2p_6 - 1s_5$, $2p_5 - 1s_4$, $2p_8 - 1s_5$ have been observed in CO_2 mixtures with added Xe, and a mechanism for this effect is suggested.

CONTENTS

CONTENTS (Continued)

CONTENTS (Continued)

1. PERTURBATION SPECTROSCOPY

1.1 Introduction

In the context of this work the term 'Perturbation Spectroscopy' will be defined as the study of the action of a radiation field on an active medium containing atoms or molecules which have energy levels resonant with the frequency of that field. Because of the high intensity and monochromaticity of a laser field the perturbations induced in the two primary levels responsible for generating that field are especially large. Consider an active medium containing atoms which have energy levels as shown schematically in figure 1.1, and which are pumped by electron impact in an electrical discharge.

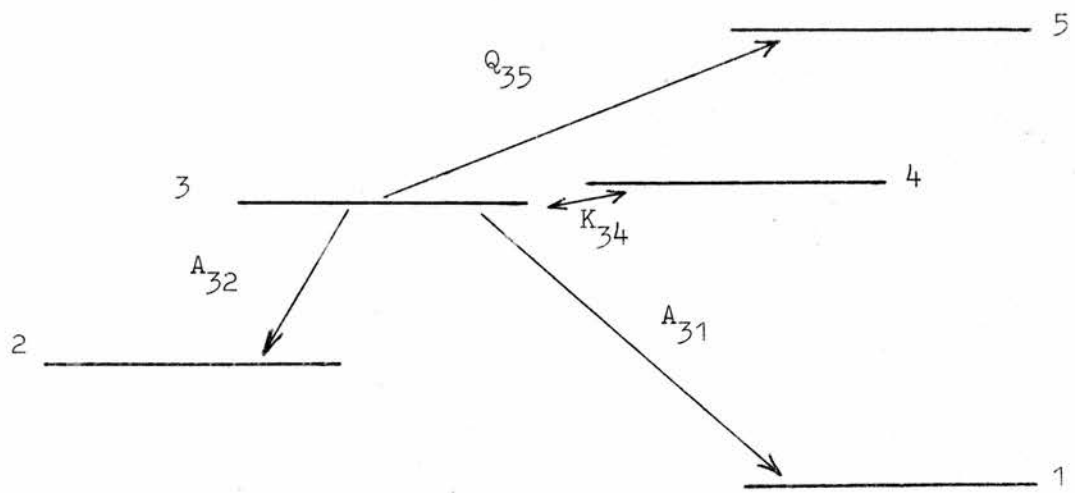

figure 1.1

Levels 3 and 1 represent the upper and lower laser levels respectively; 3 is coupled by radiative decay to levels 2 and 1 (with transition probabilities of A_{32} and A_{31} respectively), by interatomic collisions with level 4 and by electronic excitation to level 5 described by the rate constants K_{34} and Q_{35} respectively. Under equilibrium conditions the populations of the various levels are controlled by a balance between their pumping rates and their decay rates which may be by spontaneous emission or by collisional de-excitation with other atoms or electrons.

If the system is in a gain condition ($N_3 > N_1$) then an incident radiation field of frequency ν_{31} will induce stimulated transitions between 3 and 1 thereby decreasing the steady state population N_3 and increasing N_1 providing the pumping rates remain constant. If the irradiating field is now removed N_3 increases and N_1 decreases; thus a periodically varying field produces a modulation in the quantities N_3 and N_1 at the same frequency, and spontaneous transitions to 2 and 1 are modulated in intensity. If 3 and 1 are coupled by electron impact excitation, interatomic collisions, or by radiative transitions to other levels in the system (e.g. 2, 4, 5) then their populations will also be modulated. Hence by selectively perturbing two levels with a laser field it is possible to observe not only population changes in the primary levels but also changes in levels to which they are coupled, and to examine the mechanisms by which this coupling takes place.

This concept was first used by Parks and Javan (1) to study collision processes and radiative transition probabilities between optically excited levels of neon. Radiative decay processes, electron excitation cross-sections and radiative transition probabilities were also investigated (2), (3), (4) and similar studies of other laser systems including Xe (5), and CO_2 (6), (7), (8) have been carried out. Not only does the laser field modulate certain excited state populations in an active medium, it may also perturb other discharge parameters. For example current quenching effects have been observed in the helium neon system (9), low pressure Xe (5), and in the CO_2 system (10)-(13). Further discussion in this work will be confined exclusively to the CO_2 system, a brief description of which now follows.

1.2 The CO_2 Laser System

The CO_2 laser system was the first capable of generating powers of several kilowatts or more continuously with practical efficiencies of over 10% and a theoretical quantum efficiency of 40%. This performance may be compared with that of the helium neon system which generates powers of several milliwatts cw at efficiencies of about 0.07% or the argon ion laser with powers of up to several watts cw and efficiencies around 0.1%. A conventional sealed CO_2 system may contain CO_2, N_2 and He at total pressures of 20 torr in the ratio 1:2:7 as the active medium. Excitation of the gas is usually by a dc electric discharge running at a current density of the order of ten milliamps per square centimetre. A simplified energy level diagram is shown in figure 1.2 together with schematic representation of the CO_2 ground electronic vibrational modes, figure 1.3. The high efficiency of the system is due to the pumping mechanism of the CO_2 laser levels which is now described.

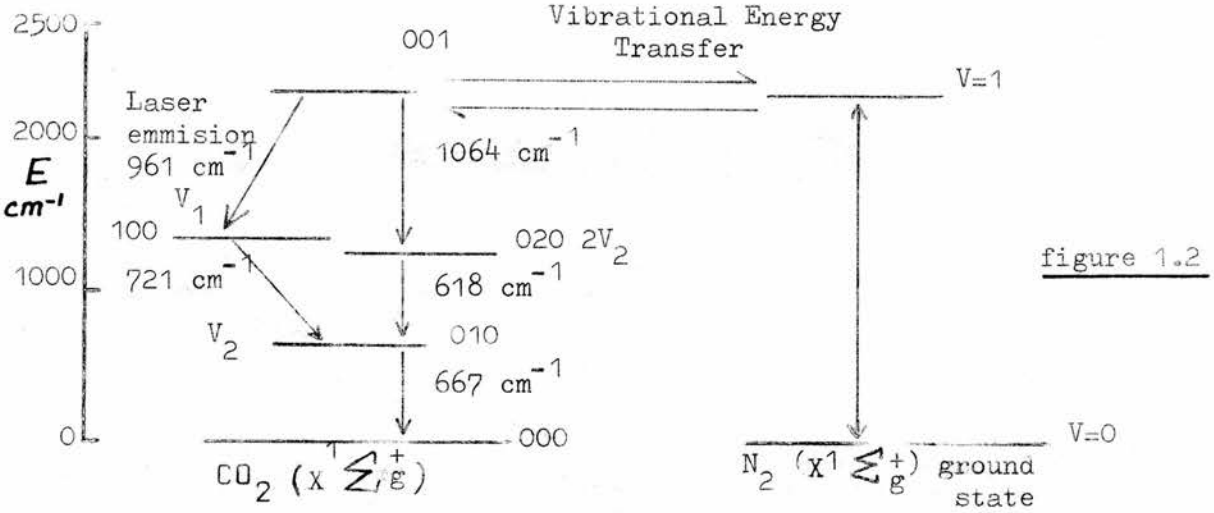

figure 1.2

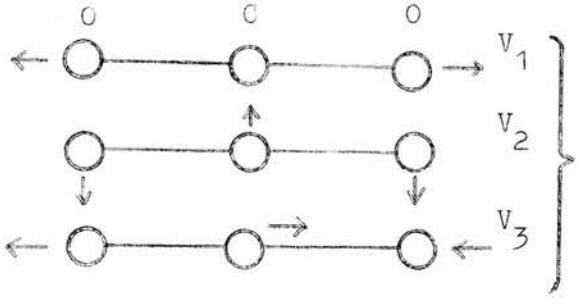

Normal Vibrations of a CO_2 molecule

figure 1.3

The electronic ground state nitrogen molecules have a relatively large electronic excitation cross-section ($\sigma(e, N_2)_{max} \approx 3 \times 10^{-16} cm^2$), leading to a high population of ground electronic vibrational levels (V = 1, 2, ...8), as many as 10 to 30 per cent of the total nitrogen molecules may lie in these levels. Because of its symmetry, dipole radiative transition from these nitrogen levels is forbidden and decay is possible only by collisional energy transfer. There is a close energy coincidence between the CO_2 001 and the N_2 V = 1 levels ($dE = 18\ cm^{-1}$) resulting in strong collisional coupling and hence selective pumping of this CO_2 level. This mechanism is generally accepted as being the predominant one in establishing a population inversion between the CO_2 001 and 100 or 020 levels. The CO_2 100 and 020 levels are in Fermi resonance and are strongly coupled via vibration-vibration and vibration-translation energy exchange processes to the 010 and 000 levels. The addition of helium is a further aid to relaxing the 100, 020 and 010 levels and also increases the thermal conductivity of the gas mixture resulting in:

(i) a reduction in gas kinetic temperature and consequent lowering in effectiveness of the thermal populating processes of the CO_2 vibrational levels.

(ii) an increase in gain since output power is a function of gas kinetic temperature ($P_{out} \propto T^{-3}/2$) in a wall dominated discharge.

The active medium normally exhibits a population inversion between several rotational sublevels of the 001 and 100 states and generation of laser radiation may take place at around 10.6μm on a number of vibrational-rotational lines with upper level J values around 19. We now consider the effect of altering the intensity of the radiation field which couples the 001 and 100 levels.

As discussed in section 1.1 if the system is in a gain condition and the radiation field is increased in intensity the 001 population is decreased, that of the 100 and 020 levels is increased. The CO_2 and N_2 molecules are closely linked by reactions of the type

$$CO_2\ (000) + N_2\ (V=n) \rightleftharpoons CO_2(001) + N_2(V=n-1) + dE \quad \ldots\ldots\ 1.1$$

where one vibrational quanta from the $N_2(V=n)$ state is given up to the CO_2 molecule which is excited to the V_3 vibrational mode. If the number of CO_2 (001) molecules is decreased then the number of $N_2(V=n)$ molecules is also decreased in order to maintain equilibrium as described by 1.1. Thus stimulated emission processes in the CO_2 system may be thought of as an effective leak of vibrational energy from these N_2 levels. Since excitation of the electronic states of N_2 responsible for generating the first and second positive bands is mainly by direct electron impact from these perturbed N_2 $X^1\Sigma_g^+$ levels then the spontaneous emission within these bands becomes modulated; a similar explanation is true for the CO Angstrom system. Further, the balance of electron energy loss by inelastic collisions with X^1 state molecules and energy gain from the electric field becomes disturbed and produces a change in electron mobility and hence discharge current. Vibrational-translational energy transfer processes between the X^1 CO_2 levels are altered leading to a gas kinetic temperature change and hence a pressure change.

The series of experiments to be described were intended to investigate the mechanisms by which perturbations to the primary laser levels of CO_2

due to a varying 10.6μm field were coupled to

i) other molecular species

ii) the electron gas

iii) macroscopic plasma parameters including discharge current and gas pressure.

1.3 Perturbation Experiements in the CO_2 Gas Laser System

Because of the relatively high gain of the CO_2 system several perturbation effects become enhanced due to strong coupling of the radiation field and the active medium, and are more easily observable than similar effects which may occur in lower gain gas systems. These include current effects, gas pressure and kinetic temperature changes, molecular vibrational temperature changes, and infra-red, optical, and ultra-violet sidelight perturbations. References concerning these specific effects may be found in the appropriate chapters below and are omitted in the following discussion for the sake of brevity. The preliminary observations made in this work, and by other investigators, on the perturbation properties of gas discharges containing CO_2 or a mixture of CO_2, N_2 and He may be summarised as follows. If the active medium is in a gain condition and is irradiated with a beam of 10.6μm radiation which is increasing in intensity,

i) the spontaneous sidelight intensity at 4.3μm from the CO_2 001→ 000 transition is decreased in intensity due to a reduction in the upper laser level population as a result of stimulated emission to the 100 level.

ii) the spontaneous sidelight in the range 2800 to 9000 Å arising from vibrational electronic transitions in CO and N_2 (Chapters 8 and 10), is modulated in intensity.

iii) the integrated sidelight intensity between 2800 and 9000 Å is reduced although certain discrete transitions in the N_2 second positive system are observed to increase in intensity.

iv) the discharge current is decreased in magnitude.

v) radial and longitudinal acoustic waves are generated.

vi) macroscopic pressure and kinetic temperature changes take place.

It is at first surprising that in a typical CO_2 laser plasma containing the additives N_2 and He that sidelight perturbations in the range 2800 to 9000 Å should occur. The 10.6μm field is coupled to CO_2 vibrational levels which lie at about 0.2eV above the ground $X^1\Sigma_g^+(000)$ state and yet optical transitions taking place at 10eV above this level are also perturbed. In order to explain this effect other plasma parameters which depend on the radiation field intensity have been investigated. Previous explanations for current changes in a CO_2 system have followed those which were applied to helium neon laser discharges and which described current changes in the latter as being due to cumulative ionisation effects from the directly perturbed lasing levels. In the case of a CO_2 discharge however the relevant perturbed levels lie many electron volts below the ionisation limit and other explanations of the current behaviour have been sought here which involve consideration of the effect of the alteration of gas temperature and pressure, due to the laser field, on discharge current as well as inelastic energy exchange between the electron gas and perturbed molecular vibrational levels.

The magnitude of the current perturbation is dependent not only upon internal parameters of the system (partial pressure of gas constituents, current, gas kinetic temperature, and optical gain) but also upon the external circuit parameters such as ballast resistance and power supply properties. In order to reduce the effects of external parameters to an absolute minimum a constant current power supply was used to excite the active medium of interest. In this way perturbed parameters which depended directly on discharge current changes were effectively eliminated, and the interaction between the irradiating field and vibrational levels of CO_2, CO, and N_2 was studied without being masked by gross discharge current

changes which were normally produced. The power supply could also be run in the more normal voltage controlled mode which allowed macroscopic current perturbations to take place, and data obtained with such discharge conditions was compared with that of other investigators. As well as current and sidelight intensity perturbations direct evidence of radiation field induced gas pressure changes was obtained; this data was used to interpret the current perturbations. Sidelight perturbation spectroscopy was carried out under current and voltage controlled modes on vibrational electronic transitions in the CO Angstrom band and N_2 first and second positive systems, and evidence of a perturbation to the Xe transitions at the wavelengths 8819, 8280, and 8231 Å was found which has not been reported before. A mathematical model based on the theory outlined by Sobolov et al and Bleekrode has been constructed which qualitatively interprets the anomalous sidelight perturbations in the N_2 second positive system purely in terms of vibrational temperature changes induced in the ground electronic vibrational states of nitrogen by stimulated emission processes.

2. EXPERIMENTAL APPARATUS

2.1 CO_2 laser and absorption cell

The cw 10.6 μm perturbing radiation field used in all the experiments was generated by a sealed CO_2 laser which was of an all quartz glass and stainless steel construction. The discharge tube consisted of a 1.2 cm internal diameter quartz envelope surrounded by a concentric quartz tube forming a water jacket through which coolant was flowed. A Hilger and Watts refrigeration unit, with a cooling capacity of 1500 watts, was used to supply cooling water to the laser and absorption cell. The coolant was maintained at $3 \pm 0.5^{o}C$ by means of a thermostat on the unit, resulting in a constant outside wall temperature of the discharge tubes. This was essential in obtaining a long term (several hours continuous operation) stable laser output, and reproducible discharge conditions in the absorption cell. The laser active discharge length of 70 cm was contained between a cylindrical platinum cathode and two, equally spaced, platinum ring anodes. To form the optical cavity it was decided to use a plane dielectric mirror anti-reflection coated for 10.6 μm on one side and of 15% transmission, and a totally reflecting gold plated stainless steel mirror of about 200 cm radius of curvature, separated by an axial distance of 118 cm. Both were mounted in steel housings fitted with a triple micrometer screw adjustment. The maximum output power cw multimode with a mixture of 0.6 torr Xe, 2.6 torr CO_2, 3.8 torr N_2 and 13 torr He was 15 watts with a beam diameter of 3 mm at the output mirror as detected on a thermal image plate. The discharge current was supplied by a Hivotronic power supply unit type 22-300-26 which gave a maximum output of 22 kV at 300 mA with 5% current ripple. The laser was found to operate stably for periods of several hours with the output power varying by less than 5% from its

maximum which was obtained after a few hours continuous running in a fresh gas mixture. It was normally operated with a discharge current of 20 mA and in a given experimental run the output was always maximised by mirror alignment.

The absorption cell was of an all quartz and stainless steel construction and, like the laser, designed around standard V.G.high vacuum components.

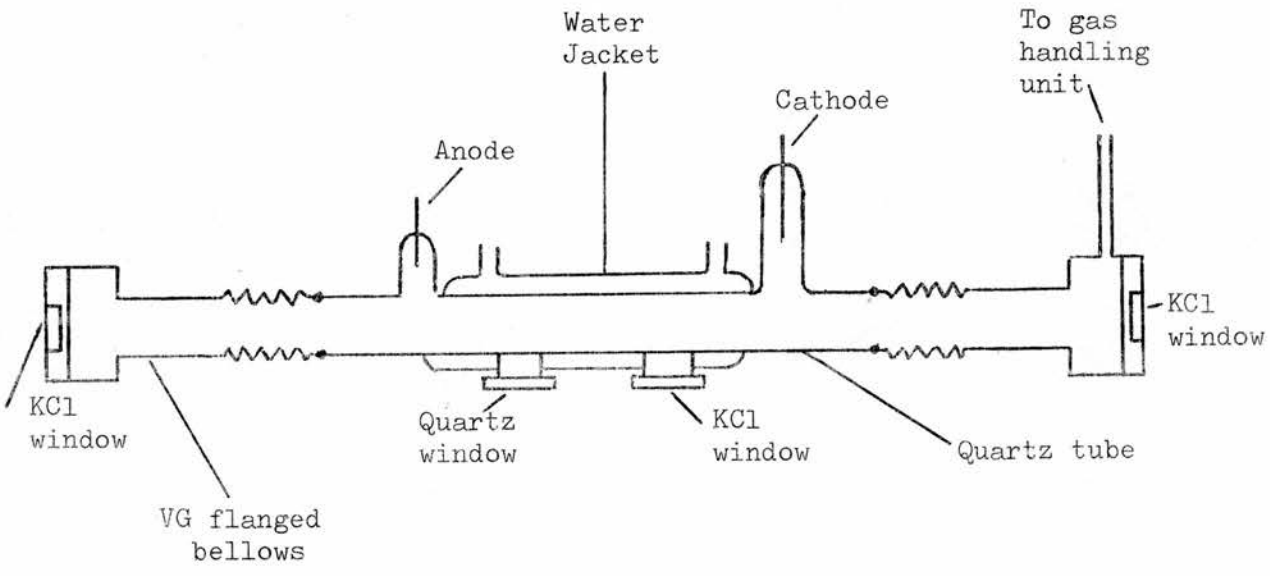

figure 2.1

The discharge tube consisted of a 1.2 cm diameter quartz envelope surrounded by a concentric quartz tube forming a water jacket through which coolant was flowed at $3^{o}C$. The active discharge length of 30 cm was contained between a cylindrical platinum cathode and a platinum wire ring anode. Near the centre of the discharge region

were two observation windows one of optically flat polished quartz (3mm thick), the other of similar optical quality KCl (5mm thick), both of 25mm diameter. They were fixed in place to quartz stubs protruding through the water-jacket using low vapour pressure epoxy resin (Varian Torrseal) and gave an uninterrupted view of the active discharge medium. Because of the similarity between the absorption cell and the laser, it was possible to create discharge conditions in the cell which closely simulated those of the active laser medium.

The 10.6μm beam from the laser was allowed to pass along the axis of symmetry of the absorption cell via two 25mm diameter x 5mm thick optically flat, polished KCl windows epoxied to V.G. stainless steel flat flanges at either end of the cell see figure 2.1 for details. The laser and cell were each mounted on two steel supports bolted to pieces of insulating material ($\frac{3}{4}$" x 6" x 6"), which were in turn rigidly fixed to aluminium channel (4" x 2"). Both tubes, together with their bases, were then placed upon insulated tables which were adjustable laterally and vertically with respect to the optical axis. The tables in turn rested on a single length of aluminium U-shaped channel (6" x 3"), which provided stability and made for ease of optical alignment of the system.

To align the laser and absorption cell the following procedure was adopted. A helium neon laser was placed approximately three metres from the CO_2 laser output mirror and readjusted positionally until its beam was reflected from the back surface of the dielectric flat along its original incident path. The absorption cell was then placed between the two lasers with the nearest of its end windows 75cm from the CO_2 laser output mirror. It was then readjusted positionally until the combined helium neon incident and reflected beams passed through the centres of the KCl end windows and hence along the central optic axis

of the cell.

2.2 Pressure measurement

For pressures below about 0.1torr a series of three Edwards pirani gauges suitably placed in the gas handling system were used, and for pressures in the range 0.1 to 20torr an Atlas MCT diaphragm-type capacitance manometer was used. The capacitance manometer had an accuracy (with respect to reproducible pressure measurement) of 2% full scale deflection on all three ranges (0 to 2, 5, and 20torr) and a minimum detectable pressure change of 10^{-2} torr, on the most sensitive range; it was used to determine the cold fill partial pressures of gases employed in all experiments with the sealed absorption cell. The measuring element was a pressure measuring condenser whose capacity was a linear function of pressure. It consisted of two vacuum tight chambers separated from each other by an elastic metal diaphragm which together with a fixed counter electrode constituted the pressure dependent cavity. Any difference in pressure between the two chambers caused a deflection of the diaphragm and the counter electrode. The measuring condenser formed one part of an a.c. bridge from which a voltage output proportional to the capacitance change was obtained. This voltage was then amplified and rectified and was a direct measure of the pressure difference. The measuring head was of high quality stainless steel and the whole unit was bakeable. Normally it was maintained at $55^{o}C$ in a thermally insulated casing, by a contact thermometer and temperature regulator. Several advantages accrue from the use of this type of instrument:

i) measurements are independent of the chemical nature of the gas

ii) composition of thegas is unaffected

iii) the measuring system has a constant volume

iv) there is a minimum of outgassing

v) non-reactive materials only are used in the system in contact with gases of interest

vi) 55°C operation avoids the effects of ambient temperature changes

2.3 Gas handling system

The gas handling system was of all metal construction and used standard stainless steel Hoke bellow valves and fittings. It had the capability of supplying mixtures of the gases CO_2 CO, N_2, He, Xe, and H_2 (all of at least 99.99% purity, as supplied by B.D.H.Chemicals Limited) to both the laser and the absorption cell. The system could be pumped by either a Genevac PL44 rotary pump fitted with a diffusion pump or by a Leybold 'Trivac' type D1 rotary pump fitted with a sorption trap containing a molecular seive. The complete system with the exception of the KCl windows and mounts and laser mirrors and mounts, was bakeable and could be pumped to below 10^{-3} torr (lower limit of the pirani gauges). A mass spectrometer, A.E.I. MS 10, was used to examine the laser, absorption cell, and associated vacuum connections for leaks and out-gassing dueto wall contamination. Residual gases were found to be mostly OH (from the cracking pattern of H_2O), O_2, N_2, H_2O, and several peaks around mass 40 which were presumed to consist of the cracking pattern of organic molecules from solvents used to clean the laser and absorption cell during assembly. After baking the quartz tubes and metal parts of the gas handling system the total background pressure in the laser, cell and vacuum connections was below 10^{-3}torr. Each gas component was reproducibly accurate to within one part in a hundred.

2.4 Differential Pressure Measurement

For the pressure fluctuations measured as described in chapter 5, an

MDC capacitance micromanometer, manufactured by Furness Controls Limited and working on a similar principle to the MAT, was used. This had an accuracy of 1% and a pressure measuring range of 0 to 100torr in five separate stages. The diaphragm in the measuring head responded to sinusoidal pressure fluctuations of up to 200 Hz, and the instrument was able to provide an ac electrical output of the order of millivolts proportional to the peak to peak amplitude of the observed pressure fluctuations. For normal dc work the electrical output was 500 m v at full scale deflection on all of the ranges. A typical frequency response curve (provided by the manufacturer) indicated a bandwidth of 150 Hz (defined at -3dB from zero Hz) although the transducer was capable of detecting signals of up to 500 Hz. The frequency response curve for the transducer had an error of 20% (manufacturer's quotation).

2.5 Power Supply Unit for the Absorption Cell

Accurate control of the current to the discharge in the absorption cell was provided by an EHT power supply unit (C1096) designed and built by Irvin Electronics. It provided up to 10kV and 50mA in either a current or voltage controlled mode. The output voltage was held to within 0.1% by a series stabilising valve controlled by solid state sensing bridges and amplifiers. The power output changed by less than 0.1% for a 10% change in mains supply; the output voltage changed by less than 0.1% for a load current change of 50mA in the voltage controlled (cv) mode, and the output current changed by less than 0.1% for a load voltage change of 10kV in the current controlled (cc) mode. The output changed by less than 0.1% per hour for a fixed load supply voltage and temperature; the temperature coefficient was less than 0.01% per degree centigrade, and the ripple less than 5μA or less than 1 volt rms under cc and cv controlled modes respectively. The important features of the unit were therefore its stability and its ability to maintain a constant current or constant

voltage under changing load conditions running in the cc or cv controlled modes respectively.

Table 1 was obtained by the method described in chapter 5. Ten torr of carbon dioxide was used in the absorption cell as this gave a current perturbation with sufficiently high signal to noise ratio to enable quantitative measurements to be made of the change in current supplied to the load $(di)_{cc}$ by the power supply unit running in the cc mode; τ is the time in milliseconds for one complete chopping cycle. Under cv controlled conditions the total voltage across the output terminals of the power supply is held constant although the response time of the unit in this mode to changes in load conditions is slow ($\sim$1 sec.).

The voltage across the ballast resistors and discharge cell vary since they are connected in series and an alternating impedance change is induced in the gas discharge at the chopping frequency, $\frac{1}{\tau}$.

Table 1

Chopping Frequency (f) Hz	$\tau = 1/f$ ms	di (arbitrary units) cv mode	di (arbitrary units) cc mode	$(\frac{di_{cc}}{di_{cv}})$ %
364	2.75	14	7.0	50
333	3.00	40	6.5	16.3
250	4.00	47	4.0	8.5
83.5	12.00	60	0.5	0.83
62.5	16.00	77	0.4	0.52
28.6	35.00	130	0.3	0.23

There was a residual signal from the phase sensitive detector (with the perturbing field switched off) which was constant and about 30% of the total $(di)_{cc}$ signal at τ = 35ms. Thus the power supply unit operating in the cc mode with a load whose value changed periodically at this frequency was capable of correcting the current to within (0.23 $\pm$ 0.08%), when operated in the cc mode.

The $(di)_{cv}$ signal was dependent upon the size of ballast resistor used, becoming larger as the ballast resistance was reduced. The $(di)_{cc}$ signal was independent of the size of ballast resistor to within the experimental error (dictated by the signal to noise value) of the measurement. Table 1 was obtained using a ballast resistor of 120kohms.

2.6 Variable Speed Chopper Motor

The operating conditions of the lock-in amplifier and the demands of certain experiments required a chopping motor whose frequency could be varied from about 10Hz to 500Hz and which was frequency stable to within 2%. For this purpose a 1/100 h.p.commutator d c shunt wound motor was used, driven by means of a power supply with a voltage sensing feedback loop (14). The circuit constructed is that shown in figure 2.2 and works on the following principle. A chain of square wave power pulses is generated by the supply which have their mark/space ratio controlled by the Schmitt trigger consisting of Q1 and Q2, phase inversion stage Q3 and delayed feedback through R3 and C1. The output is a variable-width, variable-frequency pulse whose duty cycle and frequency are a function of the d c input. The d c input is the summation of the current through R2 which is connected to the speed control potentiometer R1, and the current through Rf, the overall feedback resistor.

The output of the modulator is fed to a Darlington-connected power amplifying stage consisting of Q4 and Q5 which drives the d c motor.

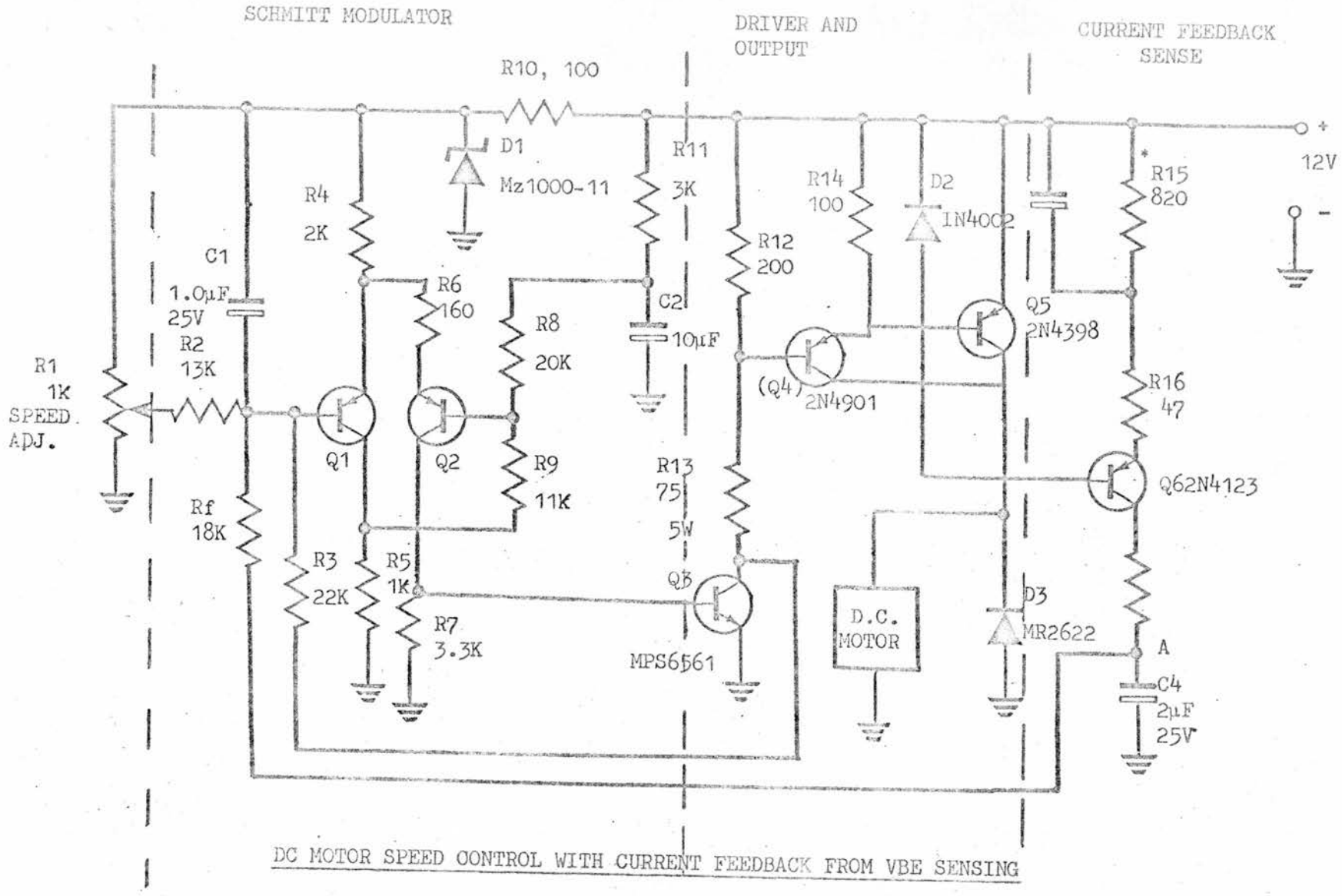

DC MOTOR SPEED CONTROL WITH CURRENT FEEDBACK FROM VBE SENSING

*ADJUST TO SUIT MOTOR

ALL RESISTORS ± 5% UNLESS MARKED

figure 2.2

The overall feedback voltage used to maintain constant motor speed is generated by sensing the forward base emitter voltage Q5, causing Q6 to conduct a greater amount of current as the load is increased. The voltage at point A then rises and Q1 begins to conduct for a shorter period of time. This means that the duty cycle of Q2 through Q5 increases and a larger average voltage is applied to the motor, thus compensating for the increased load. The frequency stability of the unit was checked by using it to drive a chopper blade which periodically interrupted the illumination between a torch bulb/photo-diode pair, and the resultant amplified signal from the photo-diode measured by means of a frequency counter. The results are shown in Table 2.

Table 2

f= 55 Hz, τ= 18ms (a)			f= 32 Hz, τ= 31ms (b)		f= 10 Hz, τ= 100ms (c)	
1	2	3	1	2	1	2
548	553	556	291	291	51	51
548	553	557	291	291	51	54
549	553	557	291	291	51	52
549	553	556	290	292	52	53
549	553	557	292	291	52	51
549	553	556	291	291	50	51
550	554	556	291	290	50	53
549	553	557	290	290	49	52
550	553	556	292	291	49	51
550	553	557	291	291	51	51

Figures in columns 1, 2 and 3 section (a) are the series of counts taken over a 10 second period, with 10 seconds elapsing between each measurement. There is a period of 10 minutes running time between the series of counts in (a), and 15 minutes running time between each series

in (b) and (c).

The frequency drift at 55, 32 and 10Hz is 0.10, 0.01, and 0.02% per minute respectively.

2.7 Signal Recovery System

The signal recovery system used an AIM phase sensitive detector. The system consisted of a stabilised power supply MPSU 101; low noise amplifier LNA133; broadband amplifier ACA 123; two tuneable filters TFO 129's; one on the reference and one on the signal input; phase shift amplifier PSA 128; and the phase sensitive detector itself, PSD 122. The amplifiers gave a total combined gain of 120 dB in 6 dB steps, and use of a tuned amplifier on the signal input gave the unit a high out of phase rejection figure. As an alternative to the preamp and amplifier in series employed in the AIM a Princeton Applied Research (PAR CR4A) low noise amplifier was used. This gave a higher signal to noise ratio than the AIM unit at the slower chopping frequencies i.e. of less than 30Hz. The d c output from the lock-in amplifier was most conveniently displayed on a chart recorder, a Honeywell continuous balance potentiometric, twin pen, type 'Electronic' 194.

For a known stable periodically varying input to the phase sensitive detector (generated by an audio frequency signal generator), the signals appearing on the chart recorder were reproducible to more than 1% accuracy, and stability was limited by drift in either the audio frequency generator (or actual experimental source), or the phase sensitive detector unit 122. However, it was found that when the phase sensitive detector was used in conjunction with the variable speed chopper its long term output stability (over a period of hours) was limited by frequency drift in the chopper motor. With the use of a high Q ($\sim$10), tuned amplifier at the signal input, any small frequency change in the signal ($\sim$2%) resulted in it

being phase-shifted when filtered through the TFO 129 module; this was sufficient to cause changes of up to 50% in the phase sensitive detector output. To maintain a useful signal to noise ratio at the phase sensitive detector input it was necessary to continually correct the phase drift in the signal channel by retuning the filter and thus maximising the d c output. Because of this measuring technique phase information concerning the input signal was lost and it was possible to satisfactorily detect phase shifts which occurred in signals from the absorption cell (as distinct from those induced by frequency changes in the perturbation signal), of only $\pi/4$ radians or greater.

The performance of the AIM was compared with that of a Brookdeal 411 lock-in, which employed a coherent filter (type 467) in the signal channel between the pre-amplifier (45) and its input. The purpose of such a filter is to lock the signal frequency to the reference frequency, thus avoiding any problems due to variations in the chopping motor speed responsible for the reference and synchronous signal frequencies. It was found, however, that the Brookdeal unit gave a signal to noise ratio at its output upwards of five times poorer than that of the AIM. Noise generated by the amplifier in the coherent filter was thought to be responsible for this; especially at the slower (i.e. less than 30Hz) chopping frequencies.

The overall noise limiting factor was discharge noise in the absorption cell. At pressures below 5torr, moving striations formed in the discharge severely modulated the spontaneous sidelight. It was thought that initially such sidelight changes were due to thermal effects in the plasma, or long term chemical dissociation and recombination of CO_2, but observation of sidelight emission at pressures of about 1torr revealed well-defined striations in the positive column of the discharge which moved past the observation windows and hence modulated the sidelight emission with a

typical period of some seconds. In later experiments involving sidelight observations gas pressures were normally greater than 6torr, and a check was made to ensure that the effects due to moving striations were not present.

Screened coaxial cable and B.N.C.connectors were employed throughout in order to minimise stray pick-up. The photomultiplier tubes were screened with mu-metal or copper shields maintained at the photomultiplier cathode potential. All electronic equipment (excluding the power supplies to the laser and absorption cell) was run from a constant voltage transformer operating at mains earth.

2.8 Optical Components and Detectors

The spontaneous and stimulated emission processes occurring in a dc. electrically excited discharge containing CO_2, N_2 and He give rise to the output of radiation over a considerable range of wavelengths. This is due to transitions between vibrational levels within a given electronic state leading to production of infra-red radiation, and transitions between vibrational levels which belong to different electronic states producing radiation in the visible and ultra-violet. It is therefore necessary to use severaltypes of detector in order to observe the complete range of wavelengths.

(a) Detection in the near infra-red

To monitor emission from the ground electronic state ($X\,^1\Sigma_g^+$), levels of CO_2 a Mullard photoconductive cell RPY 36 was used. This had an indium antimonide element sensitive to infra-red radiation of wavelengths from over 5.6 μm through the visible region and down to 0.25 μm. The peak of the spectral response was at 5.3 μm and it was used to measure the spontaneous emission at 4.3 μm from the 001 —— 000 band in CO_2. The figures of merit for this detector are given by the values of D* and the noise equivalent

power N.E.P. (15).

$D^* = 2.0 \times 10^{10}$ cm $(c/s^{\frac{1}{2}}/watt)$ typically at $70^{\circ}K$, and

N.E.P. $= 8.5 \times 10^{-12}$ (r.m.s) watt.

Both of these values represent the responsivity of the detector to monochromatic radiation incident at 5.3 μm, modulated at 800 Hz and with an electronic bandwidth of 1 Hz.

For the detection of a given quantity of energy W it is necessary in the case of an infra-red detector to use as small an area of detecting element as possible to reduce the amount of background thermal noise. For a detector which has a cut-off in the near infra-red no problem of thermal noise arises. That is because there are so few photons generated by a black body at say $300^{\circ}K$ - as can be seen from the Planck distribution curve - with wavelengths less than the minimum required to produce any photo-excitation of the detector element. Hence the figure of merit for a photomultiplier with photo cathode cut off at 9000 Å or so operating in the visible and uv will generally be greater than that of an infra-red or thermal detector.

The bias circuit used with the RPY36 is shown in figure 2.3. Power was supplied by a current stabilised power supply unit (Coutant, type LP50/50), giving 50 volts at 0.5 amps maximum. The detector was always biased at a current of 1.0mA which gave a maximum signal to noise ratio rather than optimum gain. The dwell time of the liquid nitrogen dewar was about forty minutes, but the detector output changed by less than 1% after switching off the bias current (necessitated because of exposure of the element to visible radiation when replenishing the coolant), refilling the dewar with liquid N_2, and switching the bias current back on again.

(b) Detection in the U.V.and Visible regions between 3000 and 9000Å.

In order to observe the second positive system of nitrogen (2800 to 5000Å), a photomultiplier tube, EMI9597 QUB, was used. This was a high

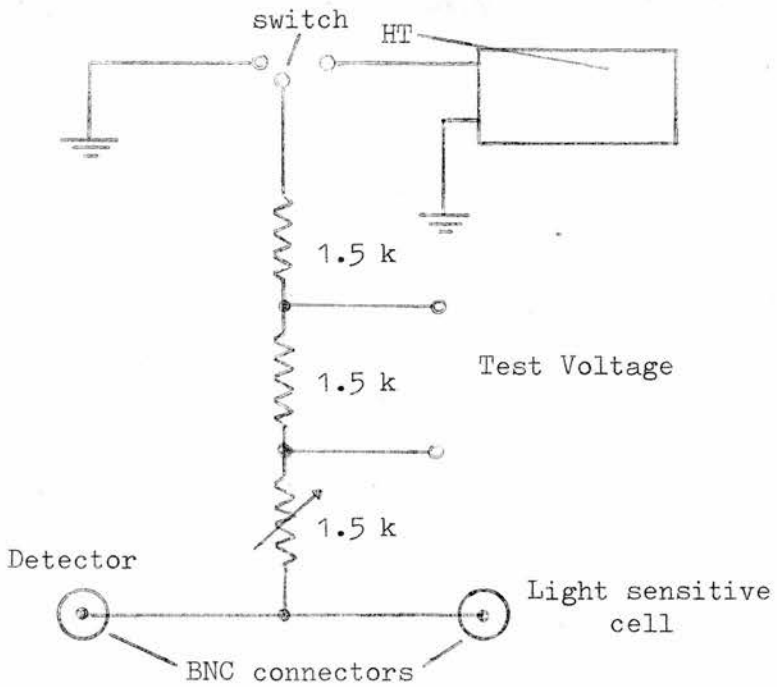

figure 2.3.

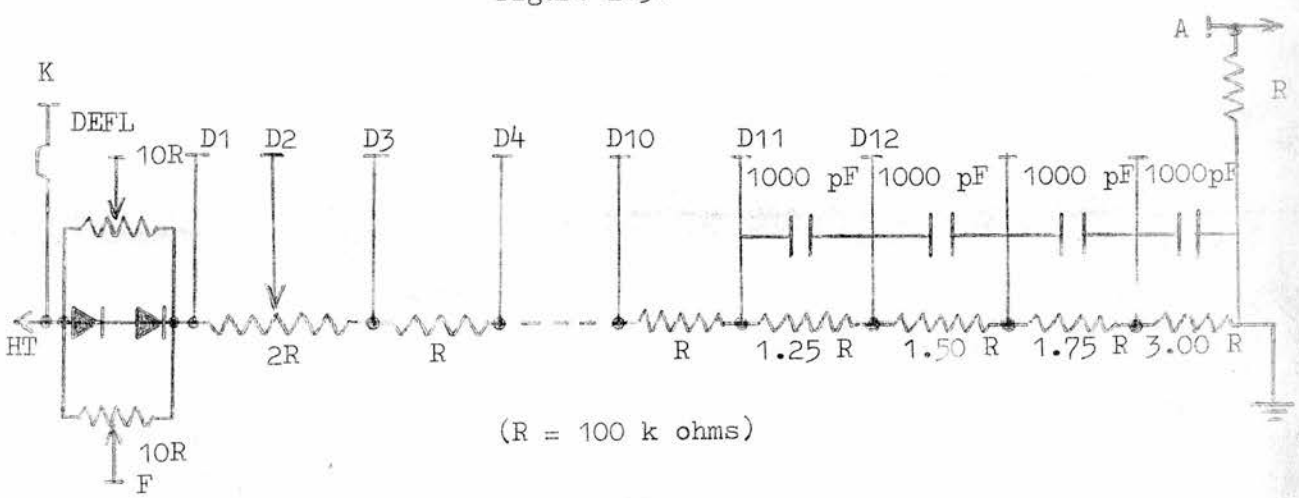

(R = 100 k ohms)

figure 2.4.

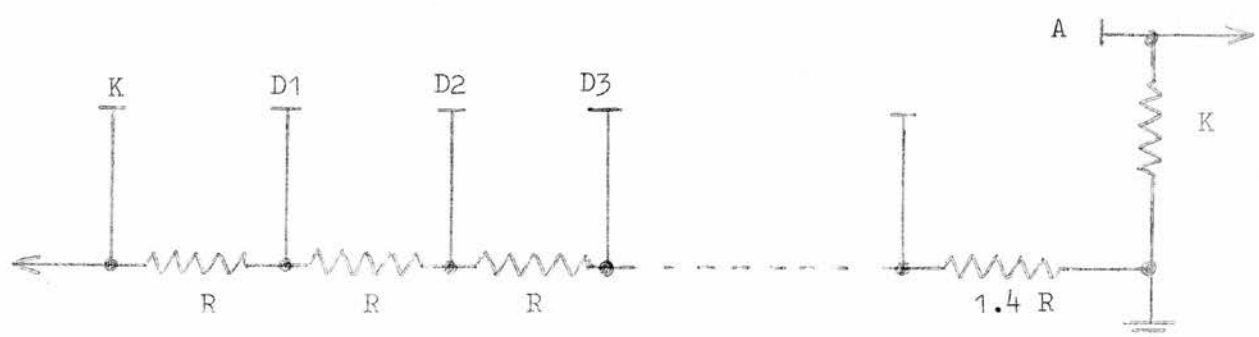

(R = 100 k ohms)

figure 2.5.

gain high output current 14-stage tube fitted with a Spectrosil quartz window and an S-20 cathode. The dynode chain used is shown in figure 2.4 and is similarto that described in (16).

The nitrogen first positive system has transitions ranging from 5000 to 10,500 Å. The EMI tube described above has no appreciable cathode sensitivity above about 7000 Å where the quantum efficiency is less than 2%. In consequence an alternative photomultiplier tube was used to examine the first positive system. This was an RCA C31034 having a cathode material of quantum efficiency greater than 8% beyond 8 600 Å. This quantum efficiency was achieved by using a gallium arsenide cathode rather than the tri-alkali material of the EMI tube. In order to reduce the dark current, the RCA tube together with its dynode chain shown in figure 2.5 was mounted in a housing which was both thermally and electrically shielded. An adaptation of the system described in (17) was designed and constructed as shown in figure 2.6. Gas boiled off from liquid Nitrogen was circulated throughout the housing as shown. Thermal and electrical insulation was provided by the inner pirtoid shield, the gas flow being such that the copper sleeves and window housing were cooled first ensuring that any residual water vapour (remaining after flushing the system with dry nitrogen at room temperature) condensed on the copper sleeves rather than the tube or dynode chain. The inner window was prevented from misting by circulating cold gas on both faces of it, and the outer window by means of a small heating element. The copper sleeves were maintained at the photomultiplier cathode voltage and provided electrostatic shielding. A flexible arrangement of soft copper wire and standard brass pin connectors was used to connect the tube to its base, and thence to the dynode chain. This precaution was necessary to avoid damage to the glass to metal seals, due to differential thermal expansion, which might have occurred had the tube been mounted

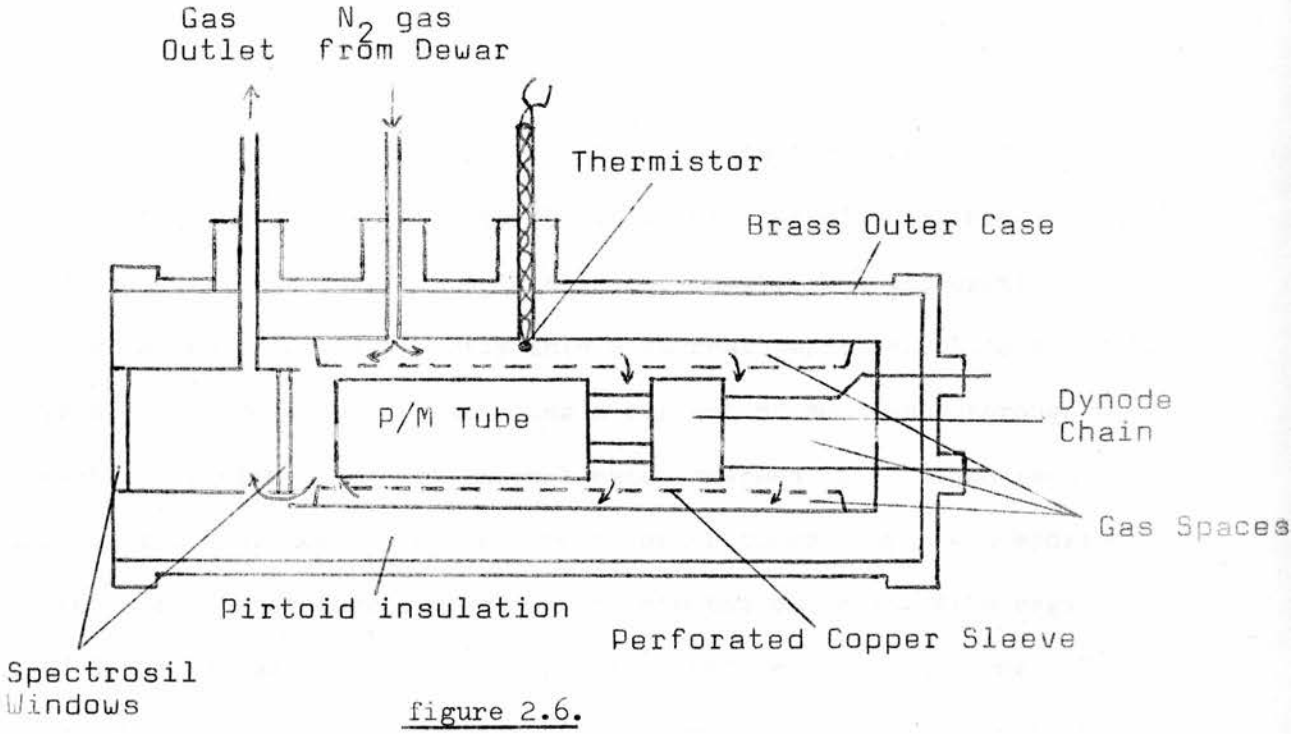

figure 2.6.

Cooled Photomultiplier Housing Schematic.

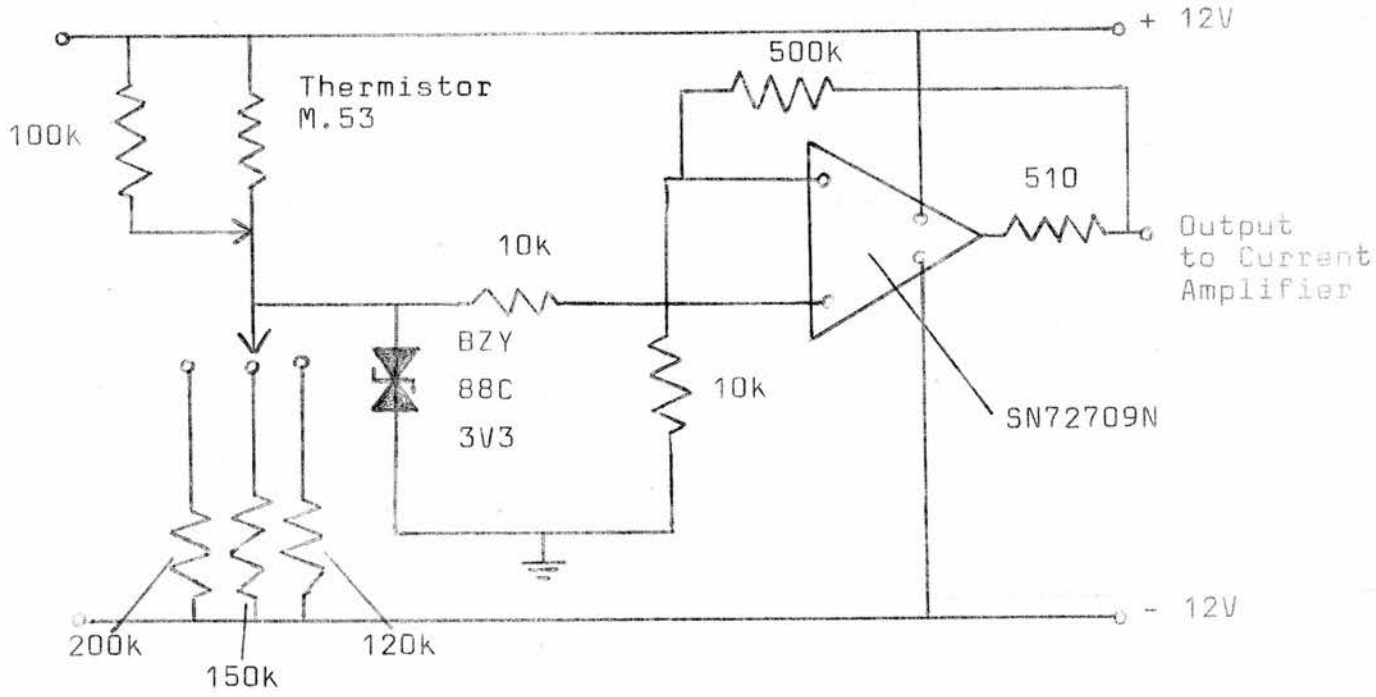

figure 2.7.

Thermistor Controlled Heating Circuit.

2800Å to 8000Å to resolve individual electronic vibrational transitions - though not their rotational substructure - in the nitrogen first and second positive systems, and carbon monoxide Angstrom band system. The monochromator was a double pass instrument (i.e.radiation passed twice through the prism before leaving the exit slit) and used a parabolic mirror of 40cm focal length. The prism and mirror were fixed together on a Wadsworth mounting such that they were permanently placed in a minimum angle of deviation configuration. The acceptance aperture of the instrument at the entrance slit was f8.4, and a condensing lens suitably placed in front of the entrance slit was used to match the instrument to the volume of plasma which was observable through the side window of the absorption cell.

The monochromator was placed on a three point mounting and beneath it was clamped a triangular section optical bench which was used to mount a helium neon laser (temporarily for horizontal optical alignment) and a convex condensing lens (spectrosil B quality) of 5cm focal length. Alignment of the complete system by the following method was carried out. The helium neon laser beam was directed through the exit slit of the monochromator and allowed to pass out through the entrance slit, through the condensing lens and onto the side observation window of the absorption cell. The lens and spectrometer were then adjusted positionally until the beam passed through the centre of both slits lens and window. Final adjustment was made by tuning the spectrometer to the peak of one particular electronic vibrational transition in the nitrogen spectrum emitted by a dc excited discharge in the absorption cell. The light signal was detected by a photomultiplier, amplified and displayed on a chart recorder. The positions of the lens and spectrometer with respect to the side window of the absorption cell were then adjusted in turn until the chart recorder output was maximised. An irtran 2 condensing

lens, suitably positioned, was used in place of the spectrosil lens when observing infra red transitions in the carbon dioxide ground electronic state. The complete experimental assembly is shown schematically in figure 2.8. Figure 2.9 shows the laser and absorption cell aligned on the optical bench together with the variable speed chopper C1 and SPM2 monochromator. Figure 2.10 shows the absorption cell in detail, and the CRL power meter, MDC manometer, and sidelight chopper, C2.

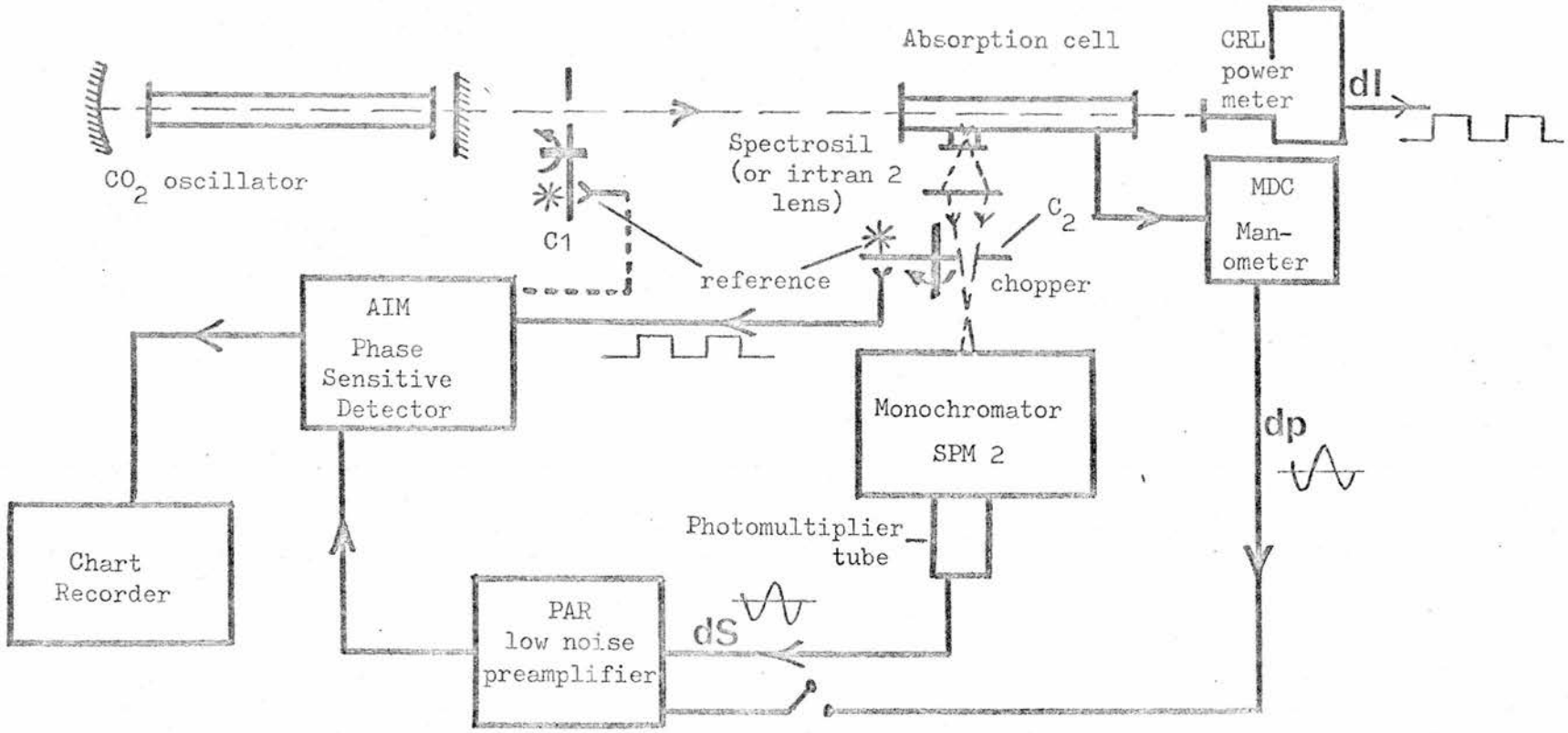

figure 2.8

Schematic of experimental set-up showing method of measuring sidelight spectra (chopped by C2) perturbation sidelight spectra (chopped by C1) and the parameter dp.

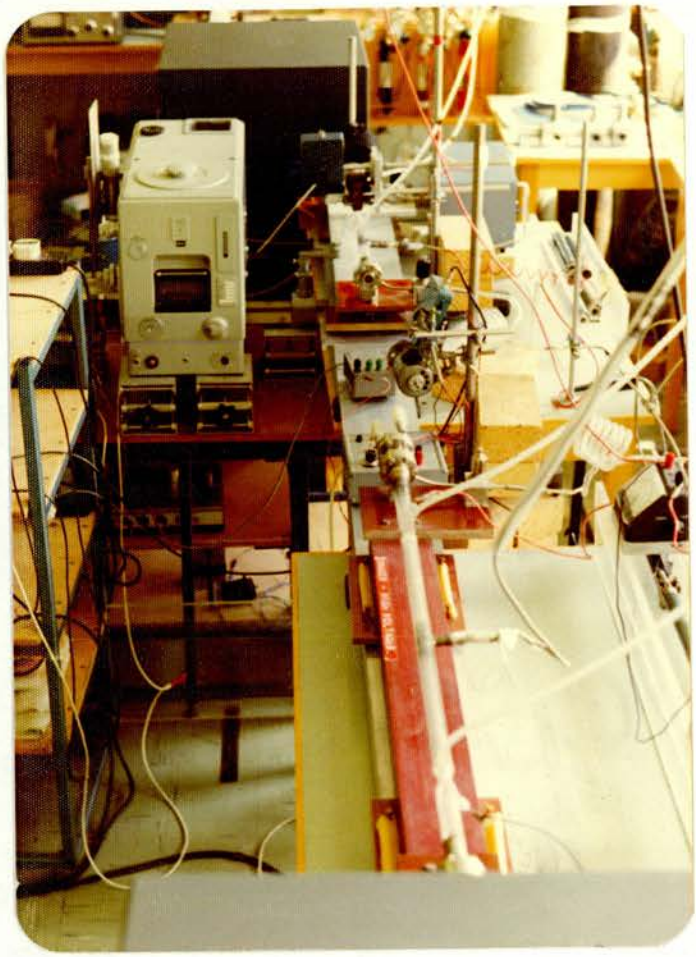

Fig. 2.9

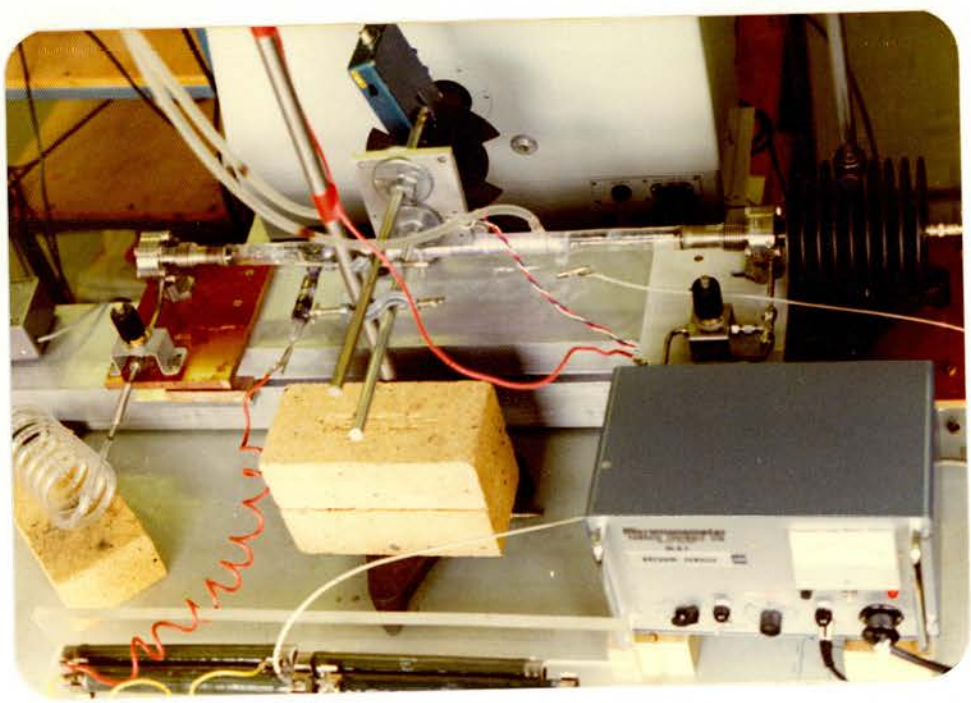

Fig. 2.10

3. CURRENT CHANGES IN A CO_2 AMPLIFIER

This chapter gives a review of previous work on the subject of current perturbations and related effects in the CO_2 laser. The first section deals briefly with the work of several authors whilst the second is a more detailed account of the subject and pays attention to aspects particularly relevant to the present work.

3.1 Previous Work in Current Perturbations and Associated Effects

It has been shown in several papers (for example references (5), (6), (13), (18) and (19)), that in a cw CO_2 laser and in CO_2 laser amplifiers, discharge current changes can be brought about by the influence of laser radiation at 10.6μm. There are various explanations of this effect. Crane and Waksberg (7) together with the authors of (13), (19) and (20) suggest that an increase in the number of CO_2 molecules in vibrationally excited ground electronic states will lead to an enhancement of the numbers of ionised molecules and electrons. This depends on the argument that molecules in the upper laser level (001), have sufficient energy (about 0.2 eV) to contribute significantly to ionisation in the plasma, as do the molecules in the lower laser (100) level, though to a lesser extent. If ionisation is more efficient from the (001) level and its population is depleted, by stimulated emission processes say, then the overall contribution to ionisation in the plasma is reduced and so the discharge current is reduced. In a cw CO_2 amplifier which is in a gain condition the 10.6μm radiation field will deplete the (001) level and the amplifier discharge current will decrease, see for example reference (19).

Rigden and Moeller (6) and Aoki et al (21) have interpreted the current change in terms of a macroscopic change in translational temperature of the irradiated molecules. Rigden and Moeller do not describe in detail the processes involved but attribute the increase in plasma current to heating of the gas. This is accomplished either by directly heating the amplifier tube walls (see also (19)) or by the resonance absorption of radiation at 10.6μm in CO_2; in both cases there is a current increase. They comment further that if radiation at 10.6μm is passed through an amplifier which contains an active medium in a gain condition, a nett amount of energy is removed by stimulated emission processes from the gas it is therefore cooled and the discharge current is decreased.

Aoki et al interpret the temperature induced current changes as being due to transient heating and cooling effects brought about by the transfer of vibrational to translational energy from the upper and lower laser levels of CO_2; this process is discussed more fully in Section 3.2. Unlike Rigden and Moeller who used a cw CO_2 laser and external amplifier, Aoki et al irradiated an intra-cavity amplifier cell by means of a Q-switched 10.6μm pulse, which allowed the study of short term ($<$ 1 millisecond), transient current changes. Comparison of these current transients with known vibrational translational relaxation times of the upper and lower laser levels revealed a strong temporal correlation between the two. No details are given, however, as to the mechanism whereby the discharge current is changed as a result of the change in translational energies of the CO_2 molecules.

Kindl, Leeb, and Schiffner (13) also pointed out in an earlier paper the order of magnitude agreement obtained between

the time constants for both rapid and slower discharge current changes, and the decay constants of the lower and upper laser levels respectively. At this point they differ from Aoki et al in their argument. They comment that since it can be assumed that it is easier to ionise CO_2 molecules in the laser discharge if at least one of the available vibrationally excited levels is populated, then the cessation of laser action provides a population increase in the (001) state, a decrease in the (100) state, resulting in the ion density - and therefore discharge current being raised by enhanced contribution from the upper laser (001) level (over its relaxation time) and lowered by the depleted contribution from the lower laser (100), level also in a time equal to its relaxation time. They show the effect not only of internal parameters of the system (partial pressure of gas components, current and gas temperature), but together with Rosenberger, the importance of external circuitry, especially ballast resistance. Rosenberger (20) gives a theoretical treatment of the problem by considering the relaxation of a three-level model whose terms (CO_2 (001), (100) and N_2(V=1)), are coupled by radiative and non-radiative transitions. To explain the current changes it is supposed that population changes in the primary laser levels are directly responsible, following the argument above of Kindl et al pertinent to ionisation from CO_2 vibrationally excited levels.

Lobov et al (22), give a different theoretical treatment. They state that when a pure CO_2 discharge is irradiated at 10.6μm the distribution of molecules among the primary laser levels, and those vibrational levels to which they are collisionally coupled, is altered. This will change the

amount of energy exchanged by them in inelastic collisions with electrons. Since the electron mobility depends directly on the inelastic electron-molecule collision processes, a change in them will affect the mobility and hence the discharge current. This is evident from the equation which describes the electron mobility as follows:

$$b_e = C \sqrt{\frac{e\lambda_1}{mpE}} \cdot (X)^{\frac{1}{4}} \qquad \ldots\ldots\ldots 3.1$$

X = average energy fraction imparted by an electron to a molecule per collision.

b_e = electron mobility

m = electron mass

e = electron charge

p = gas pressure (torr)

E = electric field

λ = electron mean free path = $\frac{\lambda_1}{p}$

C = constant dependant on the electron distribution function.

(This equation appears in a similar form in Von Engel (58), its derivation uses average values for such variables as electron energy, drift velocity and mean free path, for the electrons in a molecular gas discharge). A change in X, the energy transferred during an inelastic collision, alters b_e in equation (3.1). The change in discharge current due to the redistribution of molecules amongst the ground electronic vibrationally excited states of CO_2 is observed for various gas discharge conditions. The consequences of their model are discussed in Section 3.2 below.

3.2 A Detailed Consideration of the Models Describing Current Perturbations

(a) Vibrational-Translational Energy Transfer

Current transients brought about in a CO_2 discharge by a Q-switched 10.6μm pulse correlate temporally very closely with the relaxation times of the primary laser levels. It is thought therefore (Aoki et al (21)) that the explanation of such behaviour is as follows. For a medium exhibiting gain there is a depletion of CO_2 (001) molecules and an increase in CO_2 (100) molecules after the incident 10.6μm pulse has interacted with the discharge. The increased number of (100) molecules lose their energy over a period of several microseconds due to rapid vibrational to translational (V - T) energy exchange, and thereby induce a heating effect in the gas. This causes a short duration discharge current increase corresponding to the same time span over which these V - T processes operate. The depleted (001) molecules also lose energy via V - T processes, but do so over a typical period of several milliseconds; this results in a cooling of the gas over a similar period of time and hence a current decrease of the same duration. If the medium is in an absorption condition then the opposite effects occur, i.e. a short duration gas cooling (due to fast V - T energy exchange from the depleted (100) population) and a corresponding current decrease, followed by a longer duration gas heating (due to slower V - T energy exchange from the increased (001) population) and current increase. Exactly how the change in gas

kinetic temperature produces a current perturbation is not discussed in detail by Aoki et al (21) although it is attributed to acoustic oscillations in the gas generated by V - T relaxation of the (001) and (100) levels. A 10.6μm Q-switched pulse directed along the longitudinal axis of the absorption cell was found to produce a radially-directed sound wave (21) and therefore associated acoustic pressure waves. This being so, then there would also be molecular number density fluctuations in the gas.

Gebhardt and Smith (24) have used a Mach-Zehnder interferometric technique to measure gas density changes brought about by the absorption of a short duration 10.6μm pulse in high pressure CO_2 and CO_2 : N_2 mixes through which there is no discharge current flowing. Using a three level relaxation model (25) to interpret their results they report an initial anomalous gas cooling (density increase) on absorption of the laser pulse, over a time period τ_{10}, provided $\tau_{10} < \tau_{21}$. The relaxation times are defined as follows:

τ_{10} = time for group (1) molecules i.e. (100), (020), (010), to relax to the ground vibrational (000) state.

τ_{21} = time for group (2) molecules i.e. (00n), n = 1,2,3,... to relax to energy states in group (1).

This process is followed in turn by a heating of the gas (density decrease) over a period of time $\tau_{10} + \tau_{21}$. In conjunction with Aoki et al (21) we have then the following argument. For a sufficient condition, i.e. a gain situation in the gas, and certainly a necessary one, $\tau_{10} < \tau_{21}$, there is a short duration gas density decrease

due to the fast V - T energy exchange rate from the population enhanced (100) level, and consequent increase in gas kinetic temperature. This is followed by a much slower density increase due to the longer duration V - T energy exchange rate from the depleted (001) level. In the absorption case the reverse argument is true. Gebhardt and Smith (24) restrict their experimental conditions to those of absorption. They comment that the gas temperature changes occur over the same time scale as the V - T decay processes (and are in qualitative agreement with reference (21) in this respect), but that the gas density changes are delayed by an acoustic transit time defined as $\tau_a = \frac{D}{V_s}$ where:

D = irradiating beam diameter

V_s = velocity of sound in the gas.

So, for a constant total gas number density there is a gas kinetic temperature change followed by a gas density change, the delay being limited in this case by τ_a, and also the V - T decay processes responsible for the temperature change. For 10.6μm pulse lengths of milliseconds or longer, and gas pressures of interest to the present experiments ($\lesssim$ 20 torr) we note that τ_a is comparable with times associated with the relevant V - T decay processes. So we conclude that effectively any gas kinetic temperature change in the irradiated volume of a gas is followed after a time τ_a by a corresponding density fluctuation. The following reactions illustrate typical V - T energy exchange processes and define the associated rate constants:

$$CO_2\ (001) + M \xrightarrow{k(V_3)} CO_2\ (n, m^l, 0) + M + E_{trans} \quad ....3.2$$

$$CO_2\ (n, m^l, 0) + CO_2\ (000) \xrightarrow{k(V_1, 2V_2)} 2\ CO_2\ (010) + E_{trans} \quad ....3.3$$

where $\tau_{10} = 1/K(V_1, 2V_2)p \approx 500\mu s.$
$\tau_{21} = 1/K(V_3)p \approx 260\mu s.$
} $p = 10$ torr CO_2

In a 1 cm diameter tube:

$D = 0.5$ cm $\quad p_{CO_2} = 10$ torr $\quad V_s \approx 2.7 \times 10^4 cms^{-1}$ at 400^oK

$\tau_a \approx 0.02$ ms $\leq \tau_{10}, \tau_{21}$.

Hence the (001) level will convert its vibrational energy to translational energy after about $760\mu s = \tau_{10} + \tau_{21}$ under the above conditions.

In a gas discharge the electron mean free path is inversely proportional to the number density of gas molecules present. We may assume that Gebhardt's analysis in pure CO_2 and $CO_2 : N_2$ mixture holds also in the case of a CO_2 amplifier in which a discharge current is flowing. This will be so since the V - T processes will be similar in both cases (provided the gas temperatures in each case are comparable), although the population distributions amongst the CO_2 ground state vibrational levels will differ due to the additional process of electronic excitation. When, as before, the gas number density is reduced, the electron mean free path will increase and so, in consequence, will the electron mobility; thus we have a current increase following a density decrease. Since the electron-molecule collision time (at pressures $\lesssim 20$ torr) is of the order of a few microseconds or less, the current change will effectively follow the density fluctuations with only a small time delay.

(b) Ionisation Effects

Crane and Waksberg (7), together with the authors of references (13), (19) and (20) have suggested that since the CO_2 (001) level lies at 0.2 eV above the ground state level it contributes effectively to the ionisation in the plasma. Therefore selectively changing the (001) population would produce a primary effect on the discharge current. Little information is at present available on the variation of ionisation cross-section with vibrational energy in the ground electronic state of CO_2 with which to support this theory. There is a large difference between the energy of the (001) state and the ionisation potential of CO_2 at 0.2 eV and 13.7 eV respectively, and so ionisation from these low lying vibrational states may not be direct and may involve a complex number of intermediate processes.

Other common additive gases in CO_2 amplifiers such as CO, or NO (dissociation products) N_2, He and Xe have ionisation potentials of 9.4, 9.25, 15.5, 24.5 and 12.1 eV respectively, all lying well above the typical ground electronic state vibrational energy levels to which they are collisionally coupled, and through which they would experience any perturbations introduced into the primary laser levels of CO_2. Multistep processes in any of these species leading to ionisation need to be examined in detail to provide further evidence for this theory. Because the CO and N_2 ground electronic state vibrational levels are metastables, any ionisation by cumulative processes from these levels (which are closely coupled to the primary laser levels), would carry with it the selective pertubation introduced to the (001) and(100) states. It is possible that high-lying

electronic states (such as the $C^3\Pi u$ in N_2 lying 3.4 eV below the ionisation limit; or the metastable $A^3\Sigma^+_u$ ($\tau_{rad} \approx 1$ sec) lying 7.0 eV below) may contribute significantly to ionisation in the plasma, but again excitation and ionisation cross-sections from these states are not known. The $C^3\Pi u$ level is populated mainly by direct electron impact from vibrational levels in the $X^1\Sigma^+_g$ state of N_2 (26), (27) and would be affected by a change in the vibrational distribution of N_2 molecules in that state due to a radiation field induced perturbation introduced via the reaction:

$$CO_2\ (001) + N_2\ (V = 0) \rightleftharpoons CO_2\ (000) + N_2\ (V = 1) \quad \ldots\ldots\ 3.4$$

Crane (11) comments that excited N_2 levels lying close to the ionisation limit (e.g. $C^3\Pi u$, $B^3\Pi g$), may be collisionally mixed with the $X^1\Sigma^+_g$ metastable vibrational levels of N_2 and would by this mechanism be perturbed. Bleekrode (28), however, points out that the typical lifetimes of these electronic levels are about three orders of magnitude smaller than the $X^1\Sigma^+_g$ vibrational metastables. The $C^3\Pi u$ state has $\tau_{rad} \approx 4 \times 10^{-8}$ sec, and the $B^3\Pi g$ state has $\tau_{rad} \approx 9 \times 10^{-6}$ sec (29); hence the probability of collisional mixing of these levels with the $X^1\Sigma^+_g$ states is small.

(c) Electron Molecule Collision Processes

As discussed above a rather different theoretical account of the mechanisms responsible for current changes in a pure CO_2 discharge was proposed by Lobov et al (22) and may be briefly reiterated as follows. The factor X (average energy fraction which an electron imparts to a molecule in an inelastic collision) in equation (3.1) will change if there is a redistribution in vibrational populations amongst the ground electronic state CO_2 vibrational levels, and hence the electron mobility is changed.

They ignore any temperature and gas density changes in the irradiated cell, and their subsequent influence on the electron mean free path; they relate the <u>total</u> current change to a change in X. Like the mechanisms proposed above, this one is also able to explain why the current will always decrease in an active medium exhibiting gain when it is irradiated at 10.6μm. Their final expression for di, the change in discharge current, involves the absorption coefficient $\alpha(\lambda)$, where

$$\alpha(\lambda) = - C\left(N_u - \frac{g_1}{g_u} N_1\right) \text{ and,}$$

C = constant

N_u = upper laser level population

N_1 = lower laser level population

g_u, g_1 = level degeneracies

$$|\dot{I}(j\Omega)| = -|\gamma \alpha(\lambda) \dot{\Pi} V f(j\Omega, \tau_1, \tau_2)| \quad \ldots\ldots 3.5$$

where $\dot{I}(j\Omega)$ = complex amplitude of the time varying part of the discharge current.

γ = constant (complex) dependent on the average energy supplied per electron per vibrational transition.

$\dot{\Pi}$ = complex amplitude of harmonically varying 10.6μm field.

V = irradiated volume of discharge

and $f(j\Omega, \tau_1, \tau_2)$ is a complex function dependent on the modulation frequency of the 10.6μm field, and the lifetimes of the upper and lower laser levels τ_2 and τ_1 respectively. Evidently $|\dot{I}(j\Omega)|$ is dependent in sign on whether α is positive or negative; e.g. for a gain condition α is positive and hence $|\dot{I}|$ decreases.

If we assume that the argument of Gebhardt holds in the case of a gas discharge (Section 3.2(a)) then number density

fluctuations in the gas molecules will occur. This in turn will cause a change in electron mean free path since it is approximately inversely proportional to the gas number density. Equation (3.1) then shows that there are two possible mechanisms which can result in a change in electron mobility, i.e. a change in X or a change in λ $(= \frac{\lambda_1}{p})$.

From equation (3.1):

$$b_e = C \sqrt{\frac{e\lambda}{mE}} (X)^{\frac{1}{4}} \qquad \ldots\ldots\ldots 3.6$$

Hence the discharge current carried by the electrons is

$$j = n_e e E b_e = C^1 \sqrt{\frac{e}{m} E \lambda} (X)^{\frac{1}{4}} \qquad \ldots\ldots\ldots 3.7$$

where $j = j(\lambda, X)$.

Taking increments:

$$dj = \left(\frac{\partial j}{\partial \lambda}\right)_X d\lambda + \left(\frac{\partial j}{\partial X}\right)_\lambda dX \qquad \ldots\ldots\ldots 3.8(a)$$

and assuming that E is constant

$$dj = C^1 \left[\frac{1}{2}\left(\frac{X}{\lambda^2}\right)^{\frac{1}{4}} d\lambda + \frac{1}{4}\left(\frac{\lambda^2}{X3}\right)^{\frac{1}{4}} dX\right] \left(\frac{eE}{m}\right)^{\frac{1}{2}} \qquad \ldots\ldots\ldots 3.8(b)$$

Hence $$\frac{dj}{j} = \frac{1}{2}\left(\frac{d\lambda}{\lambda}\right) + \frac{1}{4}\left(\frac{dX}{X}\right) \qquad \ldots\ldots\ldots 3.9$$

Since $\lambda \propto \frac{1}{p}$

$$\frac{d\lambda}{\lambda} = -\frac{dp}{p} \qquad \ldots\ldots\ldots 3.10$$

From 3.9 and 3.10, with $\frac{di}{i} = \frac{dj}{j}$

$$\frac{di}{i} = \frac{1}{4}\frac{dX}{X} - \frac{1}{2}\frac{dp}{p} \qquad \ldots\ldots 3.11$$

Here di, dp and dX are the fractional changes in discharge current, gas pressure and fractional energy transfer per electron–molecule collision respectively when the perturbing field is switched on, and equation 3.11 shows explicitly the two variables responsible for the change in discharge current i.

(d) Summary

It was the purpose of the experiments described below to attempt to differentiate between the importance of the various mechanisms for current changes proposed in 3.2(c) above. Because of the lack of experimental data on ionisation from excited states of CO_2 and N_2 it is not possible to comment further on the validity of the argument in 3.2(b) except to emphasise that, in common with other theories, it can agree qualitatively with the experimental observations that:

(i) For a medium containing CO_2 which exhibits gain (absorption), the discharge current decreases (increases) upon irradiation, and increases (decreases) when the irradiation is terminated.

(ii) The transient behaviour of the current perturbations may be explained in terms of the V - T energy exchange rates.

4. EXPERIMENTAL DETERMINATION OF THE RADIATION INDUCED CURRENT AND PRESSURE VARIATIONS, di AND dp

4.1 Apparatus and Procedure

In all the experiments described below cw 10.6μm radiation from the laser was modulated by a variable speed chopper and passed into the absorption cell containing gas mixtures of interest. The cell had an active discharge region of approximately 30 cm in length and 1.2 cm in diameter and a total volume - including that of the MDC measuring chamber - of 300 cc, see Fig. 4.1 for details. The active and non-active irradiated volumes were 2.20 and 3.20 cc respectively*. The perturbing radiation field was modulated at frequencies from 10 to 500 Hz and could be adjusted in power from 1 to over 10 watts cw in a multimode output. The MDC capacitance manometer had an output of 500 mV at full scale deflection on all pressure ranges and in order to calibrate the pressure measuring system - comprising the manometer PAR preamplifier and AIM detector - the following procedure was adopted. The output from an audio frequency signal generator in the range 0 to 500 mV initially at 30 Hz was applied to the reference input of the phase sensitive detector after suitable amplification. A small known fraction of this output was also applied to the PAR preamplifier where it became amplified and was monitored on an oscilloscope and passed into the signal channel of the AIM phase sensitive detector. A dc output from the AIM was then obtained which was proportional to the amplitude of the sinusoidal voltage input; and hence the output of the

* See also the discussion in Appendix A.1.

detection system in volts was calibrated against a known periodically varying input of the order of millivolts. A response curve for the system covering input signal ranges 0 to 500 mV and 10 to 500 Hz was finally obtained. The MDC voltage output was a function of the peak to peak value of the pressure signals and by knowing the frequency response of the manometer to periodically varying pressure signals it was possible to relate quantitatively the dc output from the AIM to these pressure inputs at the MDC.

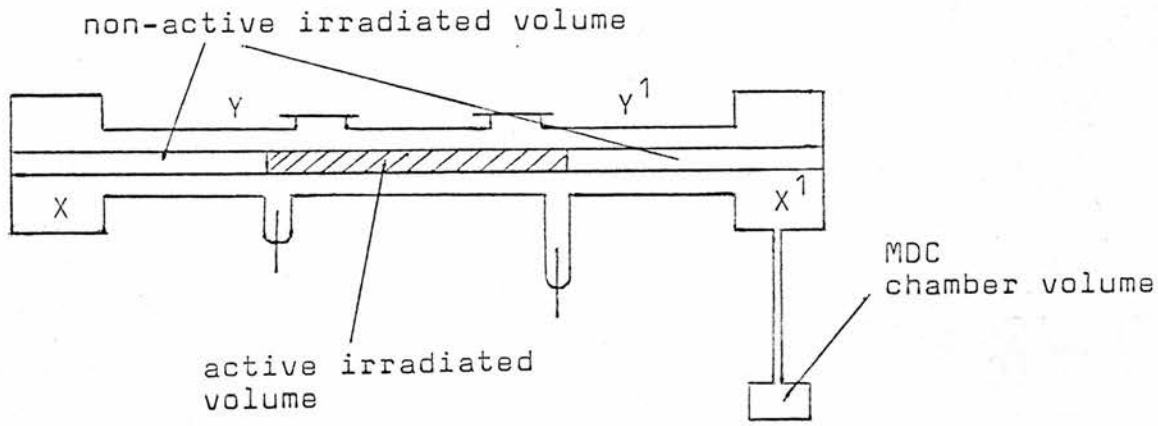

Fig. 4.1
Absorption Cell Schematic.

By a suitable choice of gas mixtures it was possible to have the active medium in the cell in a gain or absorbtion condition; this was monitored by observing the spontaneous emission at 4.3μm from the upper laser level in the (001)—(000) band. Radiation was observed through a sidewindow in the cell using the Zeiss SPM2 monochromator and Mullard RPY36 infra-red detector. The monochromator was centred on the 4.3μm band (which extends from 4.18μm to 4.35μm (30)) using an optical bandwidth of 0.18μm. Thus emission from the whole of the band was focussed on to the detector. The sidelight was modulated

at 40 Hz by means of a suitably placed mechanical chopper C2 (see Fig. 2.8). The detector output was amplified using the PAR preamplifier and passed into the lock-in amplifier. Unmodulated radiation at 10.6μm from the CO_2 laser was then passed through the cell. If the active medium in the cell was in a gain condition the 4.3μm spontaneous emission decreased due to depletion of the (001) level of CO_2 by stimulated emission. If the active medium was in an absorption condition, CO_2 molecules were pumped from the (100) to (001) level and thereby increased the spontaneous emission at 4.3μm. This technique was sufficiently sensitive to enable all of the gas mixtures of interest to be categorised in terms of whether they exhibited gain or absorption. Having examined the active medium in this way the mechanical chopper C2 was removed and the variable speed chopper inserted between the CO_2 laser and the absorption cell. This resulted in a modulated sidelight signal at 4.3μm synchronous with the chopped laser input. Using the PSA 128 phase shift amplifier the modulated signal and reference - from the variable speed chopper - were brought into phase and a dc output of defined polarity obtained.

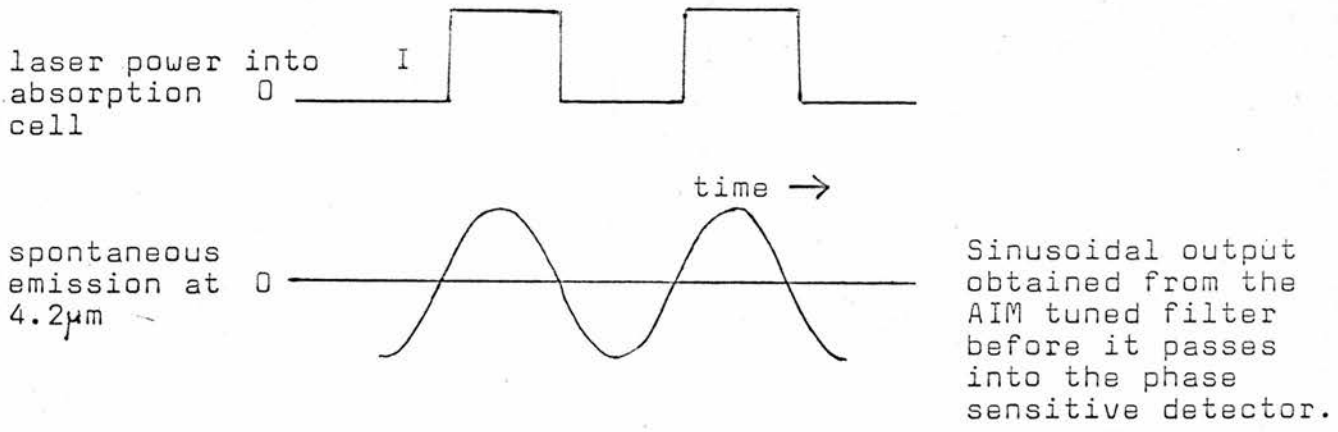

Fig. 4.2

Schematic of Oscilloscope Traces.

Fig. 4.2 illustrates the case where the upper laser level is pumped by absorption of 10.6μm radiation in the (100) level. The subsequent increase in spontaneous emission is thus in phase with the perturbing field, so determining the polarity of the lock-in dc output.

A similar experiment was performed in which the radiation field induced current changes were examined with the dc power supply to the absorption cell set in a constant voltage mode. The experimental set up is illustrated in Fig. 4.3.

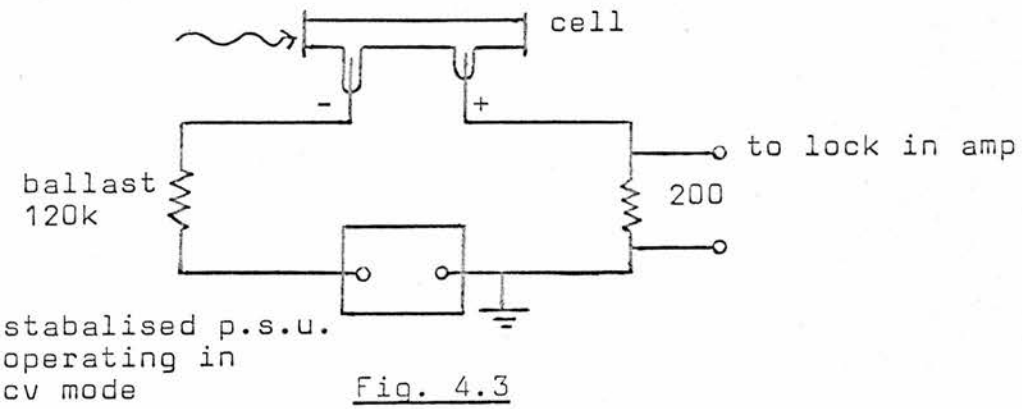

Fig. 4.3

A small dc voltage appeared across the 200 ohm resistor when a discharge was running in the cell; this was 2 volts at a typical discharge current of 10 mA. The unmodulated 10.6μm field was then allowed to pass into the cell and subsequent changes in magnitude of the discharge current were noted. It was established that if the medium in the cell exhibited gain the discharge current decreased when the cw radiation field was passing through the cell. Conversely, for an absorbing medium the current increased when the field was switched through. This is in agreement with the observations of Moeller et al (6).

The irradiating field was now modulated by C1 and an alternating voltage appeared across the 200 ohm resistor. This was passed into the AIM module and, using the phase shift amplifier, the voltage signal and reference from C1 were brought into phase, resulting in a dc output of defined polarity. Fig. 4.4 illustrates the situation where the active medium is absorbing radiation at 10.6μm (c.f. Fig. 4.2) and the discharge current is increased during the period for which the cell is irradiated. The sinusoidal output shown is the signal obtained from the AIM tuned filter before it passes into the phase sensitive detector.

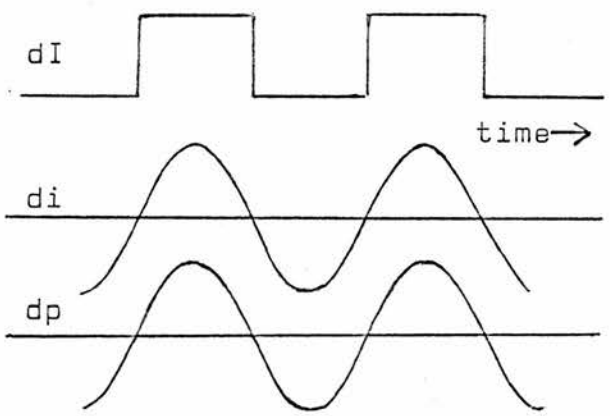

Sinusoidal outputs from the tuned filter.

Fig. 4.4

One further preliminary experiment was carried out in order to determine how the gas pressure in the absorption cell changed when continuously irradiated at 10.6μm. With the cell containing 10 torr of pure CO_2 at 10 mA discharge current, in a voltage controlled mode, the MDC capacitance manometer output was displayed on the chart recorder; this reading corresponded to an equilibrium total pressure in the cell. 10 watts of cw 10.6μm radiation was then switched through the cell and the gas pressure was observed to rise due to gas heating. (It was not possible

to find a gas mixture which, whilst exhibiting gain, gave a sufficiently large negative pressure change when irradiated to be detected in this manner). Simultaneous observation - in a similar fashion - of the direct current change revealed a current increase upon irradiation. This, then, was direct evidence of a pressure change in the cell due to gas heating correlating with a discharge current increase in the cell. The variable speed chopper C 1 was now introduced between the CO_2 laser and the absorption cell and outputs from the MDC manometer (dp) Mullard detector (dS) and current changes across the 200 ohm resistor (di), compared for phase relationship using the square wave reference dI which represented the modulated 10.6μm perturbation field. The result is illustrated in Fig. 4.5.

By replacing the 10 torr of CO_2 with a mixture of CO_2, N_2, He in the ratios 1:1:8 respectively at a total cold fill pressure of 10 torr and discharge current of 10 mA the result shown in Fig. 4.6 was obtained. With this mixture and current the cell was in a gain condition. As can be seen, all three quantities dS, di and dp retain a constant phase difference of zero degrees, and all become 180^{o} out of phase with dI. That is, the spontaneous emission at 4.3μm is decreased (since the 10.6μm field depletes the 001 level due to stimulated emission), the discharge current is decreased, and the gas pressure decreased when the active medium is irradiated.

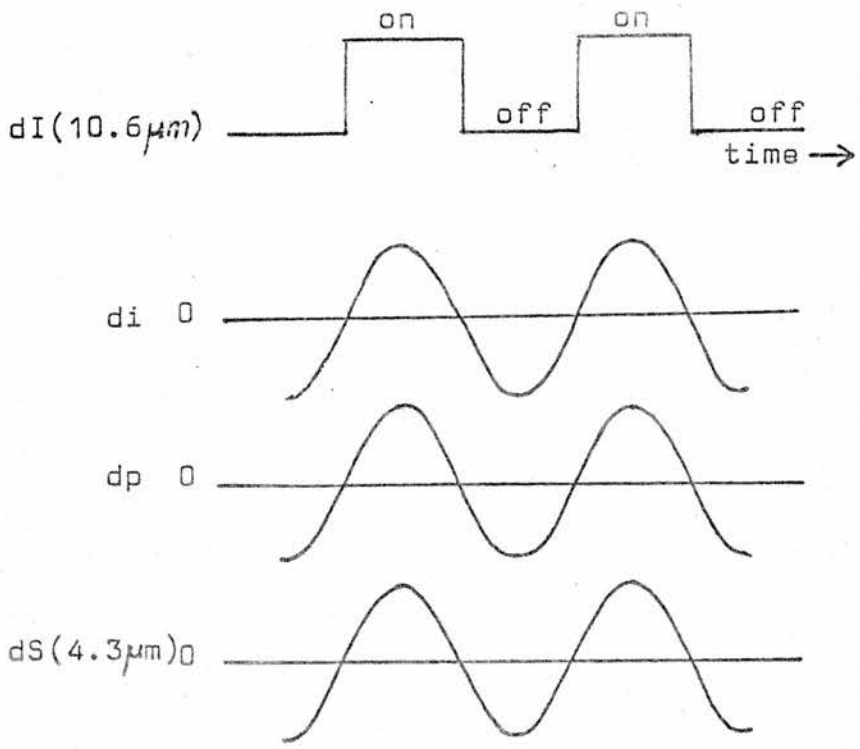

Fig. 4.5
Absorption Condition.

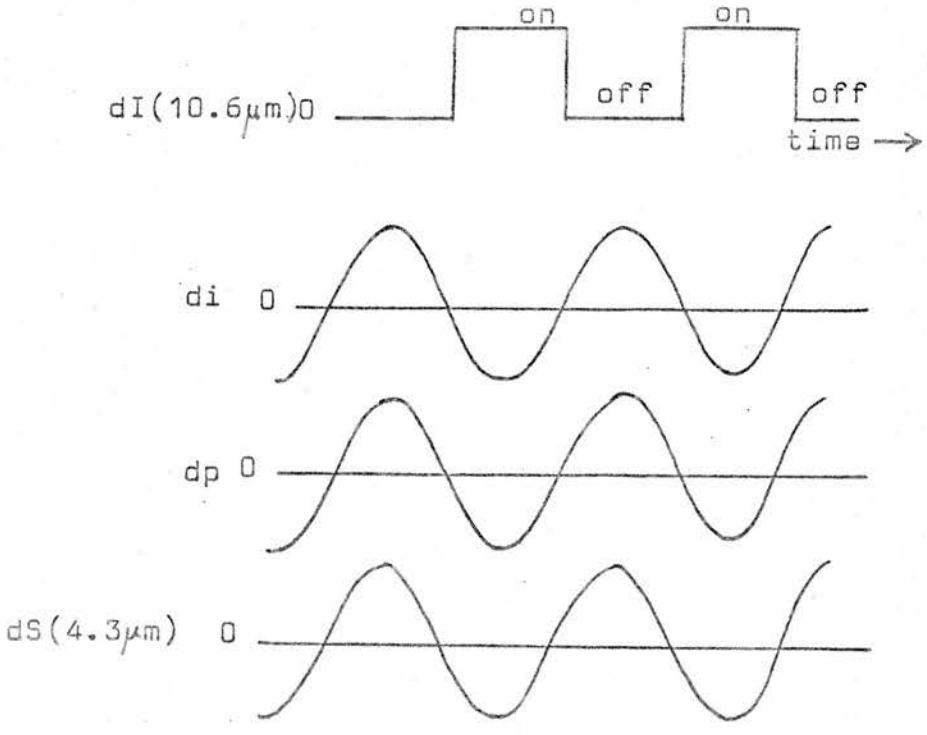

Fig. 4.6
Gain Condition.

Further results are illustrated below, but comments on the qualitative behaviour of the quantities di and dp from Figs. 4.4, 4.5 and 4.6 is required. Evidently if the gas number density in a discharge is increased by some means then the electron mean free path will become smaller. According to Section 3.2 this would mean that the discharge current would decrease. Conversely a decrease in gas pressure would likewise lead to a current increase. It would appear from Figs. 4.4, 4.5 and 4.6 that we are observing the opposite effect, i.e. a pressure increase leading to an in-phase current increase and vice versa. However, the dp illustrated in the figures is that pressure change which is measured in a non-irradiated volume of the absorption cell, and thus does not represent what is happening in the portion of active medium forming the active irradiated gas discharge region between the cell's electrodes. In this region the 10.6μm field will interact with CO_2 molecules in the following manner. In an absorption situation the gas is heated and expands and the number density of CO_2 molecules in the irradiated portion of the discharge decreases. These 'hot' molecules are driven into cooler dead-spaces in the cell by the process of thermal expansion, i.e. in these cool regions the molecular number density is temporarily increased and we thus see a pressure increase on the capacitance manometer which samples pressures from such a cooler region; the converse argument is true for a situation where the active medium exhibits gain. Thus the 'observed' phase of dp is 180^{o} out of phase with that of the pressure change taking place in the active irradiated volume of discharge. All data presented below have the phase of the observed dp signal corrected by

adding a factor of π radians. Some information involving the true nature of the detailed phase relationships between the perturbing field dI and dp and di is of course lost by the above procedure of synchronising all three signals. The graphs presented below show only maximised dc outputs obtained by tuning the phase shift amplifier (always by an amount $<30^{o}$), before each reading. Care was exercised in determining the phase difference between di and dp, however, and it was possible to measure phase differences between both to less than $\pm$ 15^{o}.

There is a time delay between the effect of the perturbing field on the active medium and its detection at the capacitance manometer head. Assuming the gas density fluctuation to travel from the interaction region to the capacitance head at the speed of sound V_s, it will require a time τ_s. If the distance from the interaction region to the detection head is d then

$$\tau_s = \frac{d}{V_s}$$

For 10 torr of CO_2 at 300^{o}K, $V_s \simeq 2.7 \times 10^4$ cm.s^{-1}.
The maximum and minimum distances of the interaction volume from the detection head are d_{max} = 110 cm and d_{min} = 20 cm respectively (points X and X^1 in Fig. 4.1).
Hence $\tau_s^{max} \approx$ 4.0 ms, and $\tau_s^{min} \approx$ 0.8 ms, giving a delay of about 3.2 ms between the two signals. The capacitance head will effectively measure a decaying pressure fluctuation for approximately 3.2 ms following the switch-off of the perturbing field. For perturbation frequencies of greater than 300 Hz (τ = 3.2 ms), there will be a complex sequence of pressure changes interfering

constructively or destructively from point to point along the cell axis according to their phase relationship; however in all experiments described here the perturbation frequencies were generally below about 30 Hz.

5. EXPERIMENTAL RESULTS ON CURRENT AND PRESSURE FLUCTUATIONS

This chapter discusses the behaviour of the current fluctuations $\frac{di}{i}$ and pressure fluctuations $\frac{dp}{p}$ in the absorption cell as the incident 10.6μm laser radiation is modulated at a frequency f $(= \frac{1}{\tau})$. In sections 5.1 and 5.2 the effects of variation of f and incident modulated power I on $\frac{di}{i}$ and $\frac{dp}{p}$ are examined. In section 5.3 the quantitative connection between the pressure fluctuation with constant voltage applied across the absorption cell $(\frac{dp}{p})_{cv}$ and the pressure fluctuation with constant current through the cell $(\frac{dp}{p})_{cc}$ is established. In section 5.4 a dependence between $(\frac{dp}{p})_{cc}$ and the gain or absorption condition of the cell is established. Section 5.5 shows that $\frac{di}{i}$ and $(\frac{dp}{p})_{cv}$ behave similarly with discharge current and finally in 5.6 the quantitative relationship between $\frac{di}{i}$, $\frac{dp}{p}$ and $\frac{dX}{X}$ is examined.

5.1 Variation of $\frac{dp}{p}$ and $\frac{di}{i}$ with perturbation frequency

In order to explain the behaviour of $\frac{dp}{p}$ and $\frac{di}{i}$ with chopping frequency f, it is necessary to consider the relaxation rates from the upper and lower laser levels. If the active medium is perturbed at values of $\tau (= \frac{1}{f})$ which are of the same order as the relaxation times of the 001 or 100 levels, then it is reasonable to suppose that the response of the system will be altered from that where the relaxation times are very much shorter than the period of the perturbation field. For example it is possible (see Table 3) to have relaxation times of the primary laser levels of up to 1 ms. If the perturbation frequency f is 500Hz (τ = 2 ms) the pressure and current

perturbations will depend in magnitude upon the population difference - between the upper and lower laser levels - which has had time to re-establish itself during the off period ($\frac{\tau}{2}$ = 1 ms) of the perturbing field. In this case 1 ms is much less than the total time required for the system to achieve equilibrium by V-V and V-T exchanges.

TABLE 3

Gas mixture	Value of τ(ms) at which $\frac{dp}{p}$ and $\frac{di}{i}$ are half-maximum		Calculated collisional (ms) relaxation times	
	$\frac{dp}{p}$	$\frac{di}{i}$	001→000	100→000
CO_2:CO, 1:9	15	10	10	5
CO_2:N_2:He, 1:1:8	$\lesssim$ 2	$\lesssim$ 2	1	< 0.1
CO_2:N_2:He:H_2, 1:1:7.75:0.25	$\lesssim$ 5	$\lesssim$ 2	0.5	< 0.05
CO_2:N_2:He:Xe, 1:1:7:1	$\lesssim$ 3	$\lesssim$ 7	1	< 0.1

Data in fig. 5.1 were obtained at 10 mA discharge current (voltage controlled mode) and 11 watts cw input pump power (I); total cold fill gas pressure was 10 torr. Maximum errors in the measurement of $\frac{dp}{p}$ were 10% arising at frequencies of about 100 Hz - this was a signal to noise limitation. The error in the frequency calibration of the MDC transducer was 20% (manufacturers quotation), hence the total error in $\frac{dp}{p}$ is approximately 30% above a perturbation frequency of 100 Hz. The values in Table 3 were obtained by assuming about 90% dissociation of CO_2 and ignoring the effects of the partial pressure of O_2 formed by associative reactions. The half-maximum values obtained for $\frac{dp}{p}$ were in active media containing

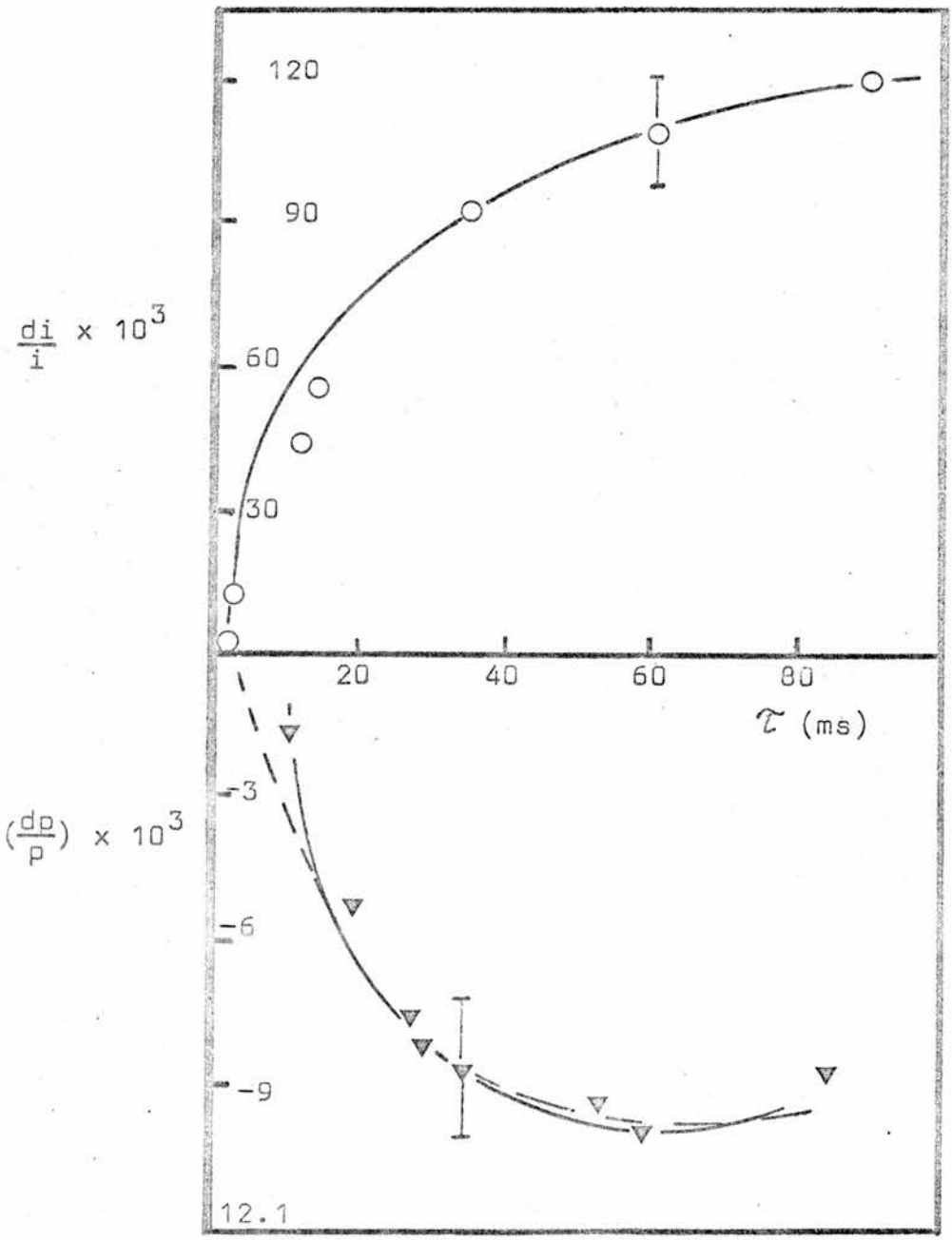

Fig 5.1

Variation of $\frac{dp}{p}$ and $\frac{di}{i}$ with τ.
10 torr CO_2; 10 mA (cv); I = 11 watts
- - - - Curve with transducer frequency response correction.

a total cold fill of 10 torr of gas running at a discharge current of 10 mA.

Response curves for the variation of $\frac{dp}{p}$ and $\frac{di}{i}$ with f are shown in fig. 5.1 for an active medium containing a 10 torr cold fill of CO_2, and it can be seen that the $\frac{dp}{p}$ value is about half-maximum at a τ of 15 ms. Similar curves were obtained for other gas mixtures used and the results are shown in Table 3. All mixtures had a total cold fill pressure of 10 torr. Due to the limited frequency response of the MDC pressure transducer there is a correction required for the values of $\frac{dp}{p}$ shown in fig. 5.1; this is indicated by the dotted curve. There is reasonable agreement between the laser level total relaxation times and the $\frac{\tau}{2}$ values (= on time of laser field) at which the $\frac{dp}{p}$ and $\frac{di}{i}$ signals become half-maximum. Thus it is necessary to place an upper limit on the perturbation frequencies suitable for analysis of various molecular systems such that the transient effects of the 001 and 100 lifetimes on the pressure and current fluctuations were reduced to a minimum. An approximate calculation showed that the pressure perturbations were of the expected order of magnitude. In a CO_2 discharge approximately one watt of power was observed to be absorbed from the laser beam which resulted in gas heating. The estimated temperature rise with this input power was between 2 and $10^{o}K$ for values of τ between 10 and 60 ms. Assuming a gas kinetic temperature of $700^{o}K$, this gives pressure changes of around 0.03 to 0.1 torr which are similar in magnitude to those observed in the cv discharge mode shown in fig. 5.1.

5.2 Dependence of $\frac{dp}{p}$ and $\frac{di}{i}$ on radiation field intensity I

The variation in behaviour of $\frac{dp}{p}$ in cc and cv controlled modes and $\frac{di}{i}$ in the cv mode at a given current setting was investigated as the input power of the perturbing radiation field was altered. This was achieved by altering the current to the CO_2 laser so obtaining a continuously variable cw output power in the range 0 to 15 watts. As the results indicate (see figs. 5.2 and 5.3 and figs. A1 - A4 in Appendix A.1) there is a linear dependence of $\frac{di}{i}$ and $\frac{dp}{p}$, in both cc and cv modes, on the laser input power I. This is particularly true near the peak of all $\frac{dp}{p}$ versus i curves (see section 5.4) and at currents of 35 mA where one would expect some evidence of saturation effects since the medium is excited by currents which are higher than those required for optimum pumping of the 001 level. This fact - together with data presented in Appendix A.1 - would indicate that the saturation parameter for these particular gas systems was in excess of 100 watts cm^{-2}.

The net rate of stimulated emission and absorption occurring in the active medium is given by:

$$(N_i - N_l)B_{il}\rho_{il} \quad s^{-1} \qquad \ldots\ldots\ldots\ldots\ldots\ldots \quad 5.1$$

Where N_i = population density of upper laser level

N_l = " " " lower " "

B_{il} = probability per unit time of a stimulated transition between levels i and l

ρ_{il} = density of radiation field of frequency ν_{il}

If $\frac{dp}{p}$ depends on the actual number of transitions per unit time taking place, it will consequently depend linearly on the radiation field density ρ_{il}. Second order effects on $\frac{dp}{p}$

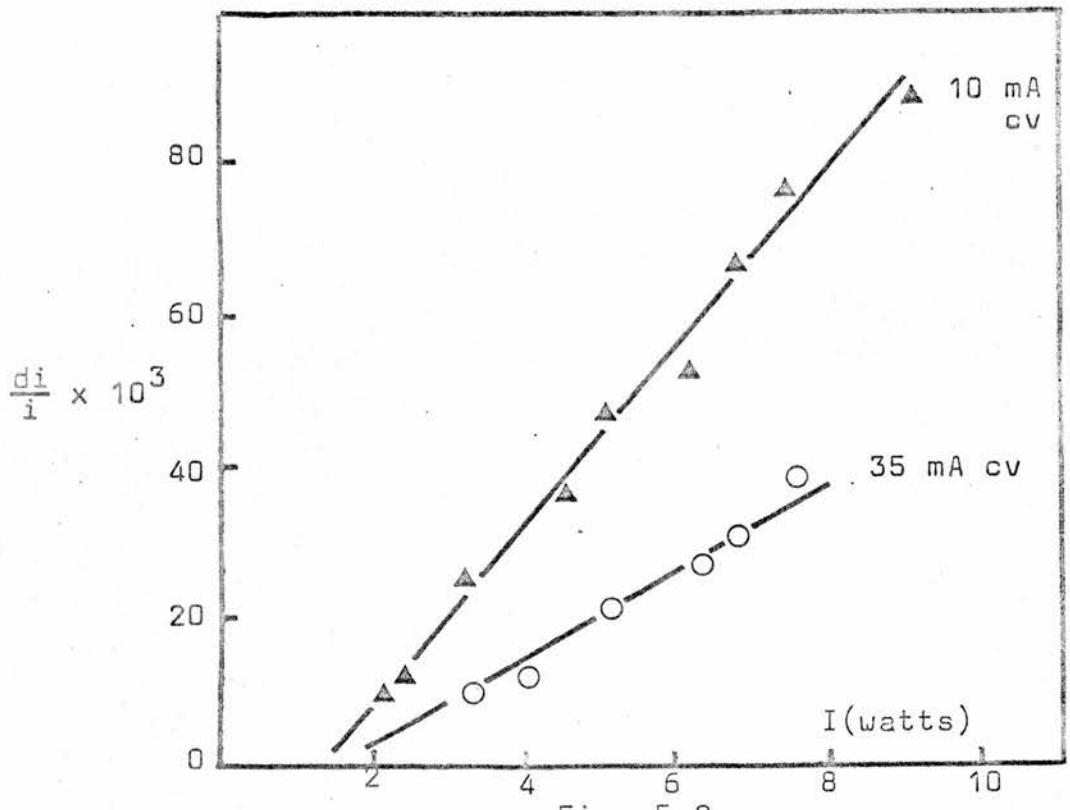

Fig. 5.2

Variation of $\frac{di}{i}$ with I. 10 torr CO_2; τ = 35 ms.

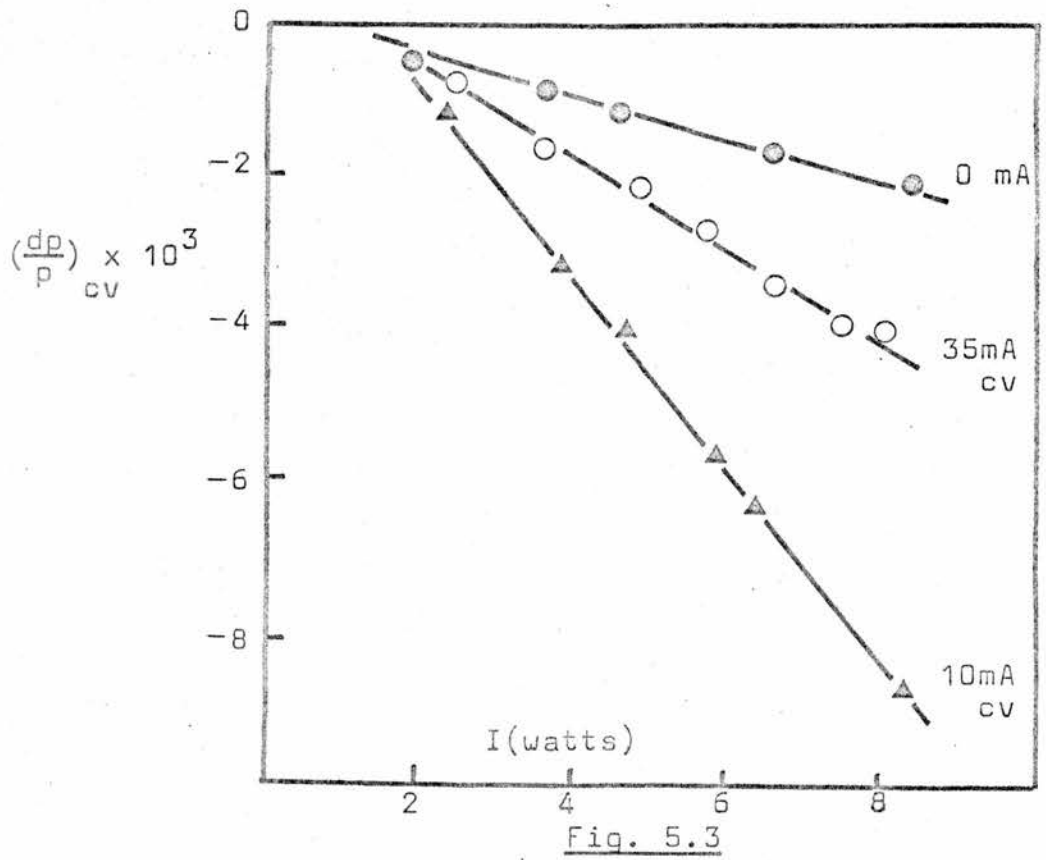

Fig. 5.3

Variation of $\frac{dp}{p}$ with I. (Data for 10mAcc is the same as data at 35mAcv to within experimental error.
10 torr CO_2; τ = 35 ms.

when the discharge was running in cv or cc controlled modes were not observed.

Lobov et al (22) give the following expression for the radiation field induced variation in X, in a dc excited CO_2 gas discharge:

$$\dot{X}(j\Omega) = \frac{-\alpha(\lambda)\dot{\Pi}}{\hbar\omega n_e \nu_e u_e} \cdot \left[\frac{\bar{U}_2}{1+j\Omega\tau_2} - \frac{\bar{U}_1}{1+j\Omega\tau_1} \right] \quad \ldots 5.2$$

Where ω = frequency of irradiating field

n_e = electron density in the discharge

ν_e = electron collision frequency

u_e = average electron energy

$\bar{U}_1, \bar{U}_2$ = average energy supplied to an electron during one transition event (721 cm^{-1} and 2342 cm^{-1} respectively).

Evidently the quantity X will depend linearly on the amplitude of the harmonically varying 10.6μm field $\dot{\Pi}$ for a given value of $\alpha(\lambda)$. If the above experimental results are used in conjunction with equation 3.11, then a linear dependence of both $\frac{di}{i}$ and $\frac{dp}{p}$ on laser input power I implies a similar dependence of $\frac{dX}{X}$ on I.

5.3 Relationship between $(\frac{dp}{p})_{cv}$ and $(\frac{dp}{p})_{cc}$

It may be seen from figs. 5.4 and 5.5 that there is a considerable difference between the quantities $(\frac{dp}{p})_{cv}$ and $(\frac{dp}{p})_{cc}$ for CO_2 and for the 1-1-8 gas mixture (see also figs. 5.10, 5.11 in section 5.4 for other gas mixtures used). It is believed that this is due to large second order gas heating effects produced by radiation induced current changes which are present in the voltage controlled mode but eliminated in the current controlled mode. As a discharge operated in a voltage controlled mode is irradiated the discharge current

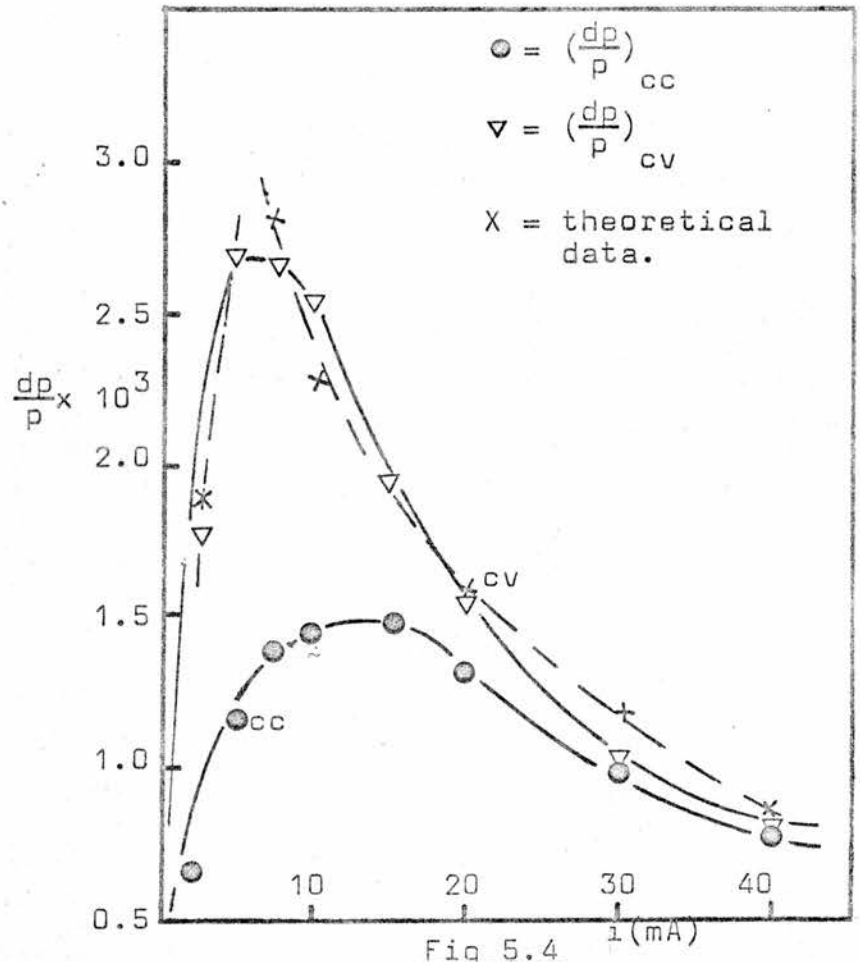

Fig 5.4

Variation of $\frac{dp}{p}$ with i. I = 13.0 watts; 1-1-8, CO_2:N_2 P: He at 10 torr. τ = 35ms.

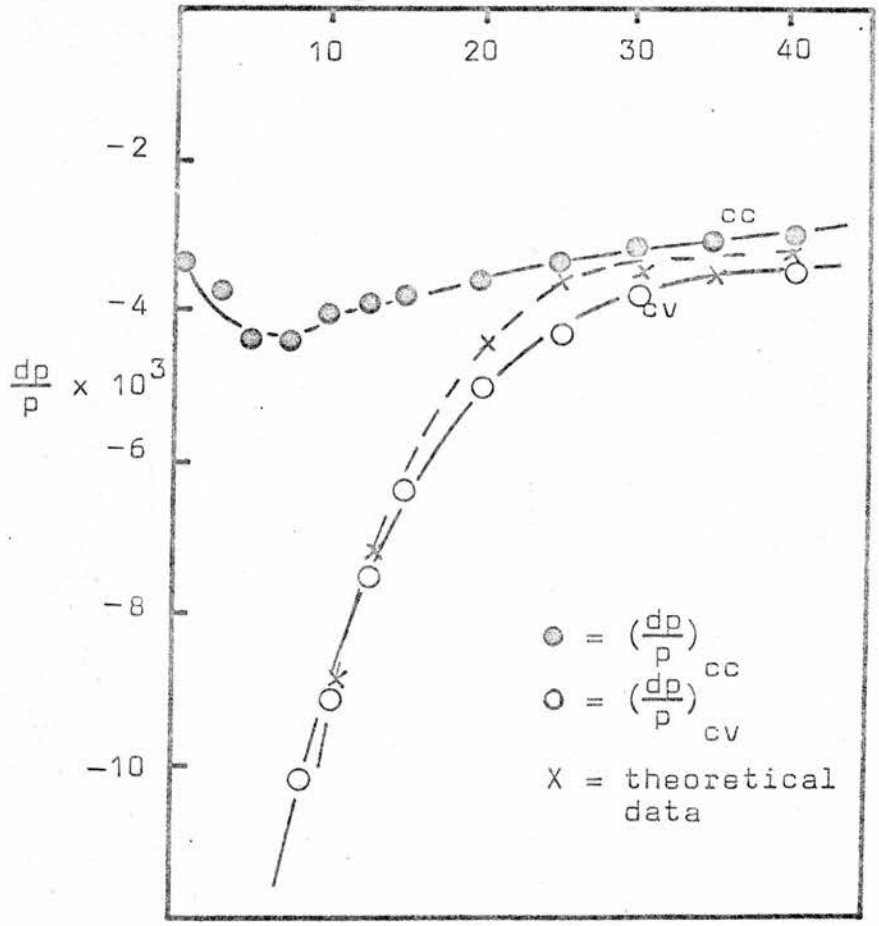

Fig. 5.5

Variation of $\frac{dp}{p}$ with i. I = 8.5 watts; 10 torr CO_2; τ = 35 ms.

is changed and so its heating effect on the gas molecules will be altered and hence there will be a current induced gas pressure change. Thus the effect of irradiating, for example, a pure CO_2 discharge will result in a gas pressure change due to:

(i) gas heating due to absorption of radiation and finally V-T energy transfer processes.

(ii) gas heating due to an increase in current through the discharge when its impedance is lowered.

If we assume the gas pressure in the active irradiated volume to be described by a function of two variables, i.e.

$p = p\ (I,i)$, where

I = intensity of perturbing radiation

i = discharge current,

and then take increments:

$$dp = \left(\frac{\partial p}{\partial I}\right)_i dI + \left(\frac{\partial p}{\partial i}\right)_I di \qquad \ldots\ldots\ldots 5.3$$

$$\text{hence } \frac{dp}{p} = \frac{1}{p}\left(\frac{\partial p}{\partial i}\right)_I di + \frac{1}{p}\left(\frac{\partial p}{\partial I}\right)_i dI \qquad \ldots\ldots\ldots 5.4$$

The normalised pressure change measured in the voltage controlled mode where $di \neq 0$ is thus described by the full expression in 5.4 above. In the current controlled mode, however, $di = 0$ and,

$$\left(\frac{dp}{p}\right)_{cc} = \frac{1}{p}\left(\frac{\partial p}{\partial I}\right)_i dI \qquad \ldots\ldots\ldots 5.5$$

$$\text{Hence } \left(\frac{dp}{p}\right)_{cv} = \left(\frac{dp}{p}\right)_{cc} + \frac{1}{p}\left(\frac{\partial p}{\partial i}\right) di \qquad \ldots\ldots\ldots 5.6$$

The term $\frac{1}{p}\left(\frac{\partial p}{\partial i}\right)_I di$ can be determined from a graph of the static characteristic p versus i - giving p and $\left(\frac{\partial p}{\partial i}\right)_I$ - and a knowledge of di versus i. The quantity $\left(\frac{dp}{p}\right)_{cc}$ may also be measured and hence the value of the right hand side of equation 5.6 determined.

The total pressure change in a CO_2 gas discharge due to an increase in current is a result of gas heating and dissociation of CO_2. In determining the variation of p with i it was observed that the output from the MDC monitoring p displayed two time constants when reaching equilibrium at each current setting. The first was of about 5 seconds duration and represented the new pressure equilibrium between gas in the positive column and gas occupying the dead space volume. The second change in p of about 10 minutes duration was only 10% or less of the first transient in magnitude. It was thought to be due to thermal diffusion of hot gas from the cathode bulb into the remainder of the system. The current results, di, and pressure results, p and dp, were recorded over a period of two to three minutes after each new current setting, during which time thermal diffusion was taking place. Hence there was an additional uncertainty in the magnitude of the measured parameters di and dp as both were functions of the pressure in the irradiated active volume. Results were normally averaged over a series of experimental runs and were reproducible to within 15% accuracy. The theoretical values obtained from equation 5.6 for $(\frac{dp}{p})_{cv}$ are shown (x) in figs. 5.4 and 5.5 and agree with the measured values of $(\frac{dp}{p})_{cv}$ to within the stated experimental accuracy.

Thus we may conclude that the $(\frac{dp}{p})_{cc}$ curves represent the direct effect of the incident modulated radiation field, and the larger amplitude $(\frac{dp}{p})_{cv}$ curves are due to gas heating effects brought about by large current perturbations. This effect may be represented by a movement of the discharge operating point along the p - i static characteristic.

5.4 Pressure Variations in the current controlled mode

By eliminating any current changes taking place in the active irradiated volume, no gas heating due to the current feedback effect can take place, and the $(\frac{dp}{p})_{cc}$ curves for all gas mixtures show a pronounced maximum. To consider the way in which the pressure change is brought about by the radiation field perturbing two specific energy levels, some knowledge of the variation in population of these levels with discharge current is necessary. The number of induced transitions (either by stimulated emission or absorption) is proportional to the difference in number density of molecules in the upper and lower states of such a transition, and the generation of a pressure change is due to heating or cooling of the discharge by V - T processes from both the upper and lower levels. In a gain situation only the upper level contributes to the long term (>1 ms) cooling effect, and in absorption again it is the upper level which causes the long term gas heating. First consider the gain situation. Maximum cooling of the gas due to minimum V - T energy transfer from the depleted 001 level will occur when the population inversion (or gain coefficient $\alpha(\lambda)$) is a maximum. The induced pressure changes should therefore exhibit similar qualitative variation with discharge current as the gain for that medium. The gain properties of the present gas systems have not been examined but it is possible to obtain compatible data from references (32), (33), (34), (35) and (36). The results concerning pressure perturbations in individual gas systems are now discussed.

(a) 1-1-8 mixture of CO_2 : N_2 : He

The variation of $(\frac{dp}{p})_{cc}$ in the current controlled mode in a 1-1-8 CO_2: N_2 : He mixture - cold fill 10 torr - is shown in fig. 5.6. The position of the maximum pressure perturbation at 12 mA and the shape of the curve compare well with the gain versus current curve one would expect such a medium to possess. From (32) the gain at 40 mA is about 50% less than the maximum at 10 mA in 9 torr of CO_2 : He (3:6) in a 12 mm bore sealed tube; it is not expected that the presence of N_2 in quantities similar to those used in the present three part mix would significantly alter the gain curve. The observed decrease in $(\frac{dp}{p})_{cc}$ is 50% between 10 mA and 40 mA. It is worth noting that this active medium (1-1-8) shows a transition from gain to absorption in the region of 1 mA. At zero current $(\frac{dp}{p})_{cc}$ has a value of $- 0.9 \times 10^{-3}$ and upon switching on the discharge the pressure perturbation signal is observed to change in phase by 180^{o}.

Fig. 5.8 shows the variation in observed spontaneous sidelight from the 001 to 000 transition at 4.3μm. Points below the current axis represent a reduction in intensity of the phase lock signal at 4.3μm as the medium is irradiated. The peak (i.e. maximum reduction of 4.3μm intensity) occurs at currents coinciding with the peak in $(\frac{dp}{p})_{cc}$ and in gain. Again the transition between gain and absorption can readily be observed as the discharge current is switched off, and the point above the axis at zero current represents the enhancement of the 4.3μm spontaneous emission due to direct pumping of the 001 level by the irradiating field.

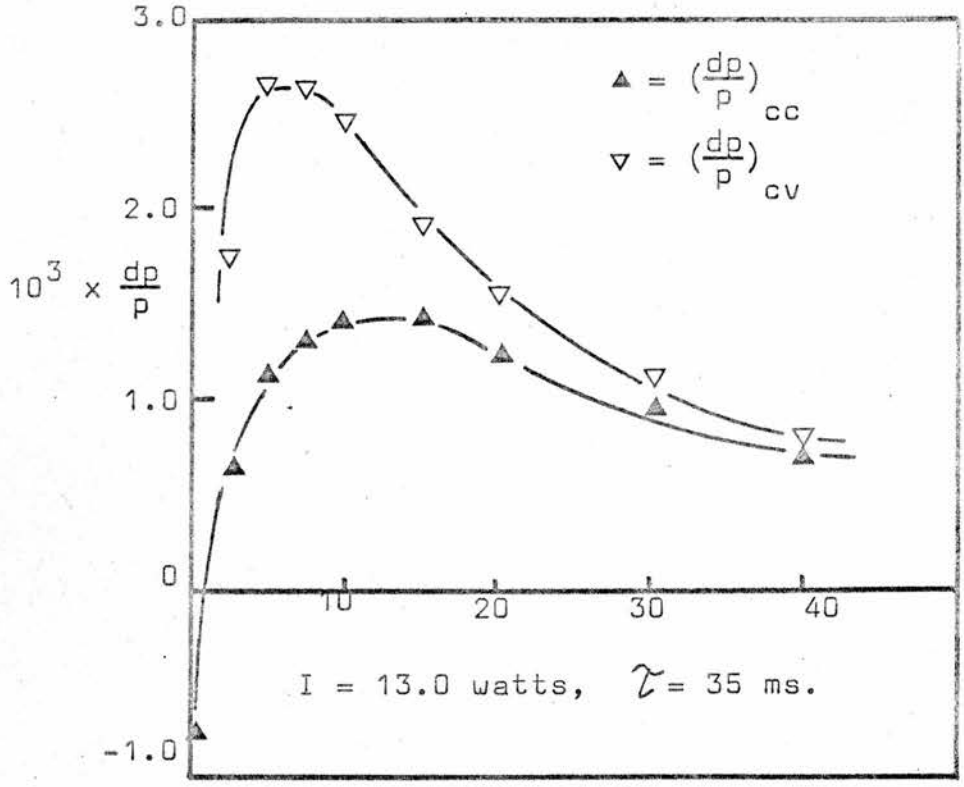

Fig. 5.6

Variation of $\frac{dp}{p}$ with i
1-1-8, CO_2 : N_2 : He at 10 torr.

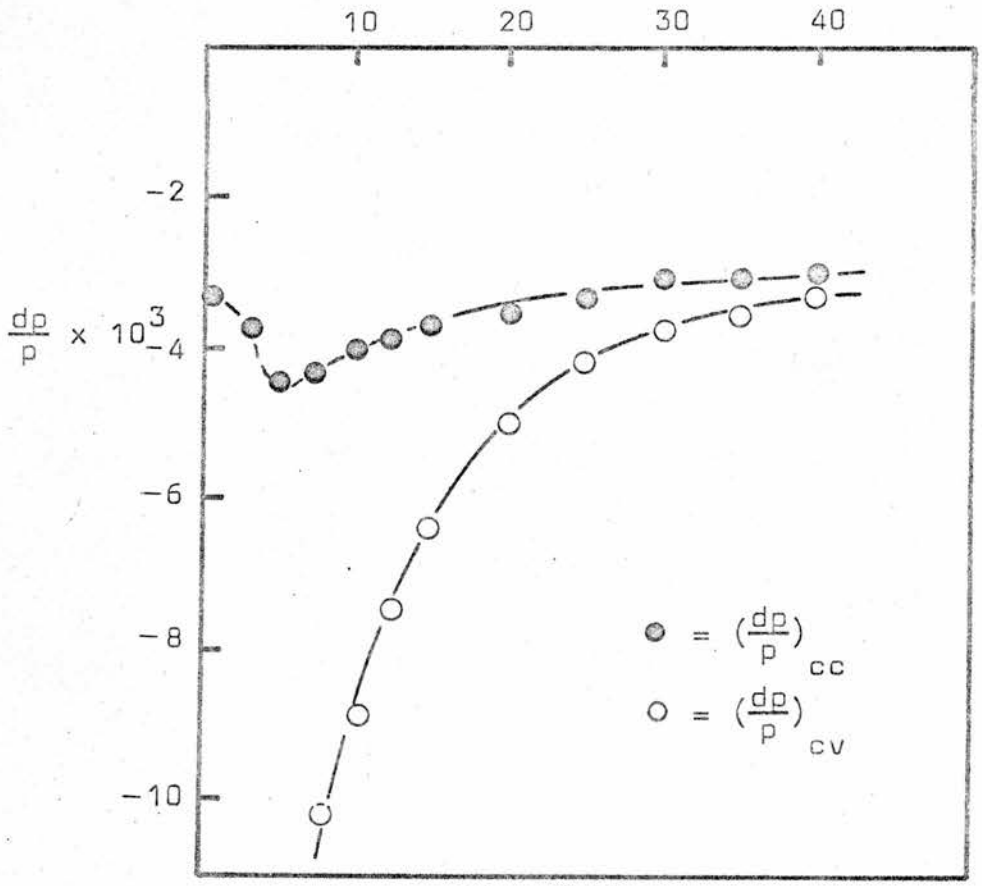

Fig. 5.7

Variation of $\frac{dp}{p}$ with i. I = 8.5 watts;
10 torr CO_2, τ = 35 ms.

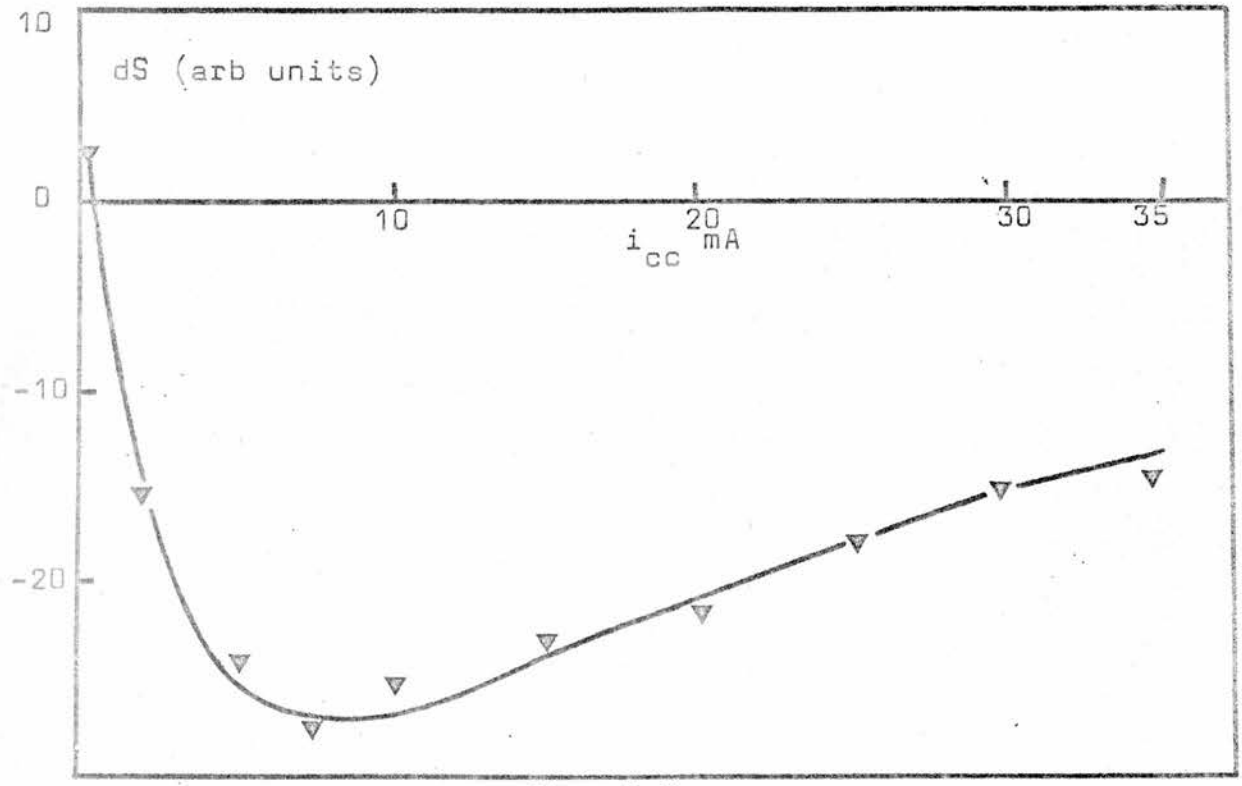

Fig. 5.8

Variation of spontaneous emission at 4.3μm (dS)
CO_2 (001 - 000), with i.
I = 13.0 watts; 1:1:8, CO_2 : N_2 : He; τ = 35 ms.

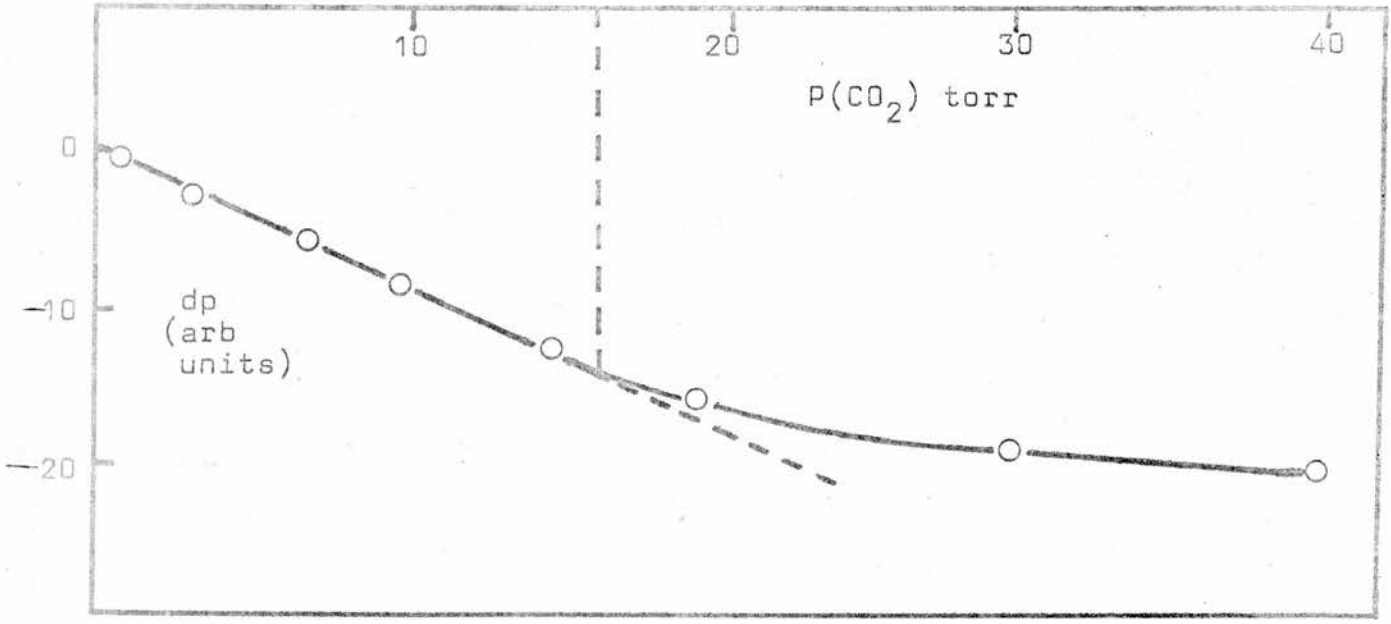

Fig. 5.9

Variation of dp with CO_2 pressure.
I = 8.5 watts; i = 0 mA; τ = 35 ms.

(b) Pure CO_2

From reference (34) it can be seen that at a total CO_2 pressure in excess of about 2 torr, a flowing system of pure CO_2 exhibits absorption. This is attributed to the low pumping rate of the 001 level by collisional transfer with CO (V=n) states and also the high gas temperature (leading to enhanced collisional de-excitation of the 001 level and high thermal population of the 100 level) because of the low thermal conductivity of CO_2. The work of McQuillan et al indicates that in a sealed system containing progressively greater pressures of CO_2 (>1 torr), the gain becomes less, and above 3 torr where the CO partial pressure can be expected to be high, there is no gain for currents above 10 mA. In the present system containing a cold fill of 10 torr of CO_2 observation of the amplifier sidelight at 4.3μm due to spontaneous emission from the 001$\rightarrow$ 000 transition, shows that the upper laser level was being pumped by the 10.6μm irradiating field at all discharge currents. It was not possible to determine the quantitative (as in fig. 5.8) variation in magnitude of the modulated 4.3μm sidelight with discharge current, due to adverse signal to noise. The $(\frac{dp}{p})_{cc}$ versus current curve in fig. 5.7 shows a well defined peak in the region of 5 mA; there was a decrease in pressure in the active discharge region at all currents and no evidence of a switch in polarity of the pressure perturbation.

The gas absorption coefficient $\alpha(\lambda)$ is defined by:

$$\alpha(\lambda) = - C \left(N_u - \frac{g_u}{g_l} N_l\right) \qquad \ldots\ldots\ldots 5.7$$

The expression shows that $\alpha(\lambda)$ is proportional to the population difference between the 001 and 100 levels. We would expect higher values of $\alpha(\lambda)$ at a fairly low gas temperature (i.e. low discharge currents) on the evidence of the following argument. Assuming excitation of the ground electronic state vibrational levels of CO_2 only (we neglect the processes of direct electron impact excitation) the following ratios of number densities are to be expected for gas temperatures T_1 and T_2:

$$T_1 = 273^{o}K; \quad \frac{N_{100} + N_{020}}{N_{001}} \approx 3.44 \times 10^2$$

$$T_2 = 400^{o}K; \quad \frac{N_{100} + N_{020}}{N_{001}} \approx 0.7 \times 10^2$$

It appears that the population ratio is reduced by any increase in gas temperature hence $\alpha(\lambda)$ will always decrease as the current (and hence T) increases. The experimental data for $\left(\frac{dp}{p}\right)_{cc}$ in a pure CO_2 discharge (fig. 5.7) show its absolute magnitude to be a slowly decreasing function of current between 10 and 40 mA. However there is a pronounced maximum below 10 mA. This is attributed to the effect of optimum electron pumping of CO_2 ground state levels on the low current behaviour of $\alpha(\lambda)$ and hence $\left(\frac{dp}{p}\right)_{cc}$.

The variation in pressure perturbation as a function of the total (pure) CO_2 pressure with no discharge current flowing is shown in fig. 5.9. It is approximately linear with CO_2 pressure up to 18 torr at which point the curve levels off to a plateau. This is because the absorption

coefficient for an inhomogeneously or Doppler broadened transition $\alpha(\lambda)$ is given by:

$$\alpha(\lambda) = -\frac{1}{8\pi}\left[\frac{\lambda_o^3}{c\tau_r}\left(\frac{Mc^2}{2\pi kT}\right)^{\frac{1}{2}}\right]\left[\left(N_u - \frac{g_u}{g_1}N_1\right)\right] \quad \ldots.5.8$$

Where τ_r = radiative lifetime of the vibrational rotational transition

k = Boltzmann's constant

T = gas temperature

N_u and N_1 are the 001 and 100 populations and g_u and g_1 their respective degeneracies.

In a collision or homogeneously broadened case:

$$\alpha(\lambda) = \frac{1}{8\pi}\left[\frac{\lambda_o^3}{\tau_r \nu_c}\right]\left[\left(N_u - \frac{g_u}{g_1}N_1\right)\right] \quad \ldots\ldots 5.9$$

Where ν_c is the molecular collision frequency.

In the Doppler broadened case $\alpha(\lambda)$, and hence dp, is proportional to the total CO_2 pressure. However, in the collision broadened case ν_c is also proportional to CO_2 pressure and hence $\alpha(\lambda)$ is now independent of the total gas pressure. Evidently the transition from Doppler to collision broadening takes place in the region of 18 torr. This is in reasonable agreement with reference (37).

(c) <u>1-1-0.25-7.75; CO_2: N_2 : H_2 : He</u>

From the basic 10 torr three part mix containing CO_2, N_2 and He, 0.25 torr of helium was substituted with the same partial pressure of hydrogen. There are two important roles which hydrogen can play. It can efficiently de-excite the 010 level as well as the mixed states (100,020) leading to enhanced population inversion. Hydrogen is also responsible for reducing the dissociation of CO_2 in a sealed device; the addition of small amounts may decrease the percentage dissociation by over half leading to a greatly enhanced power

output, (31). It may be seen that in fig. 5.10 the qualitative behaviour of $(\frac{dp}{p})_{cc}$ with current is very similar to that in the 1-1-8 mix, however the maximum value is about 0.8×10^{-3} in the hydrogen mix which is about half the maximum value in the 1-1-8 mix.

The addition of 0.25 torr of hydrogen will reduce the dissociation of CO_2 from over 80% to below 40%. Hence in the present system with a 1-1-8 mix containing a cold fill partial pressure of 1 torr of CO_2, there will be less than 0.2 torr of CO_2 in the active discharge region. The addition of hydrogen will maintain the CO_2 pressure at over 0.6 torr under typical discharge conditions, thus effectively increasing the CO_2 partial pressure by approximately a factor of three. From fig. 5.9 it can be seen that the magnitude of dp increases with the pressure of CO_2 in the active medium, and there is a linear dependence between dp and CO_2 pressure up to 18 torr. Increasing the pressure of CO_2 in the gas mixture by a factor of three would lead to an increase in dp by the same factor. The relaxation rate of the upper laser level is increased by a factor of two due to the addition of 0.25 torr of hydrogen as can be seen from Table 3. As a result the population inversion may be adversely affected producing a smaller value for the gain coefficient $\alpha(\lambda)$ and hence for dp. The sum of the two effects has led to the decrease in $(\frac{dp}{p})_{cc}$ in the hydrogen mix by a factor of somewhat less than two. Again it can be seen that the medium exhibits the transition from absorption to gain at about 1 mA.

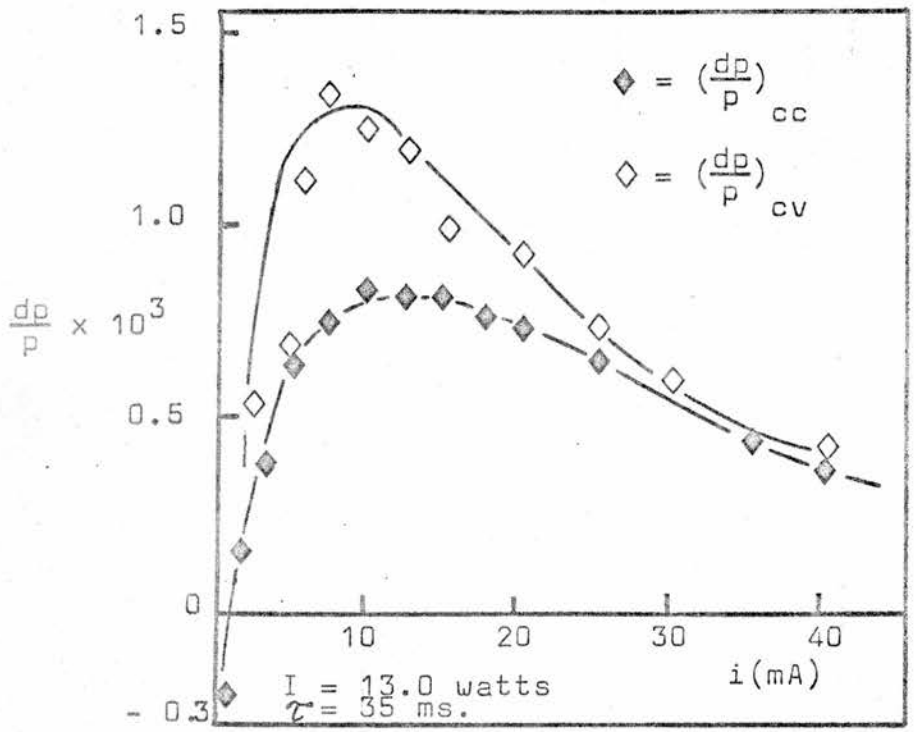

Fig. 5.10

Variation of $\frac{dp}{p}$ with i.

1:1:0.25:7.75, CO_2 : N_2 : H_2 : He.

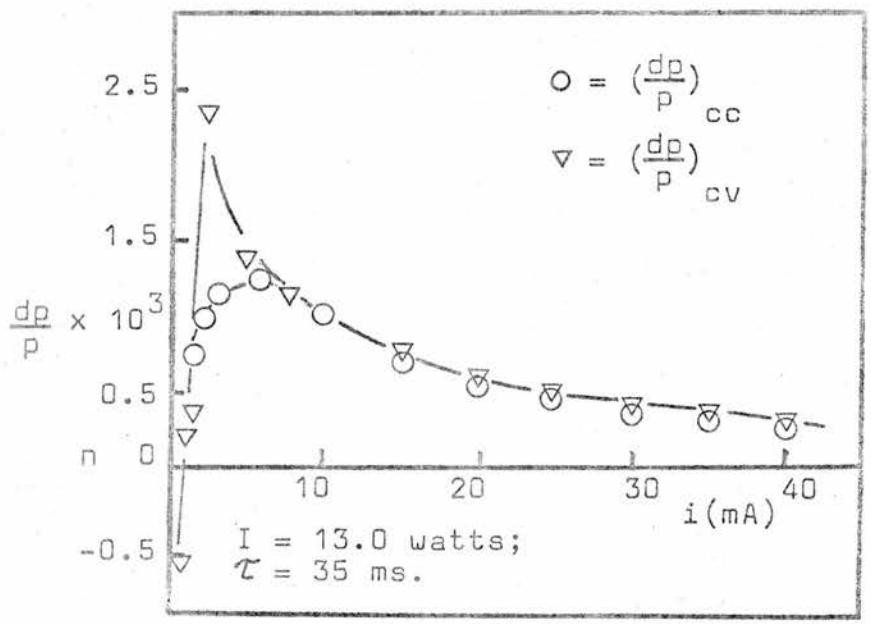

Fig. 5.11

Variation of $\frac{dp}{p}$ with i.

1:1:1:7, CO_2 : N_2 : Xe : He.

(d) 1-1-1-7 CO_2 : N_2 : Xe:He mix

It is known that the addition of xenon to the basic three part laser mixture will increase the conversion efficiency of electrical power to coherent radiation (38). The reasons as given in (39) are as follows:

(i) The number of electrons having the most probable electron energy is increased slightly.

(ii) The number of electrons in the high energy tail of the distribution has been significantly reduced.

(iii) The number of low energy electrons is increased.

(iv) The electron temperature is significantly reduced.

Because of the increase in number density of low energy electrons the pumping of the vibrational levels participating indirectly in laser action is enhanced (40). No information is available on the gain curves for a laser mix containing xenon, although it appears that devices using this additive achieve maximum power output at higher currents than with a three part CO_2, N_2, He mixture.

In view of this fact it is surprising that the peak of $(\frac{dp}{p})_{cc}$ curve - fig. 5.11 - in the xenon mix used in the present experiments occurs at a lower current than that of the CO_2, N_2, He mix. In other respects the curves for the above two mixtures are comparable in magnitude, although that for the xenon mix is more sharply peaked at a lower current than that for the 1-1-8 mix.

5.5 The variation of $(\frac{di}{i})$ with discharge current

Using the experimental arrangement shown in fig. 4.3 the behaviour of $(\frac{di}{i})$ with discharge current in the four gas mixtures of interest was determined. The results are shown in figs. 5.12 to 5.15. All the curves have a similar monotonically decreasing form above 10 mA and it can be seen that the current perturbations are negative in the gas mixtures thought to exhibit gain, and are positive in the case of the absorbing CO_2 medium. The curve for each individual active medium is now discussed in detail.

(a) CO_2

The discharge was found to be unstable below approximately 10 mA but over the 30 mA current range available $(\frac{di}{i})$ was observed to change by about one and a half orders of magnitude. No inversion of the perturbation signal was observed, and the form of the curve is similar to that in fig. 5.7. Quantitative comparisons are made in section 5.6 below. In this gas, especially at currents below 10 mA, it is evident that the electron gas is coupled strongly to the primary laser levels - this will be further discussed below.

(b) The gas mixtures $CO_2 : N_2 : He$; $CO_2 : N_2 : X_e : He$; $CO_2 : N_2 : H_2 : He$.

These curves have the same form as that for CO_2 above 10 mA but at lower currents reach a maximum and, in the case of the hydrogen mix only, become positive. The signal to noise at low currents was poor, reaching around 2 below 5 mA. The $(\frac{di}{i})$ signal in the xenon mixture was the largest in magnitude, exceeding even that obtained in pure CO_2. The form of each of these curves is very similar to that of its $(\frac{dp}{p})_{cv}$ counterpart.

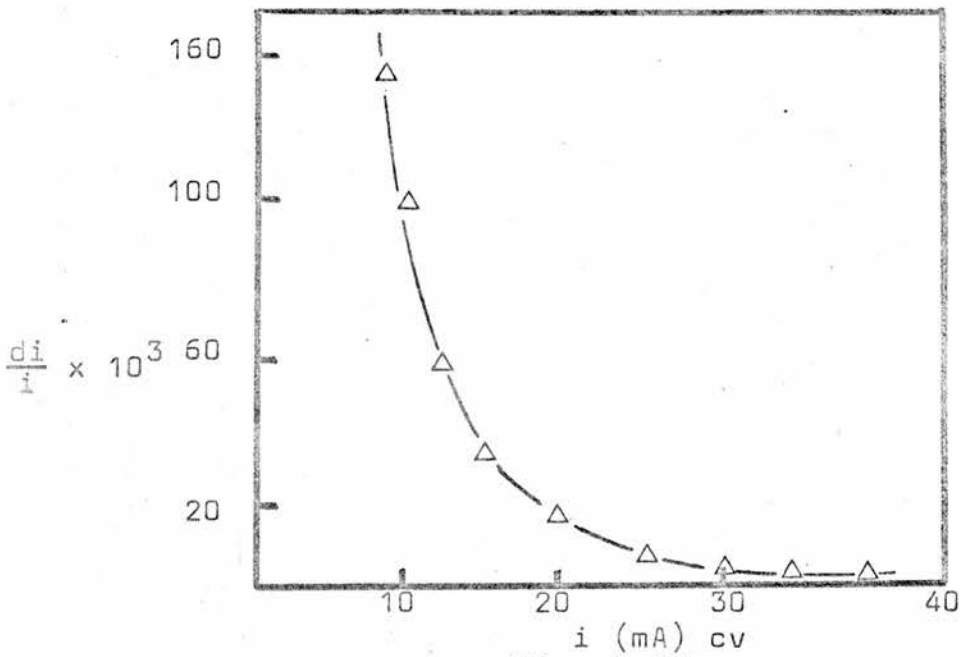

Fig. 5.12

Variation of $\frac{di}{i}$ with i.

I = 11.0 watts; 10 torr CO_2; τ = 35 ms.

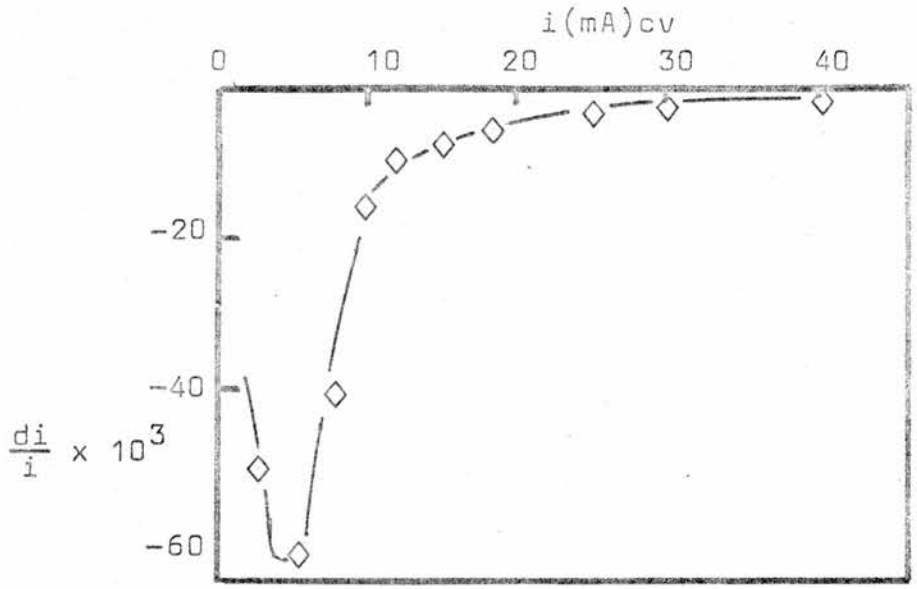

Fig. 5.13

Variation of $\frac{di}{i}$ with i.

I = 13.0 watts; 1:1:8, CO_2 : N_2 : He;
τ = 35 ms.

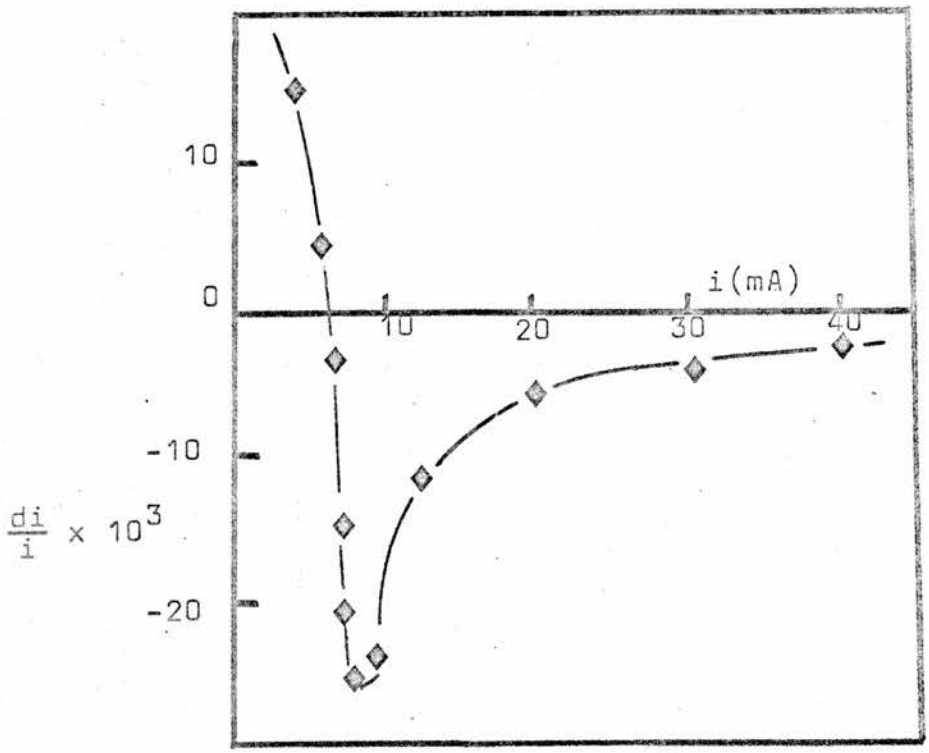

Fig. 5.14

Variation of $\frac{di}{i}$ with i.

I = 13.0 watts; 1:1:0.25:7.75, CO_2 : N_2 : H_2 : He;
τ = 35 ms.

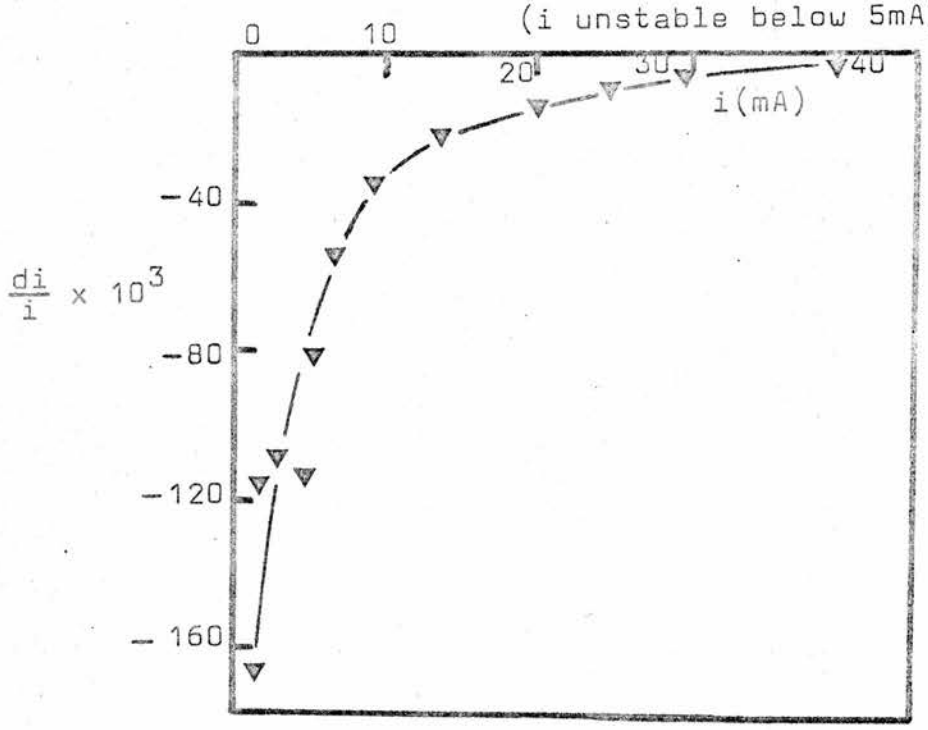

Fig. 5.15

Variation of $\frac{di}{i}$ with i.

I = 13.0 watts; 1:1:1:7, CO_2 : N_2 : Xe : He;
τ = 35 ms.

For example, 5.13 can be compared with 5.6, and so on, the peaks in the current perturbation curves occurring at similar current values to those at which the $(\frac{dp}{p})_{cv}$ peaks occur.

The discharge mixture containing hydrogen was the most stable at very low currents and showed the smallest changes in current perturbation. It is known that trace amounts of hydrogen are beneficial to laser output power using a sealed three part CO_2 : N_2 : He mixture (e.g. Smith and Browne (69)). However, partial pressures above approximately 0.1 torr may have a detrimental effect since they would lead to enhanced depopulation of the upper laser level, although still maintaining a high partial pressure of CO_2 due to back reactions involving hydrogen and carbon monoxide. It would appear that in the hydrogen mixture used for the present experiments the gain was reduced below that for the basic three part mix and that containing Xe as the only additive. Since the magnitude of the pressure variation (and that of the current) is a function of the gain of the medium, then the mix containing hydrogen is exhibiting low gain and hence correspondingly small fluctuations in current and pressure over those observed in pure CO_2 and mixtures with hydrogen absent. The addition of xenon to a CO_2 gas discharge reduces the number of high energy electrons and increases the number of electrons with energies suitable to interact with vibrationally excited molecules. Because of this stronger coupling between the electron gas and the vibrational states of nitrogen, carbon dioxide and carbon monoxide, perturbing these states will induce a larger current

change than in a discharge with xenon absent.

It can be seen that the relative changes in pressure $(\frac{dp}{p})_{cc}$ or $(\frac{dp}{p})_{cv}$ in the helium, hydrogen and xenon mixes are comparable and yet the relative perturbation current changes $(\frac{di}{i})$ differ markedly. It is possible that in the case of the xenon mix an enhanced contribution to the current perturbation via a change in the parameter X takes place. This is not unreasonable in view of the strong coupling between the electron gas and ground electronic vibrational states in the xenon mix. This is discussed further in section 5.6 below.

5.6 Results for $\frac{di}{i}$ and $\frac{dp}{p}$ as a function of discharge current

In the theory presented in section 3.2(c) the following relationship was derived:-

$$\frac{di}{i} = \frac{1}{4}\frac{dX}{X} - \frac{1}{2}\frac{dp}{p} \qquad \text{.....5.10}$$

From the work of Lobov et al (22) the absolute magnitude of the time varying part of X is given by,

$$|\dot{X}| = C(\tau_1, \tau_2, \Omega)\frac{\pi\alpha(\lambda)}{\hbar\omega\nu_e n_e u_e} \qquad \text{.....5.11}$$

It is necessary to differentiate between the interpretations of dX and X in 5.10. $|\dot{X}|$ is directly equivalent to dX since both represent the integrated change in the fractional electron energy loss per collision as a result of perturbing the active medium at 10.6μm. Because the magnitude of the population inversion in any active medium is a function of the discharge current $|\dot{X}|$ is also dependent on the discharge current; it is inversely proportional to n_e, ν_e and u_e all of which are complicated functions of the parameter $\frac{E}{n}$, (41), (42).

The quantity X refers to one specific collision event and depends on the type of particles colliding, their mass, state of excitation and energy. Increasing the discharge current will change $\frac{E}{n}$ resulting in a redistribution of populations in the various excited levels (both electronic and vibrational) and hence an alteration in the average amount of energy exchanged by an electron per collision. Superimposed on this we have a change in the vibrational populations of the lasing levels of CO_2 (and others to which they are collisionally coupled) which results in a further change in X, i.e. the time varying part $|\dot{X}|$ or dX.

It is difficult to determine experimentally or theoretically the exact behaviour of the quantity $\frac{dX}{X}$; however, if we assume $\frac{dX}{X}$ to be small compared with $\frac{dp}{p}$ then $\frac{di}{i}$ will be approximately proportional to $\frac{dp}{p}$. A summary of the results for $(\frac{dp}{p})_{cv}$ and $\frac{di}{i}$ is presented in figs. 5.16 and 5.17 below. The graphs have the same perturbation frequency and input perturbation power. They show a marked departure from linearity at currents below 25 mA in each case. If the quantity $\frac{dX}{X}$ in equation 5.10 were constant (or small in magnitude compared with $(\frac{dp}{p})_{cv}$), then the relationship would have been linear with a slope of -2; however it is evident that some mechanism other than direct pressure fluctuations contributes to the variation in discharge current especially at the lower currents. It has been shown earlier (section 5.3) that gas heating due to an increase in discharge current in an absorbing plasma takes place. Initially the impedance of the discharge is lowered by the laser field resulting in a higher current flow and hence more gas heating.

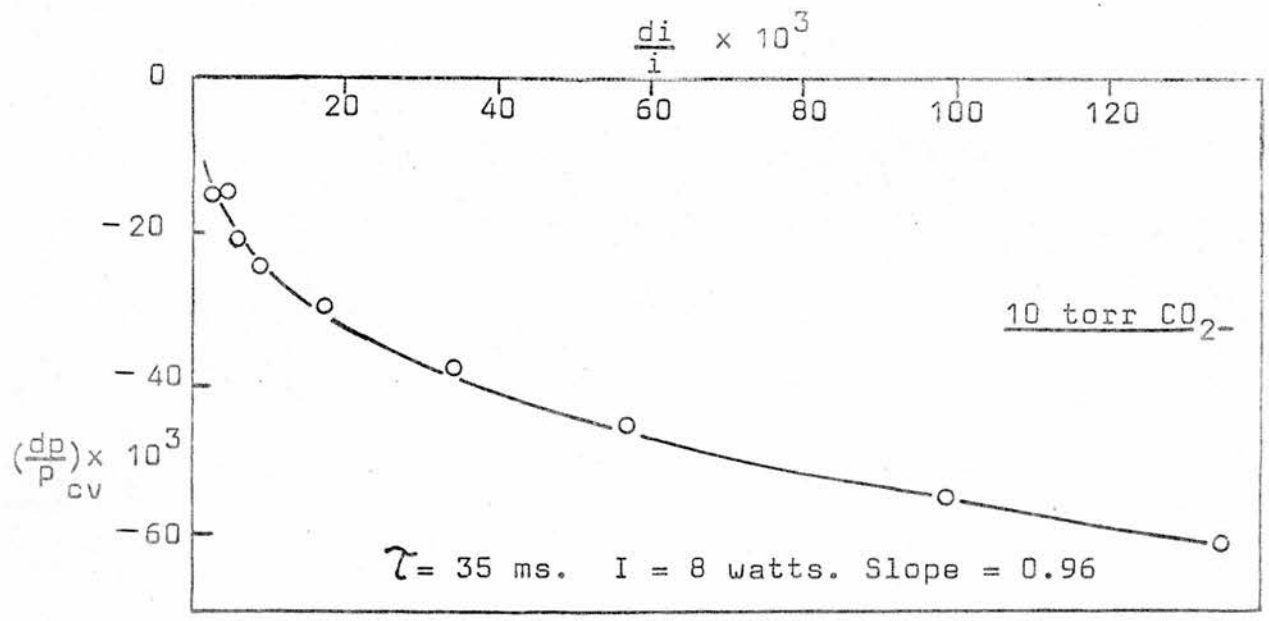

Fig. 5.16

Variation in $(\frac{dp}{p})_{cv}$ with $\frac{di}{i}$ in 10 torr CO_2

($(\frac{dp}{p})_{cv}$ values are corrected as indicated in A.2)

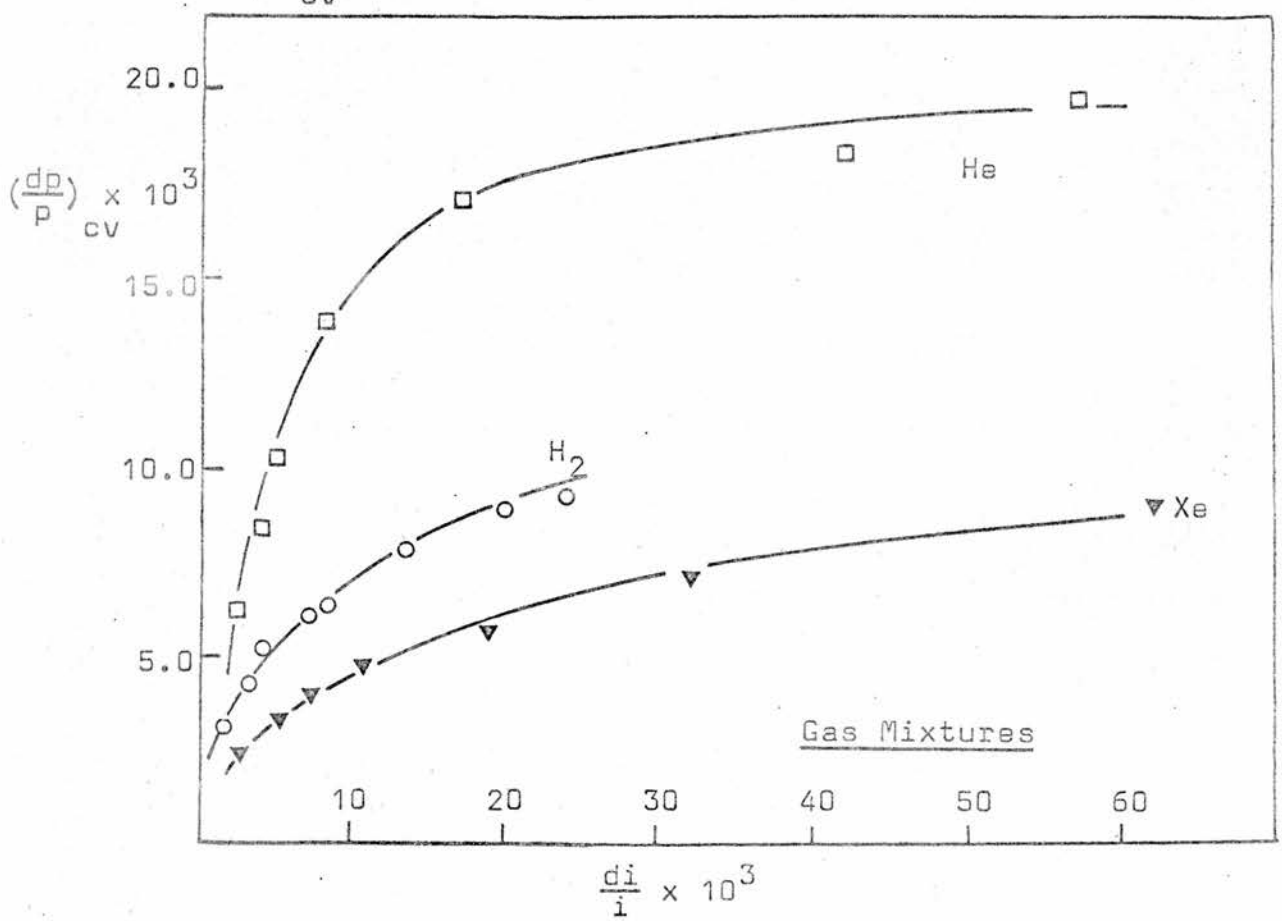

Fig. 5.17

Variation in $(\frac{dp}{p})_{cv}$ with $(\frac{di}{i})$ in the gas mixtures.

($(\frac{dp}{p})_{cv}$ values are corrected as indicated in A.2)

τ = 35 ms; I = 11 watts; Slopes: Xe = 0.3
He = 1.54
H_2 = 0.68

As hot molecules diffuse from the active irradiated volume the discharge impedence is lowered further. The positive feedback effect of the increasing discharge current thus leads to enhanced pressure fluctuations. Furthermore, as was pointed out by Carswell and Wood (8) amplified discharge impedance (and therefore discharge current) changes take place in a molecular plasma because of the following reason. Molecular gas discharges have voltage-current, or impedance-current, characteristics with very high negative slopes in the low current operating regions, see fig 5.18. The lowering of the discharge current by a perturbing radiation field moves the discharge to an operating position on the R_p - i characteristic with a higher impedance causing a further lowering of the discharge current. Thus, at low currents especially, a small radiation induced current change becomes amplified considerably resulting in a large observed value for di; this is the value plotted (as $\frac{di}{i}$) in figs. 5.16, 5.17. A knowledge of the amplification factor of the circuit would enable the true laser induced current perturbation to be calculated. This is not known for the system used in the present experiments. However, Carswell and Wood have measured circuit gains of the order of 10 in a directly perturbed CO_2 laser. The current perturbations measured here are amplified at currents of 10 mA and less and hence the slopes from fig. 5.17 of $\frac{dp}{p}$ versus $\frac{di}{i}$ are smaller than those expected from equation 5.10.

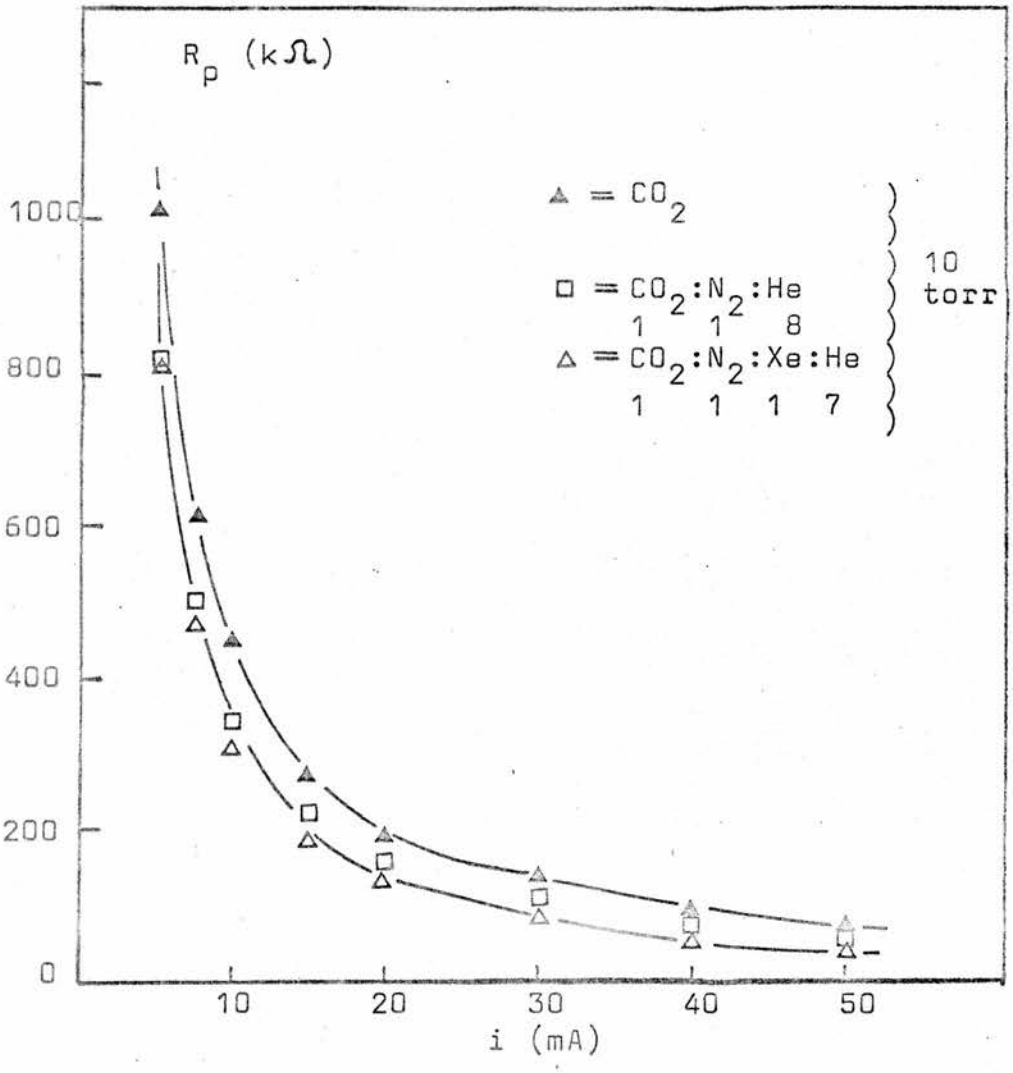

Fig. 5.18

Discharge impedance versus current for various gas mixtures (static characteristics).

5.7 Summary

The series of experiments described above have demonstrated the following concerning pressure and current perturbations in an active CO_2 medium. Pressure perturbations are generated by the 10.6μm radiation field due to molecular V - T transitions. The gas number density increases in the irradiated volume of an active medium in a gain condition when it is perturbed and decreases in that volume of an active medium in an absorption condition when it is perturbed. The magnitude of the pressure and current perturbations is dependent upon the frequency $(\frac{1}{\tau})$ of the perturbing 10.6μm field and drops to half its maximum value when $\frac{\tau}{2}$ approaches the value of the slowest relaxation time of the primary laser levels. Current and pressure perturbations are linearly proportional in magnitude to the intensity of the perturbing field; no evidence of saturation effects was observed in the system under study. Current feedback effects in the voltage controlled discharge mode caused an amplification in the magnitude of the pressure perturbations in both gain and absorption conditions. It was possible to describe the total pressure change in such a situation as a sum of the contribution due to the radiation field only $(\frac{dp}{p})_{cc}$ and that due to gas heating (or cooling) due to the macroscopic current change, $(\frac{\partial p}{\partial i})_I di$. The curves for $(\frac{dp}{p})_{cc}$ followed the gain curves expected for each particular gas system and pressure perturbations in pure CO_2 with zero discharge current were explained by the transition from inhomogeneous to homogeneous broadening of the absorption coefficient $\alpha(\lambda)$. Although the values of $(\frac{dp}{p})_{cc}$ in either discharge mode were comparable in

magnitude in all the gas systems the values of $\frac{di}{i}$ differed markedly. This was believed to be due partially to the influence of the radiation field on the parameter X. Plots of $(\frac{dp}{p})_{cv}$ against $(\frac{di}{i})$ showed a marked variation for different gas systems, but were linear in all cases in the current range of 20 to 40 mA.

6. SIDELIGHT EMISSION FROM CO_2 DISCHARGES

6.1 Introduction

In gas mixtures normally used in sealed and flowing CO_2 laser systems, the visible sidelight emitted is due predominantly to electronic-vibrational transitions in N_2 and CO. Figure 6.1 shows simplified energy level diagrams for the appropriate transitions in N_2 (second positive 2+, 2800 tc 5000 Å; first positive H, 5000 to 10500 Å), CO(Angstrom band 4100 to 6600 Å), and NO (γ or third positive 3+, 2500 to 3400 Å) respectively. Excitation mechanisms leading to the population of the electronic states responsible for emission at these wavelengths may be complex. Excitation cross-sections between, for example, vibrationally excited states in different electronic levels are not known; it is necessary, therefore, to make certain assumptions (see for example (4), (7), (48), (50)), in order to explain data obtained from the sidelight spectroscopy in such discharges.

6.2 The excited states of CO_2, N_2 and CO

It is the purpose of this section to describe the ground electronic vibrationally excited states found in each of the molecules CO_2, N_2 and CO.

(a) CO_2

Carbon dioxide is a symmetric, linear tri-atomic molecule which has three normal modes of vibration described by the quantum numbers V_1, V_2 and V_3, the so-called symmetric stretch, bending and asymmetric stretch modes respectively. The energy level diagram of the $X^1\Sigma_g^+$ ground electronic state is shown in fig. 6.2. It should be noted that the lower laser levels (020) and (100) exhibit Fermi resonance which perturbs

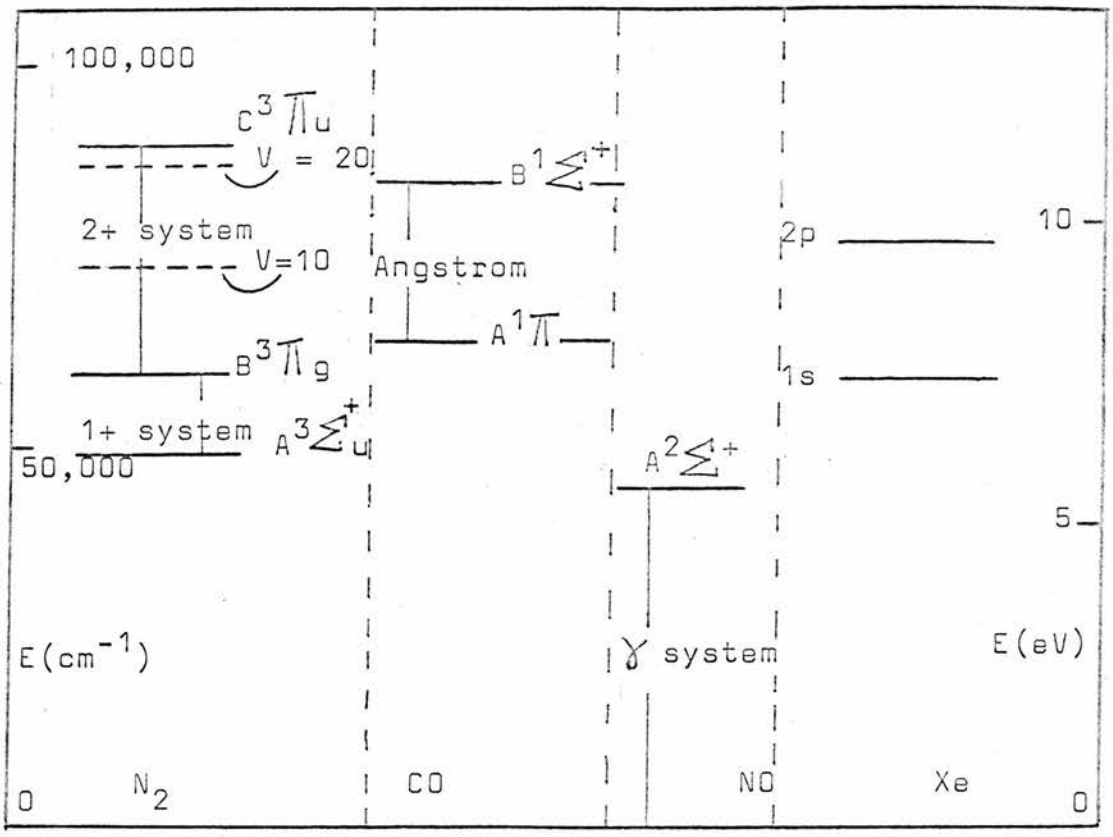
100,000
$C^3\Pi_u$
V = 20
$B^1\Sigma^+$
2+ system
V=10
Angstrom
$A^1\Pi$
$B^3\Pi_g$
1+ system
$A^3\Sigma^+_u$
50,000
$A^2\Sigma^+$
2p
1s
10
5
$E(cm^{-1})$
γ system
E(eV)
0
N_2
CO
NO
Xe
0

Fig. 6.1

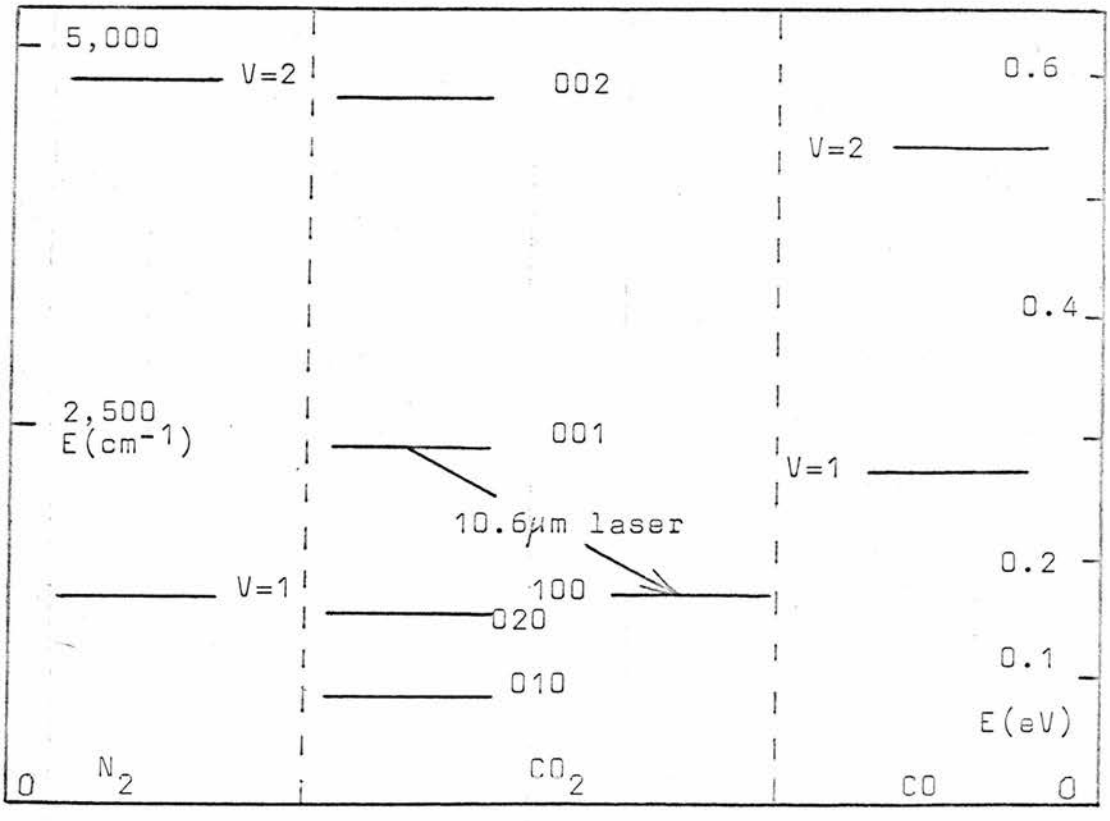
5,000
V=2
002
0.6
V=2
0.4
2,500
$E(cm^{-1})$
001
V=1
10.6μm laser
V=1
100
0.2
020
0.1
010
E(eV)
0
N_2
CO_2
CO
0

Fig. 6.2

their energy separation and leads to a strong mixing of their wave functions. Thus each level is no longer separate from the other but is a mixture of both and is expressed in the form $(020,100)'$. Superimposed on every vibrational level is a rotational substructure described by a Boltzmann energy distribution, with an inter-level spacing of the order of kT; the levels may be considered to be in thermal equilibrium due to their rapid rotational - rotational relaxation rate typically 10^{7} torr $^{-1}$ s^{-1}. Table 4 gives the values for the radiative lifetimes of the vibrational levels of interest in a typical dc excited low pressure CO_2 discharge.

TABLE 4

Level	τ(untrapped) seconds	τ^1(trapped) seconds
001	2.4×10^{-3}	5.0×10^{-2}
002	1.3×10^{-3}	
010	1.1	
$02^{0}0$	1.0	~3.0 (Even J)
$02^{2}0$	0.26	~1.0 (Odd J)
100	1.1	

Table 5 shows the approximate wavelengths of the infra-red transitions in the $X^1 \Sigma_g^+$ state of CO_2.

TABLE 5

Upper Level	Lower Level	λ (μm)	Integral absorption indices $\int k\, d\nu$
001	000	4.3	2700
001	100	10.6	0.02
001	020	9.4	0.05
100	010	13.9	7.5
020	010	16.2	-
010	000	15.0	330

This latter data was taken from Table V of ref. (46). The values were obtained in an infra-red device of medium dispersion with pressure broadened rotational lines at a temperature of $300^{o}K$.

(b) $\underline{N}_2$

Because nitrogen is a linear, symmetric, diatomic molecule, transitions between vibrational levels in the ground electronic state are forbidden in the dipole approximation, and hence they are all metastables with natural radiative lifetimes of the order of 10^3 seconds. The energy level diagram of the $X^1\Sigma_g^+$ vibrational levels is shown in fig. 6.2 where the close coincidence of the N_2 (V = n) and CO_2 (00n) levels is evident. The N_2 (V = n) levels are coupled by reactions of the type

$$N_2\ (V = n + 1) + N_2\ (V = n - 1) \rightleftharpoons 2N_2\ (V = n) \quad \ldots\ldots\ 6.1$$

Nitrogen exhibits only a slight anharmonicity and so we can assume that its molecular potential is parabolic (similar to that associated with a simple harmonic oscillator), with equally spaced energy levels. Hence the above reaction constitutes a resonant transfer of energy (no energy loss), with a high cross-section extending to values of $V \gg 4$. It has been calculated that at 1 torr of N_2 pressure the rate of excitation of N_2 (V = n) is equal to 10^{18} sec^{-1} cm^{-3} leading to over 10% of the N_2 population lying in these metastable levels and the consequent high power outputs of CO_2 lasers, (Sobolov and Sokovikov (46)).

(c) CO

A considerable amount of dissociation takes place (Smith and Browne (69)) in a CO_2 gas discharge producing CO. The V = n vibrational levels in the $X^1\Sigma_g^+$ state are, like those of N_2, in close proximity to the (00n) levels of CO_2 and it is for this reason that population inversion is possible (by direct pumping of the CO_2 molecules by the CO (V = n) molecules), in 'pure' CO_2 discharges. The collision cross-sections for direct electron excitation of the V = n levels are comparable with those of N_2 (Schultz (47)) and their radiative lifetimes are of the order 1 to 3 x 10^{-2} seconds.

6.2 Relaxation Processes in a CO_2 discharge

Energy exchange processes concerning the interaction of CO_2 and other molecules may be summarised by the following reactions. The rate constant for a particular reaction is denoted by K_e, K_{V_3}, etc.

Excitation Processes

$$N_2\ (V = 1) + CO_2\ (000) \underset{K_e^1}{\overset{K_e}{\rightleftharpoons}} N_2(V = 0) + CO_2(001) + 18cm^{-1} \qquad \ldots\ldots 6.2$$

$$CO_2\ (000) + CO(V=1) \xrightarrow{K_e(CO)} CO_2\ (001) + CO(V=0) + 206cm^{-1} \qquad \ldots\ldots 6.3$$

6.2 and 6.3 are examples of resonant energy transfer by which the 001 level is pumped.

Relaxation Processes

$$CO_2(001) + M \xrightarrow{K_{V_3}} CO_2\ (n, m^1, 0) + M + dE \qquad \ldots\ldots 6.4$$

$$CO_2\ (02^0 0, 10^0 0)^1 + CO_2\ (00^0 0) \xrightarrow{K(V_1, 2V_2)} 2CO_2\ (01^1 0) + 50cm^{-1} \quad .....6.7$$

$$CO_2\ (02^0 0, 10^0 0)^{11} + CO_2(00^0 0) \xrightarrow{K(V_1, 2V_2)} 2CO_2(01^1 0) + 52cm^{-1} \quad .....6.8$$

$$CO_2\ (01^1 0) + M \xrightarrow{K V_2} CO_2(00^0 0) + M + 667cm^{-1} \quad .....6.9$$

The rate coefficients, K, are related to the exponential relaxation time, , by the expression:

$$K = (p\,\tau)^{-1} \quad torr^{-1}\ s^{-1} \quad .....6.9$$

where p is the gas pressure in torr. The total collisional relaxation time for a molecule in a particular level V due to collisions with molecules of differing species, i, is

$$\frac{1}{\tau_v} = \sum_i \left(\frac{1}{\tau_i}\right) \quad .....6.10$$

Use was made of these equations in conjunction with data by Moore et al (25) to obtain Table 3 in section 5.1 which gives typical collisional lifetimes for vibrationally excited molecules in gas mixtures which were used in the experiments.

7. SIDELIGHT PERTURBATIONS

7.1 Introduction

One of the first reported examples of sidelight perturbation in a CO_2 laser was that due to Moeller and Rigden (6) who noted that the spontaneously emitted light from the side of a laser tube increased considerably in intensity when the lasing action was interrupted by means of an intracavity shutter. They interpreted this as due solely to thermal effects in the plasma. More detailed investigation by Crane and Waksberg (7) revealed that several spectral lines in the N_2 2+ system decreased in intensity when laser action was prohibited although the average sidelight intensity was increased. They believed that this effect could be explained in terms of direct collisions between N_2 molecules in the $C^3\Pi_u$ state and those in the $X^1\Sigma^+_g$ vibrational levels which were involved in the lasing process (i.e. those with V = 0 1, 2, ...8 in the $X^1\Sigma^+_g$ state). They also showed that under certain discharge conditions those lines which normally decreased in intensity could be made to increase in intensity as the laser action was stopped, i.e. the polarity of the perturbation of these lines was changed.

Carswell and Wood (8) showed that in their system changes in sidelight emission were due to amplified current changes (see also Chapter 5 of this work), resulting from the large variation of discharge impedance with current, and, in a later paper using an intracavity chopping technique Kindl et al (13) demonstrated complex temporal changes taking place in the discharge sidelight. Weiss et al (48) observed the spontaneous sidelight from a CO_2 laser in a lasing and non-lasing condition and by assuming a Boltzmann distribution

of molecules amongst the vibrational levels of the $C^3\Pi_u$ state were able to calculate vibrational temperatures in that state. It is apparent from their experimental results that N_2 2+ lines arising from the V = 0 and 1 vibrational levels of the $C^3\Pi_u$ state decreased in intensity in the non-lasing condition whilst those lines arising from the V = 2, 3, and 4 levels increased in intensity. Bleekrode (28) explained the behaviour of the N_2 2+ system in a CO_2 laser by assuming the $C^3\Pi_u$ vibrational levels to have a quasi vibrational temperature which he showed, by band strength analysis, to be hotter in the non-lasing than the lasing condition. By assuming a thermal distribution of N_2 molecules in the $X^1\Sigma^+_g$ vibrational levels, he calculated various population distributions in the $C^3\Pi_u$ vibrational levels which were qualitatively similar to his measured values.
He also pointed out that variations in the vibrational 'temperature' (or population distribution) of the $X^1\Sigma^+_g$ state would be manifested predominantly in changes in the relative vibrational population of the $C^3\Pi_u$ state. Crane and Waksberg's collisional theory was questioned on the grounds that the radiative lifetime of the $C^3\Pi_u$ state was about three orders of magnitude less than the time for vibrational energy exchange between CO_2 and N_2 (see ref. (28)).
Bleekrode (49) also showed in a similar experiment that the vibrational temperatures in the N_2 1 + system were independent of lasing (or non-lasing) conditions and hence the mode of $B^3\Pi_g$ excitation did not involve molecules which interacted with vibrationally excited CO_2. Bletzinger and Garscadden (10) emphasised that use of a stabalised current supply to the laser was necessary, otherwise amplified impedance changes

in the discharge associated with current changes (8), (13) would mask the interactions between the laser field and vibrationally excited molecules which produced the sidelight perturbations. This appears to be the only paper which emphasises the difference between performing perturbation experiments in a system using a current stabalised power supply over those performed using a voltage stabilised power supply. Novgorodov et al (50) used experimental methods and theoretical calculations similar to Bleekrodes' and produced data on the variation of temperature and population of the $X^1\Sigma_g^+$ N_2 vibrational levels with gas mixture and discharge current which agreed essentially with the work of Bleekrode.

None of the above authors, however, explain why certain lines in the $N_2$2+ spectrum increase in intensity whilst simultaneously others in the same band system decrease in intensity as laser action is stopped, or why these latter transitions can exhibit a switch in the polarity of their perturbation when suitable discharge conditions are chosen. There is also some discrepancy in the estimate of vibrational temperature in the $C^3\Pi u$ and $X^1\Sigma_g^+$ states of N_2 as Table 6 shows. The Russian authors together with Bleekrode obtain a value of around 1000^{o}K for somewhat similar systems, whereas Weiss et al and Legay-Sommaire obtain considerably higher values for the $C^3\Pi u$ state which do not agree with those interpolated from Novgorodov's work.

TABLE 6

Vibrational Temp. ^{o}K			Author	Experimental Method
$C^3\Pi_u$	$X^1\Sigma_g^+$	dT_v		
5000		330	(a) Weiss et al	Perturbation method in flowing 1:1:7 CO_2, N_2, He (9 torr) system. 45mA 1" bore tube.
4600			Weiss et al	Band strength analysis.
4600			(b) Legay et al (63)	Band strength analysis.
2400	1000	320	(c) Bleekrode	Band strength analysis in lasing and non-lasing system. CO_2: N_2: He mix. 20mA.
2500*-3500	1000*-2000	-	(d) Novgorodov et al	Band strength analysis. Flowing CO_2: N_2 mixtures at ~ 5 torr, 20mA in a 20mm bore tube; 1:3:8 CO_2, N_2, He* mixtures 9-2 torr at 20mA.
2500	1000	-	(e) Mikaberidze (64)	Band strength analysis. Flowing 1:3:6, CO_2, N_2, He mix, 6.9 torr at 20mA in a 23.5mm bore tube.
		500 to 700 ^{o}K	(f) Avivi et al (62)	Perturbation technique (external and internal cavity chopping). Flowing CO_2, N_2, He mix 0.6: 1.8:8.6 torr.

Investigations have been carried out to determine the vibrational temperature change in the N_2 $X^1\Sigma_g^+$, (c) and (f), or $C^3\Pi_u$, (a), levels when going from a lasing to a non-lasing condition and these values are shown in the column dT_v in Table 6.

The ideas of Weiss, Bleekrode and Novgorodov et al are used in the present work to try and explain the peculiarities of the N_2 2+ perturbation spectrum. Both current and voltage controlled power supply systems are employed in an effort to clarify the important differences in the sidelight perturbation spectra and compare results with those of the above mentioned authors. First, however, the terminology used in CO_2 perturbation spectroscopy is outlined in the remainder of this chapter and the two main proposed perturbation mechanisms are summarised.

7.2 Sidelight Perturbations

In CO_2 laser discharges changes in spontaneous sidelight emission in the optical region may be brought about by perturbations to the 10.6μm field. It is proposed here that there are at least two separate mechanisms which couple the radiation field to the optically excited states; they will be termed 'current' and 'collision' mechanisms and may be described as follows:

(i) Current Mechanism

As described in chapter 4 in a CO_2 active medium exhibiting gain the discharge impedance is increased and the current greatly decreased as the radiation field intensity becomes larger. The primary effect of a decrease in current is that the electron impact excitation to the various electronic molecular states is decreased and hence the integrated sidelight intensity is decreased. Secondary effects such as molecular number density changes, and hence changes of $\frac{E}{n}$, will also affect the excitation rates in a complex way. If the active

medium is in an absorption condition the opposite situation arises as the radiation intensity is increased, i.e. the discharge impedance decreases, the current increases, the electron pumping is increased and hence the overall sidelight intensity is increased.

(ii) Collisional Mechanism

If the discharge current is held constant and the radiation field increased in intensity in the active medium a different situation from (i) above will arise. Although the total current is maintained at a constant value it is possible that the electron energy distribution will be altered due to a change in the $\frac{E}{n}$ value in the discharge, for example via radiation induced pressure fluctuations such as those described in chapter 5. As a consequence the amounts of energy channelled into specific excitation processes (and in particular those involving electron pumping of optical electronic levels) will be altered (41). More importantly the distribution of molecules in their ground electronic vibrational states is altered due to V-V interactions with the perturbed primary laser levels. Because excitation to higher electronic levels, e.g. $C^3\Pi u$, is normally by direct electron impact from the $X^1\Sigma^+ g$ levels, the distribution in these higher states is also altered. It is believed that this change in molecular vibrational temperature brought about by perturbing the 10.6μm field is predominantly responsible for the changes in optical sidelight when the discharge is operated under current controlled conditions.

Crane and Waksberg (11), (12) and Carswell and Wood (8) have described the behaviour of a dc CO_2 discharge operating under voltage controlled conditions as follows. They consider the sidelight intensity, S, to be a function of the 10.6μm field intensity I, and of the discharge current, i, so S = S(I,i). Taking increments we have,

$$dS = \left(\frac{\partial S}{\partial I}\right)_i dI + \left(\frac{\partial S}{\partial i}\right)_I di \qquad .....7.1$$

where di is the corresponding induced current change and dI(=I) is the change in perturbing field intensity. The term $\left(\frac{\partial S}{\partial i}\right)_I di$ represents the variation in S due to discharge current changes only, the term $\left(\frac{\partial S}{\partial I}\right)_i dI$ the variation in S due to collisional effects only. (By collisional effects we must now consider intermolecular collisions in the ground electronic states of N_2 and CO_2 not the types of collisions originally referred to in (11)).

In order to test the validity of this equation and gain some understanding of the collisional effects of molecules on spontaneous sidelight, the quantity $\left(\frac{\partial S}{\partial I}\right)_i dI$ was:

(a) observed directly (by determining the sidelight perturbations in the current controlled discharge mode with di = 0, $dS_{cc} = \left(\frac{\partial S}{\partial I}\right)_i dI$.

(b) calculated - following Waksberg and Carswell - from measurements of dS in the voltage controlled discharge mode. The quantity $\left(\frac{\partial S}{\partial i}\right)_I di$ was obtained from the S - i static sidelight characteristic and di, the absolute current perturbation. It was then subtracted from the measured value of dS (= dS_{cv}), and the two values for $\left(\frac{\partial S}{\partial I}\right)_i dI$ were compared.

It is expected that changes in $\frac{E}{n}$ occur in both cc and cv controlled discharge modes and the resultant contribution to the sidelight perturbations will always be present. Section 10.4 presents the results of experiments used to determine $(\frac{\partial S}{\partial I})_i dI$. One important definition involving the polarity of such sidelight perturbations must be emphasised, i.e. if the intensity of a particular optical transition is observed to increase as the laser field is increased, the transition is defined to be positively perturbed or to have a positive polarity; if the intensity is decreased as the laser field is increased, the transition is defined to be negatively perturbed or to have a negative polarity.

8. PERTURBATION SPECTROSCOPY IN THE CO ANGSTROM BAND

8.1 Pure CO_2 Discharges

An investigation of the sidelight emission in the range 4800 to 8000 Å showed that the transitions involved in a nominally pure CO_2 discharge containing 10 torr (cold fill) of gas were those of the Angstrom system in the 0 - V band between the $B^1\Sigma^+$ and $A^1\Pi$ CO electronic levels. All transitions from 0 - V (V = 0, 1, ...5) were found to be modulated by the laser field and depended linearly in magnitude upon the intensity of the field. Their variation in magnitude and phase with respect to discharge current (in cc and cv controlled modes) and with perturbation frequency was determined; the results are shown in Figs. 8.1 and 8.2.

Two mechanisms must be considered in the qualitative explanation of this data:

(i) Collisional coupling between the $X^1\Sigma^+_g$ vibrational levels of CO and the primary laser levels.

(ii) Laser induced changes in the discharge current. The system is in an absorption condition at all currents, consequently the 001 level population is selectively increased by optical pumping at 10.6μm. By a reaction such as 6.3

$$CO_2\ (000) + CO\ (V=1) \xrightarrow{K_e} CO_2\ (001) + CO(V=0) + 206\ cm^{-1}$$

the CO molecule may exchange vibrational quanta with the upper laser level and the ground vibrational level, ($K_e \approx 0.79 \times 10^4$ torr^{-1} sec^{-1}). It is also effective in relaxing the lower laser level (100) by reactions of the type 6.4, 6.5, 6.7 and 6.9 for which $K(V_1, 2V_2) \approx 4.1 \times 10^3$ torr^{-1}s^{-1} and $K(V_2) \approx 2.5 \times 10^4$ torr^{-1}s^{-1}. The CO (V = 1) population will be

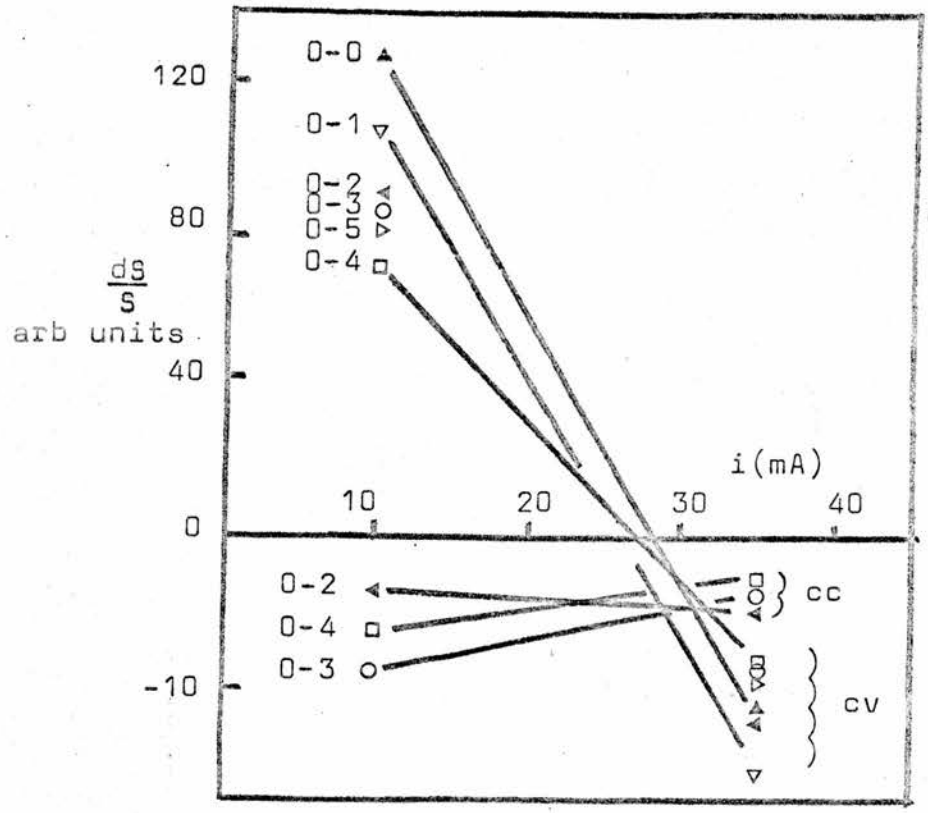

Fig. 8.1

Variation of sidelight intensity S with i (cc and cv) for transitions in the CO Angstrom band. 10 torr CO_2; τ = 35 ms.

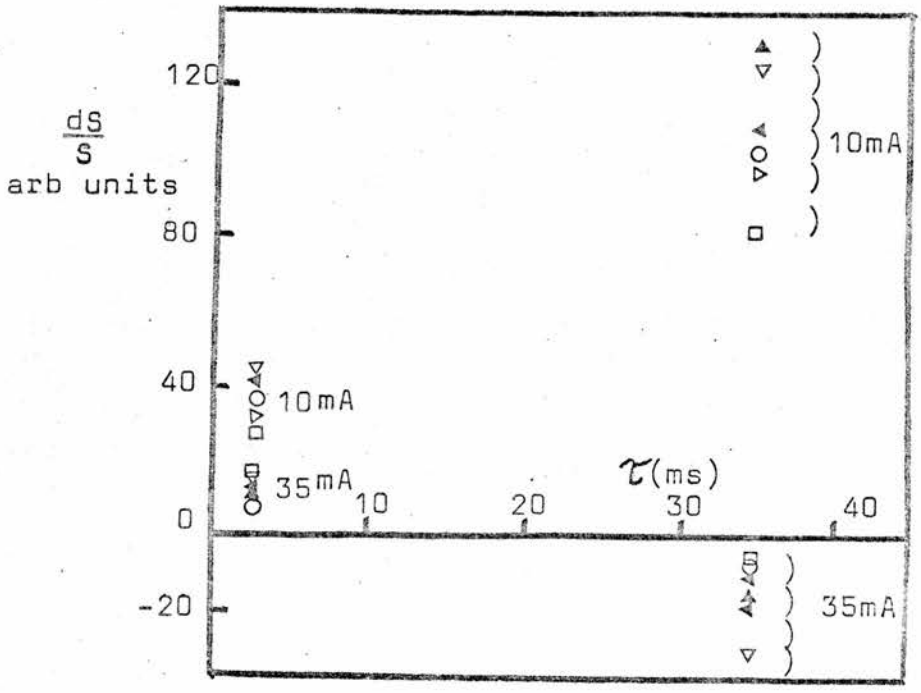

Fig. 8.2

Variation of sidelight intensity with τ for transitions in the CO Angstrom band. 10 torr CO_2; i = 10mA(cv); i = 35mA(cv).

enhanced when the irradiating field is switched on, at the expense of depleting the CO (V = 0) level. We will assume that the primary mechanism for populating the CO $B^1\Sigma^+$ state is by direct electron impact from the $X^1\Sigma^+_g$ state. Following the authors of (28) and (50) we will assume that the average cross-section for electron excitation $\langle v\sigma\rangle_{v^1_B\, v^{11}_X}$ is proportional to the Franck Condon factors for the $B^1\Sigma^+ \rightarrow X^1\Sigma^+_g$ transition (see also (53) and Appendix A.3). It can be seen that excitation to the $V^1_B = 0$ level of the $B^1\Sigma^+$ state is primarily from the $V^{11}_X = 0$ level of the $X^1\Sigma^+_g$ state, the Franck Condon factors for transitions from the $V^{11}_X = 1, 2, \ldots n$ levels being less by about two orders of magnitude (54). Thus, the perturbation to the $X^1\Sigma^+_g$ state will only be transferred to the 0 - V transitions of the $B^1\Sigma^+ - A^1\Pi$ system by excitation from the $V^{11}_X = 0$ level of the $X^1\Sigma^+_g$ state. In a purely absorbing system of CO_2 : CO the $X^1\Sigma^+(V^{11}_X = 0)$ level is always depleted by the action of the laser field and hence transitions in the Angstrom band will be reduced in intensity.

From the results it can be seen that in the constant current mode at all currents used (10 to 40 mA) the sidelight perturbations are negative. It would appear that the decreased electron excitation from the depleted $X^1\Sigma(V^{11}_X = 0)$ state qualitatively explains the behaviour of $\frac{dS}{S}$ under cc controlled conditions.

$(\frac{dS}{S})_{cv}$ for the 0 - V transitions where V = 0, 1, ...4 inverts, i.e. changes polarity, between 25 and 35 mA in the cv controlled mode and this effect cannot be explained in terms of di (or dp) since neither of these parameters shows an analogous

change in polarity. dp and di both decrease monotonically and reach their minimum values at around 30 mA. Below 25 mA the polarity of $\frac{dS}{S}$ and $\frac{di}{i}$ is the same, i.e. both increase as the laser field is turned on. Hence the cv value of $\frac{dS}{S}$ is opposite in phase to that in the cc mode because of the increased pumping of the $B^1\Sigma^+$ level overcompensating for the collisional depletion of the $X^1\Sigma^+(v_X^{11} = 0)$ level of CO. Above 25 mA the increased pumping by electron impact is insufficiently large and hence the collisional perturbation predominates, and the Angstrom band transitions invert. The relative magnitudes of the signals are within 10% accuracy at best (i.e. as measured under cv controlled conditions at 10 mA) and at worst the signal to noise ratio is about 2 on the signals observed at the higher currents ($>$ 20 mA) in both current modes. As plotted in 8.1 the magnitudes of the $(\frac{dS}{S})_{cv}$ values exceed those of the equivalent $(\frac{dS}{S})_{cc}$ values but this is not felt to be significant in view of the error involved in their determination.

The behaviour of $(\frac{dS}{S})_{cv}$ as a function of chopping frequency, fig. 8.2, may be explained following similar lines to the above arguments. The collisional induced perturbation between the CO_2 (001) and CO (000) levels (reaction 6.3) has a rate of 0.79×10^4 torr $^{-1}$ sec^{-1}. Assuming that approximately 10 torr of CO and 1 torr of CO_2 exist in the active medium under typical discharge conditions, we obtain a relaxation time of less than 0.01 ms for equilibration of these two levels, which is very much faster than the highest perturbation frequency used, (about 500 Hz, $\tau \approx 2$ ms) hence this mechanism should not be affected by a change in τ. However it can be seen from fig. 5.1 that $\frac{dp}{p}$ and $\frac{di}{i}$ are both greatly affected when τ becomes

less than 20 ms. At τ = 2 ms the current perturbation at 10 mA has decreased appreciably, i.e. the influence of increased electron pumping has been diminished, hence $(\frac{dS}{S})_{cv}$ becomes smaller but does not invert.

The behaviour of $(\frac{dS}{S})_{cv}$ at 35 mA with decreasing τ cannot be explained. One would expect $\frac{di}{i}$ to decrease as τ decreased and hence the collisional mechanism to become increasingly dominant since it is relatively independent of τ. Thus $(\frac{dS}{S})_{cv}$ at 35 mA would be expected to become increasingly negative as τ decreased rather than switch in polarity as observed. The data taken at τ = 2 ms must be treated with caution, however, since the signal to noise is about 2 or worse in this region.

8.2 Two part CO_2 : N_2 mixture

This gas mixture consisted of equal partial pressures of CO_2 and N_2 at a total cold fill pressure of 10 torr. The perturbed sidelight from this active medium showed transitions in the N_2 2+ and 1+ bands, and the Angstrom bands of CO. Unfortunately discharge noise prevented an accurate quantitative analysis of vibrational - vibrational transitions; however the results for CO may be summarised as follows:

(i) At τ = 35 ms in the cv mode at 15 mA CO transitions in the Angstrom band were in phase with the current perturbation and were therefore increased in intensity when the discharge was irradiated; at higher currents the CO lines became negative in polarity.

(ii) At τ = 35 ms in the cv mode at 35 mA the Angstrom band transitions were out of phase with the current.

None of the CO lines were able to be resolved in the cc mode of discharge. It was observed that the current perturbation decreased monotonically but did not change in phase from 10 to 35 mA; therefore collisional effects between the CO $X^1\Sigma^+$ levels and the CO_2 (001) and (000) states are responsible for inverting these transitions. Since the medium is in a state of absorption at all currents (as evidenced by the increase in discharge current induced by the radiation field) the CO_2 (001) level is continually pumped optically. As discussed in 8.1 above, this results in a net depletion of the CO $V_X^{11} = 0$ vibrational population by reaction 6.3. Hence the number of molecules excited electronically in the CO system from $X^1\Sigma^+(V_X^{11} = 0)$ to $B^1\Sigma^+(V_B^1 = n)$ states will be less and the sidelight intensity decreased, as was observed at 35 mA. Hence collisional effects responsible for perturbing the CO Angstrom band dominate over the current effects at higher currents in this gas mixture.

8.3 Three part gas mixtures

A series of experiments similar to those using the pure CO_2 gas were also performed on a mixture of CO_2, N_2 and He in the proportions 1:1:8 at a total cold fill pressure of 10 torr. Typical scans of the perturbed sidelight in a cc discharge mode may be seen in fig. 8.3 where transitions in the N_2 2+ and 1+ systems as well as the CO Angstrom system are clearly evident. The O - V band exhibited the following behaviour in the above mixture and in similar mixtures containing Xe and H_2 at 1 and 0.25 torr cold fill pressures respectively:

Fig. 8.3

Sidelight perturbation spectrum in 1:1:8 Mix CO_2 : N_2 : He (a = 20mA; b = 10mA; c = 5mA; d = 2.5mA).

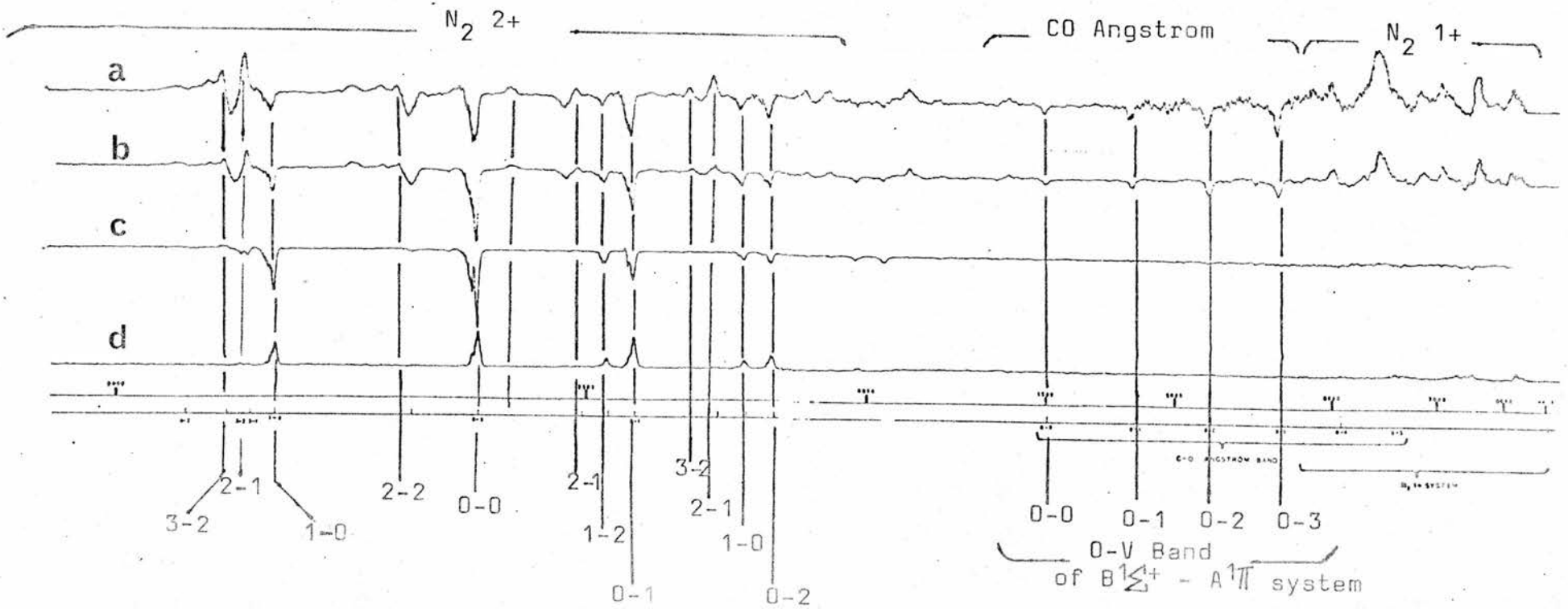

(i) In a current controlled mode the 0 - V transitions were positive at all currents between 2.5 and 40 mA.

(ii) In a voltage controlled mode the 0 - V band showed an inversion at about 7mA; for currents $0 < i < 7mA$ the perturbation was negative and in the range $7 \leq i < 40mA$ the perturbation was positive.

A possible mechanism describing the behaviour of this CO system is indicated below.

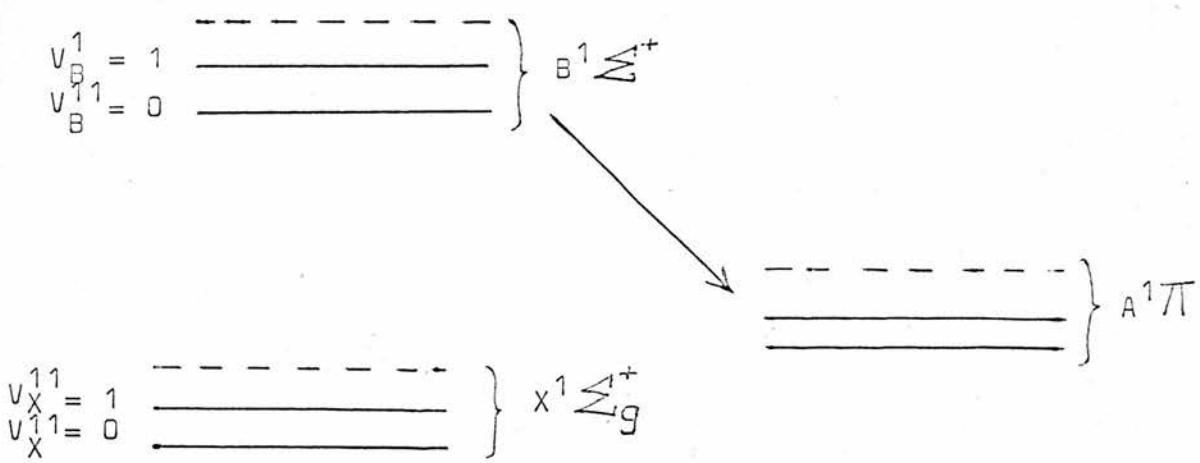

Fig. 8.4

In section 8.1 which dealt with a CO_2 : CO mixture it was assumed that excitation to the $B^1\Sigma^+ V_B^1 = 0$ level was primarily be electron impact direct from the $X^1\Sigma^+ V_X^{11} = 0$ level. If the gas system here is in a gain condition the laser field will deplete the 001 level of CO_2 and hence, by a reaction of the type 6.3 the CO ($V_X^{11} = 1$) level will also be depleted and the CO ($V_X^{11} = 0$) level population enhanced. Thus the CO $B^1\Sigma^+ V_B^1 = 0$ level population will be increased and so also will the intensity of spontaneous optical transitions in the 0 - V Angstrom band.

If current effects are eliminated (i.e. operating in the cc mode) then sidelight perturbations in this band will be positive; this is in fact what is observed here. However, in the voltage controlled mode the current is allowed to decrease as the laser field increases, thus leading to a reduced electron pumping rate of the $B^1\Sigma^+$ state. If this current decrease is large enough (i.e. when the total discharge current is below 7 mA) then the sidelight perturbation is also negative. When the current is increased above 7 mA the effect of the current perturbation on the $B^1\Sigma^+$ pump rate is reduced and the collisional perturbation effect becomes more dominant and so the sidelight perturbation becomes positive. We thus have a similar argument to that in 8.1 except that here we have a gain situation whereas before it was an absorbing gas mixture that was considered. The effect of substituting quantities of He in the three part mix with a corresponding partial pressure of H_2 did not appear to affect the switching behaviour of the CO transitions. Using chopping rates of up to 400 Hz ($\tau \approx 2.5$ ms) did not alter the appearance of the CO perturbation spectra in the voltage controlled mode. This is to be expected since equilibrium conditions are achieved collisionally in times of less than 2.5 ms in the three part mixtures used. Scans of the perturbed CO Angstrom band under identical conditions performed both in the cc and cv discharge modes at 10 mA showed that all lines were positive in polarity in both cases. It was also observed that the peak heights under cv conditions were about 40% less in magnitude than those in the cc mode. The explanation may be

that the current perturbation is diminishing the optical pertubration in the cv mode but, of course, this does not happen in the cc mode. From equation 7.1

$$dS = \left(\frac{\partial S}{\partial I}\right)_i dI + \left(\frac{\partial S}{\partial i}\right)_I di$$

and in this case $\left(\frac{\partial S}{\partial I}\right)_i dI$ is positive whereas $\left(\frac{\partial S}{\partial i}\right)_I di$ is negative, and it is this latter term which would account for the 40% lowering of the peak heights in the cv discharge mode.

8.4 Summary

From the above discussions it can be seen that the polarity and, to some extent the magnitude, of CO Angstrom band perturbations may be interpreted for the three gas systems examined. In particular for the data obtained in the cc mode the assumption of electron impact excitation from perturbed ground electronic vibrational levels, coupled to the CO_2 laser levels via reactions of type 6.3, appears to interpret the observed spontaneous emission spectra quite well. In the cv mode such effects will also be present but in general are masked by the large discharge current changes which are particularly dominant at low currents.

9. POSITIVE AND NEGATIVE SIDELIGHT PERTURBATIONS

Before discussing observed spectra of the more complex N_2 2+ and 1+ systems in further detail, it is intended at this point to examine a mathematical model of the excitation and decay of the N_2 2+ system under lasing and non-lasing conditions. The properties of the model will then be compared with experimental results.

9.1 A Model which Demonstrates Simultaneous Positive and Negative Perturbations in the N_2 2+ system.

The following assumptions have been made.

(i) Following Bleekrodé (28) and Novgorodov et al (50), the excitation probability of the vibrational levels of the $C^3\Pi_u$ state from the ground $X^1\Sigma^+_g$ state due to electron impact are taken to be proportional to the Franck-Condon factors for the Tanak system $C^3\Pi_u - X^1\Sigma^+_g$. This is reasonable in view of the fact that the electronic excitation process occurs in a time much smaller than the natural period of vibration of the molecule (see also Appendix A.3).

(ii) We take the populations in the $X^1\Sigma^+_g$ state of N_2 to be distributed according to the Boltzmann law because of the closeness of the energy level spacing to that of a simple harmonic oscillator.

(iii) The total distribution of molecules in the $X^1\Sigma^+_g$ state can be defined by an effective temperature T_{Vx}.

(iv) We assume that the electron excitation rates are unaltered between the lasing and non-lasing states.

A simple model of the excitation and decay process is seen in Fig. 9.1.

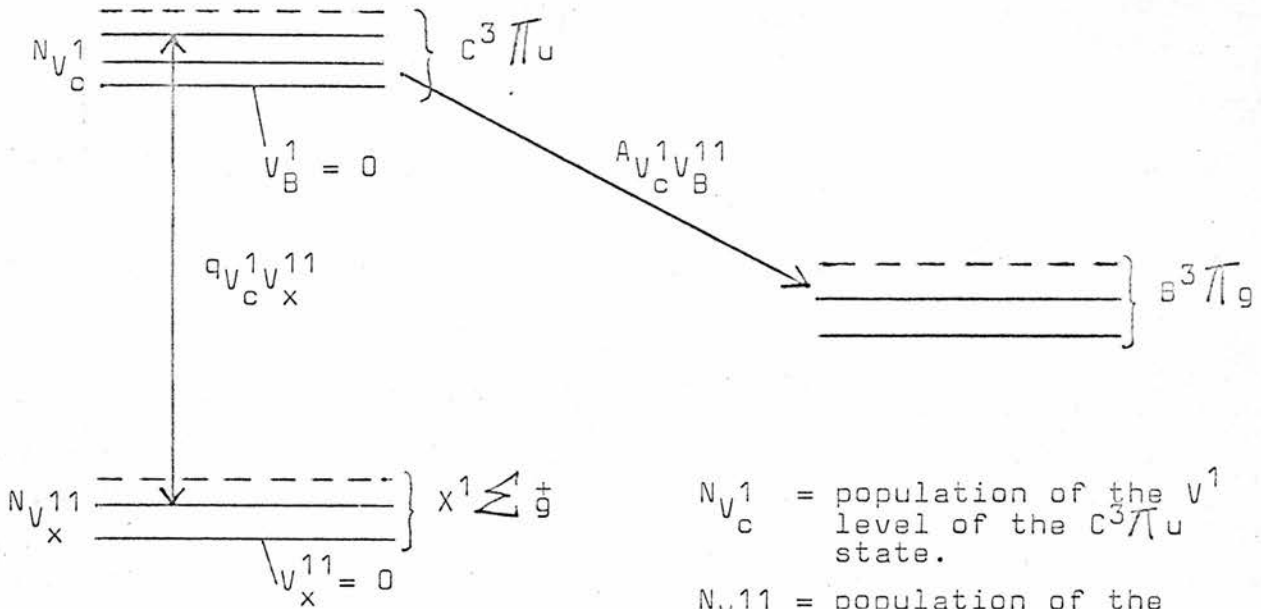

Fig. 9.1

$N_{V_c^1}$ = population of the V^1 level of the $C^3\Pi_u$ state.

$N_{V_x^{11}}$ = population of the V^{11} level of the $X^1\Sigma_g^+$ state.

$q_{V_c^1 V_x^{11}}$ = Franck Condon factor for the $V_c^1 \rightarrow V_x^{11}$ transition.

Excitation to the $C^3\Pi_u$ state from the $X^1\Sigma_g^+$ is predominantly by electron impact (26), (55) and (27), followed by radiative decay to the $B^3\Pi_g$ state. We may write the population of a particular vibrational level in the $X^1\Sigma_g^+$ state as follows:

$$N_{V_x^{11}} = \frac{N_{Tx}}{Q_V} \exp\left(- G_o (V)\, hc/k\, T_{Vx}\right) \quad \ldots\ldots 9.1$$

where N_{Tx} = total number of N_2 molecules in the $X^1\Sigma_g^+$ state.

T_{Vx} = effective vibrational temperature of the $X^1\Sigma_g^+$ state.

Q_V = partition function $(= Q_V (T_{Vx}))$

$G_o(V)$ = energy (in cm^{-1}) of the V'th level above the ground vibrational state.

Now, with the above assumptions, the population of a particular vibrational level in the $C^3\Pi_u$ state may be written

$$N_{V_c^1} \propto Ne \sum_{V_x^{11}} \langle v\sigma \rangle_{V_x^{11} V_c^1} N_{V_x^{11}} \quad \ldots\ldots 9.2$$

where Ne = electron density,

and since $N_{V_c^1} \propto (A_{V_c^1 V_B^{11}})^{-1}$ $\quad \ldots\ldots 9.3$

$$N_{V_c}^{1} = \frac{Ne}{A_{V_c}^{1} V_B^{11}} \cdot \sum_{V_x^{11}} \left\{ \langle v\sigma \rangle_{V_x^{11} V_c^{1}} \cdot N_{V_x^{11}} \right\} \quad \ldots\ldots 9.4$$

we now take $$\langle v\sigma \rangle_{V_x^{11} V_c^{1}} \propto q_{V_c^{1} V_x^{11}} \quad \ldots\ldots 9.5$$

Then $$N_{V_c}^{1} = K \sum_{V_x^{11}=0}^{4} q_{V_c^{1} V_x^{11}} \; N_{V_x^{11}} \quad \ldots\ldots 9.6$$

where K is a constant independent of V_x^{11} and we have assumed that only the first five levels in the $X^1\Sigma_g^+$ state contribute towards populating the $C^3\Pi_u$ vibrational levels.

From Herzberg we have the following expressions for $G_o(V)$ and Q_V

$$G_o(V) = \omega_o V - \omega_o x_o V^2 + \omega_o y_o V^3 + \ldots\ldots \quad \ldots\ldots 9.7$$

$$\omega_o = \omega_e - \omega_e x_e + \tfrac{3}{4}\omega_e y_e \quad \ldots\ldots 9.8$$

$$\omega_o x_o = \omega_e x_e - \tfrac{3}{2}\omega_e y_e \quad \ldots\ldots 9.9$$

$$\omega_o y_o = \omega_e y_e + \ldots\ldots \quad \ldots\ldots 9.10$$

Hence

$$G_o(V) = V(\omega_e - \omega_e x_e + \tfrac{3}{4}\omega_e y_e) - V^2(\omega_e x_e - \tfrac{3}{2}\omega_e y_e) + \omega_e y_e V^3 + \ldots\ldots \quad \ldots\ldots 9.11$$

where ω_o = fundamental molecular vibrational frequency

V = vibrational quantum number, and the other terms represent corrections to the single harmonic oscillator model of N_2 due to the anharmonicity of the actual molecule.

Thus $G_o(0) = 0$; $G_o(1) = \omega_e - 2\omega_e x_e + \frac{13}{4}\omega_e x_e$; etc. $\quad \ldots\ldots 9.12$

The partition function is given by

$$Q_V = 1 + \exp\left(-\frac{G_o(1) hc}{kTv}\right) + \exp\left(-\frac{G_o(2) hc}{kTv}\right) + \ldots\ldots \quad \ldots\ldots 9.13$$

for N_2 in the $X^1\Sigma_g^+$ state

$\omega_e = 2359.6\ cm^{-1}$

$\omega_e x_e = 14.46\ cm^{-1}$

$\omega_e y_e = 0.0075\ cm^{-1}$

Hence $G_o(0) = 0$; $G_o(1) = 2330.6$; $G_o(2) = 4632$;

$G_o(3) = 6905$; $G_o(4) = 9149$. (all values in cm^{-1}).

Assuming a range of vibrational temperatures T_{Vx} between 6000°K and 2000°K values of $N_{V_x}^{11}$ were computed for each temperature, from equation 9.1. By using equation 9.6 and Franck Condon factors from Zare R.N. et al (56), corresponding values for the $N_{V_c}^{1}$ populations in the $C^3\Pi u$ state were then calculated employing $N_{V_x}^{11}$ values between the temperatures 6000°K and 2000°K. A selection of results is presented in Figs. 9.2 to 9.4.

9.2 Discussion of Theoretical Results

It can be seen from Fig. 9.2 that as T_{Vx} is increased then the populations in the $C^3\Pi u$ state with quantum numbers $V_c^1 = 0, 1$ decrease, whilst those with $V_c^1 = 2,3,4$ increase. This behaviour may be compared with that of the $X^1\Sigma_g^+$ state vibrational populations shown in Fig. 9.3. It can be seen how a modification in the behaviour of the $N_{V_c}^{1}$ populations - as a function of temperature - is affected by the weighting of the Franck Condon factors in the excitation processes between individual $N_{V_x}^{11}$ and $N_{V_c}^{1}$ populations when compared with the corresponding behaviour of the $N_{V_x}^{11}$ populations. If we consider that there is a vibrational temperature decrease (dTv_x) in the $N_{V_x}^{11}$ levels as the medium goes from a non-lasing to a lasing condition, then the $N_{V_c}^{1}$ populations are affected as follows. The $V_c^1 = 0$ and $V_c^1 = 1$ levels are selectively increased and the $V_c^1 = 2$, 3 and 4 levels are decreased as illustrated in Fig. 9.4. Hence spontaneous emission from the 0 - V and 1 - V bands will be enhanced (positive perturbation) whilst that from the 2, 3 and 4 - V bands

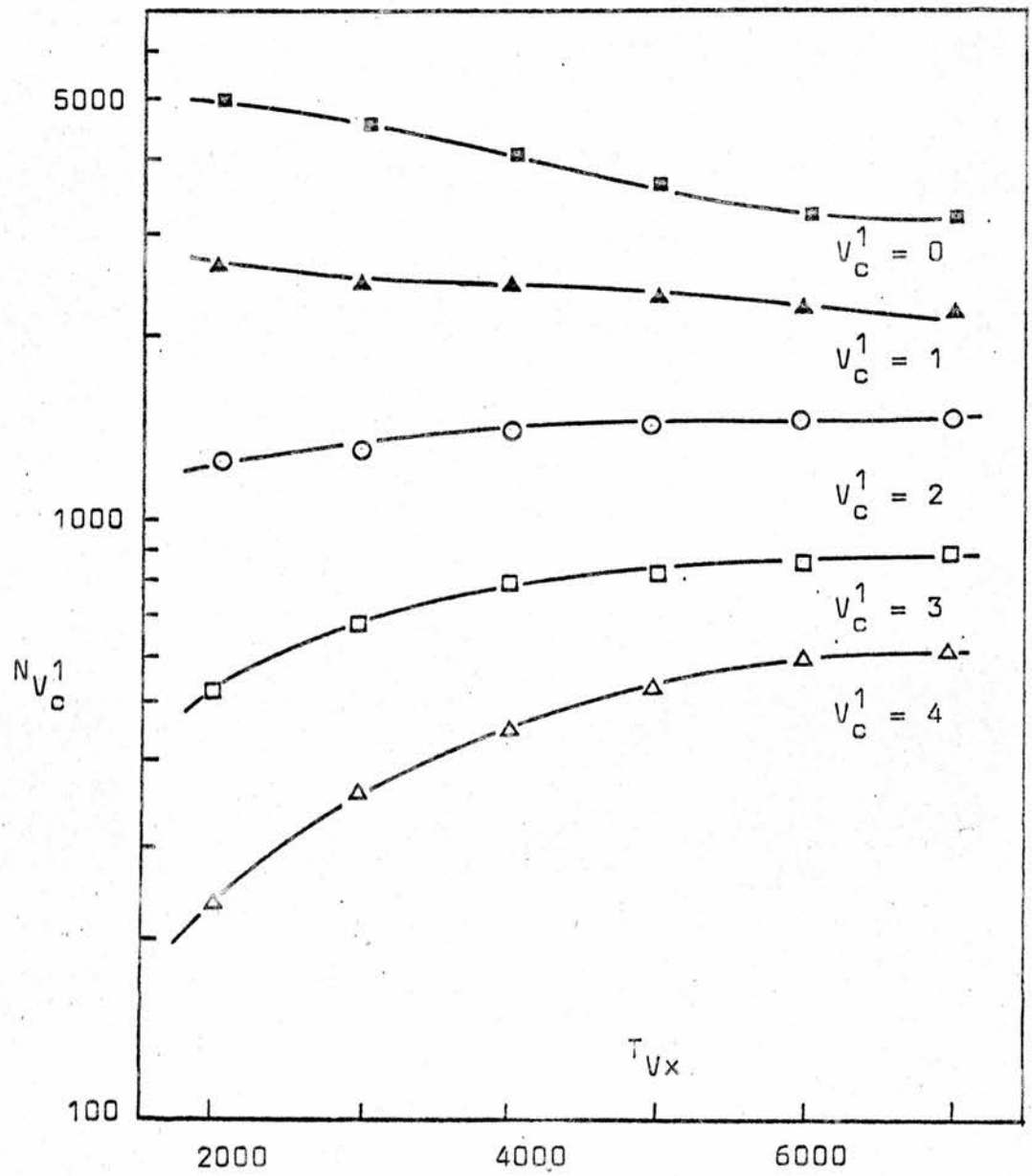

Fig. 9.2

Variation of the $C^3\Pi_u$ vibrational populations ($N_{V_c^1}$) with vibrational temperature in the $X^1\Sigma_g^+$ state.

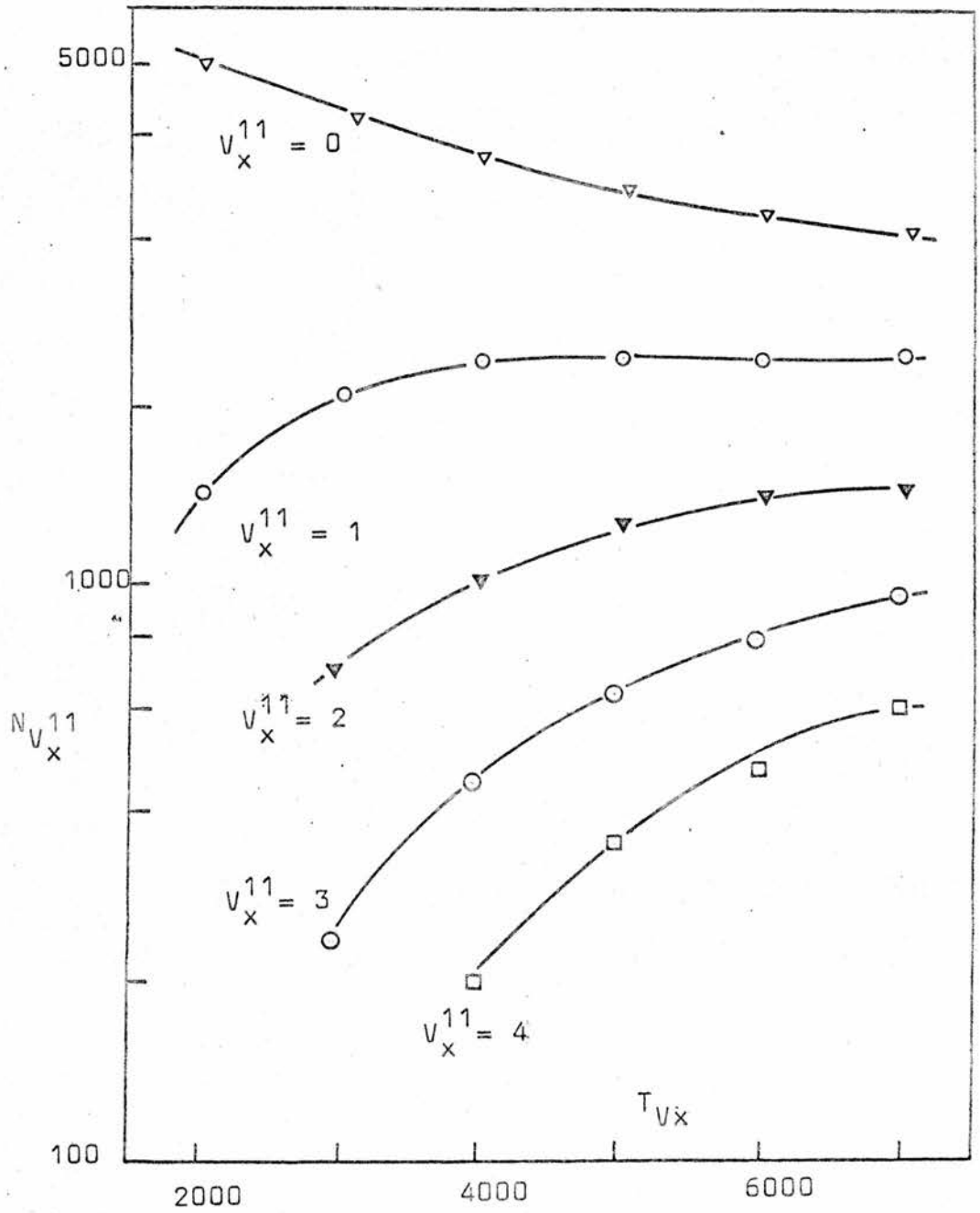

Fig. 9.3

Variation of the $X^1\Sigma_g^+$ vibrational populations ($N_{V_x^{11}}$) with vibrational temperature in the $X^1\Sigma_g^+$ state.

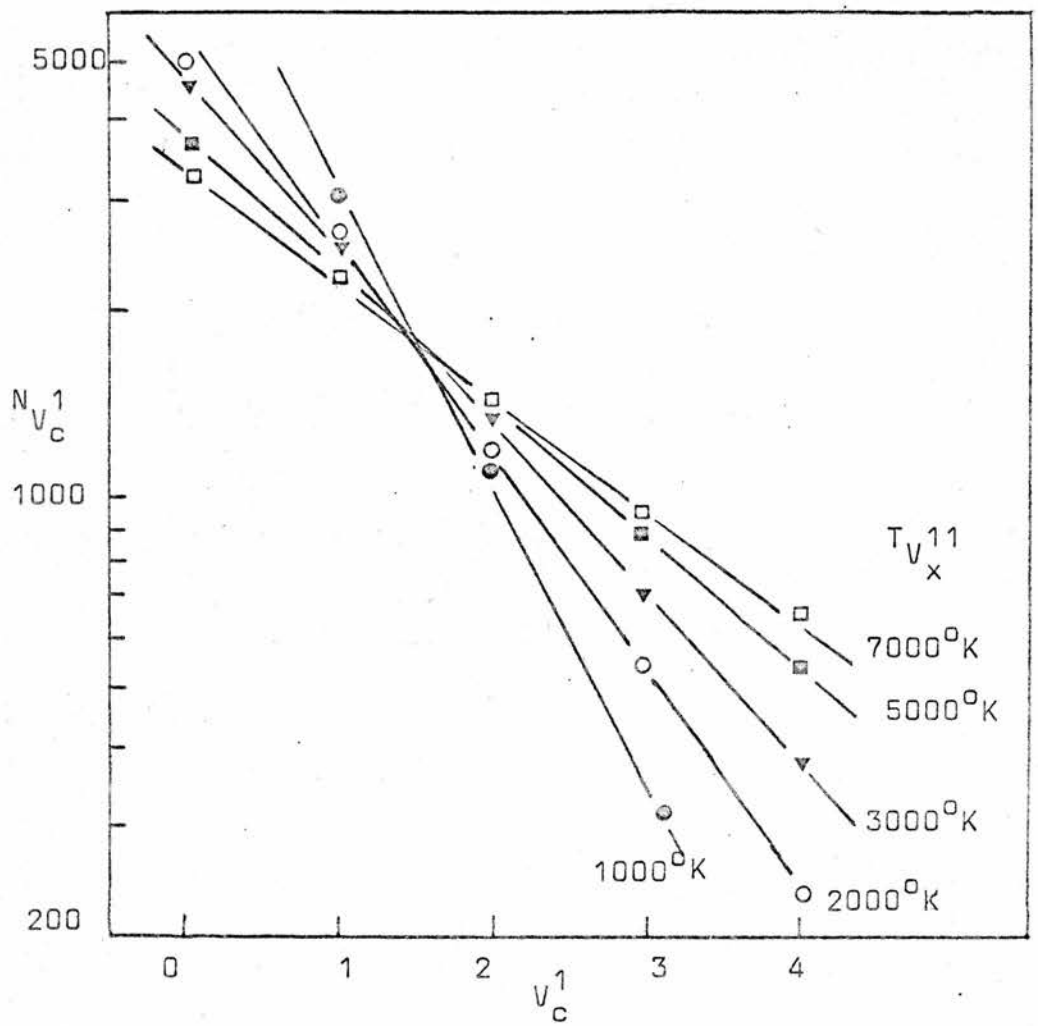

Fig. 9.4

Vibrational $C^3\Pi u$ populations ($N_{V_c^1}$) as a function of quantum number V_c^1 for various temperatures T_{Vx}.

will be diminished (negative perturbation). It is evident that perturbations in vibrational temperature cause the greatest fluctuations in the $^{N}V_{c}^{1}$ levels at the lower equilibrium vibrational temperatures (i.e. $< 3000^{o}K$) where the $^{N}V_{c}^{1}$ populations vary most rapidly with temperature. This corresponds to the experimental observation that the maximum sidelight perturbations occur at lower currents ($\approx$ 10mA), i.e. at lower vibrational temperatures, and then tend to decrease and become of constant lower magnitude as the current is increased, c.f. ref. (50).

10. N_2 PERTURBATION SPECTROSCOPY

10.1 Two part CO_2: N_2 Mixture

This gas mixture is the same as that described in chapter 8.2 and an analysis of the N_2 perturbation spectrum is now discussed. The results may be summarised as follows:

(i) at τ = 35 ms in the cv discharge mode at 15 mA all transitions in the N_2 2+ and 1+ bands are in phase with the current perturbation and are therefore increasing in intensity when the discharge is irradiated. These transitions (unlike those in the CO Angstrom band) remained positive in polarity at higher currents.

(ii) at10mA in the cc discharge mode only the $N_2$2+ transitions were resolvable. The 0 - V and 1 - V transitions appeared to be negative in polarity whilst the remainder were positive.

The $C^3\Pi_u$ system is assumed to be populated by direct electron impact from the $X^1\Sigma_g^+$ (V_x^{11} = n) levels (see for example Haworth (27)); we take the average excitation cross-section for such processes as proportional to their respective Franck Condon factors in the Tanak system ($C^3\Pi_u$ - $X^1\Sigma_g^+$). The vibrational temperature in the $X^1\Sigma_g^+$ state will be increased when the molecules are irradiated due to pumping of the CO_2 (001) level and vibrational energy transfer to the N_2 molecules via reactions of type 6.2. From Fig. 9.4 it can be seen that such a temperature change will be accompanied by a decrease in the populations of the $^NV_c^1$ levels with V_c^1 = 0 and 1 and an increase in the populations of the other levels, hence the

0 - V and 1 - V transitions in the $N_2$2+ system ($C^3\Pi u - B^3\Pi g$) will be negative and the remainder will be positive. This is the situation observed in the cc discharge mode where current feedback effects are eliminated. In the cv mode of discharge the current perturbation is sufficiently large to mask the effects of such temperature changes and simply increases the pumping to all the $C^3\Pi u$ vibrational states since all $N_2$2+ transitions are observed to be positive in the current ranges in which they were observed.

10.2 Three and Four Part Gas Mixtures - General Observations

The gas mixture of CO_2 : N_2 : He (1:1:8) is the same as that described in 8.3. Typical scans of the perturbed sidelight with the discharge in the cc mode are shown in Fig. 8.3. The scans closely resemble those of a normal sidelight spectrum of the discharge shown in Fig. 10.1. A combined scan of the sidelight and the perturbed sidelight - performed by simultaneously chopping the sidelight at 60 Hz and perturbing the discharge with a 10.6μm field modulated at 28 Hz and coupling the signal to a twin parallel arrangement of lock-in amplifiers tuned to either frequency - revealed that all the peaks of maximum perturbation coincided in wavelength with the peaks in the sidelight spectrum as both were plotted on a two channel pen recorder. It must be noted that before each perturbation scan was made the lock-in amplifier was tuned with respect to phase and frequency such that a maximum signal on one of the $N_2$2+ 0 - V or 1 - V transitions was produced. Hence the phase of all subsequently observed lines is referenced to the particular transition initially chosen.

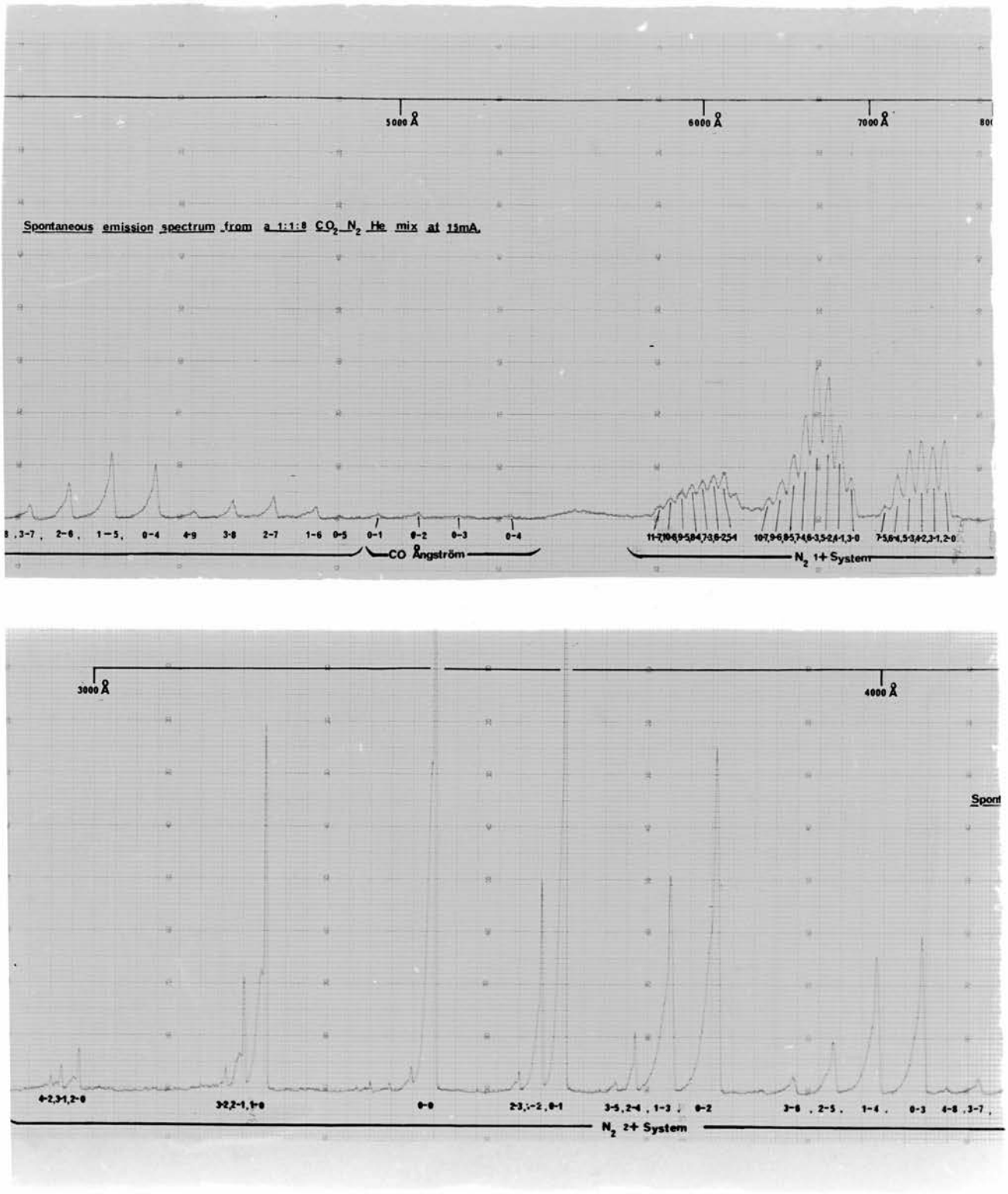

Fig. 10.1

Normal sidelight spectrum obtained from a 1:1:8 (CO_2 : N_2 : He) mixture running at 15 mA.

Referring to Fig. 8.3 it may be seen that at 20 mA (a) and 10 mA (b) all transitions in the 0 - V and 1 - V bands of the $N_2$2+ system are positive in polarity (the intensity increases positively below the zero level) as are the CO Angstrom transitions in the 0 - V band; the $N_2$1+ system is negative in polarity for all transitions. The $N_2$2+ 2 - V band for transitions with V = 4, 5 appear well defined and negative. However the 2 - 2, 2 - 1, 2 - 0 and, to some extent, the 2 - 3 transitions appear to have anomolous positive perturbations at the short wavelength tail of each (J > 20) in this particular set of scans and it is thought to be due to inaccurate phase tuning to the reference $N_2$2+ peak at the initial part of the scan. At 5mA current (c) the $N_2$1+ and CO Angstrom systems are no longer clearly visible. The 0 -V and 1 - V bands of the $N_2$2+ system are positive at this current. At 2.5 mA (d) these bands can be seen to have switched in polarity and are now decreased in intensity by the increasing laser field; they are now in phase with the remainder of the 2+ spontaneous transitions. The addition of quantities of hydrogen did not alter the behaviour of the 0 - V and 1 - V bands in this respect; i.e. at high currents ($\gtrsim$ 7mA) both bands were positive in polarity the remainder were negative. Switching of the 0 - V and 1 - V bands was generally obtained at a very low discharge current which was possible only under current controlled conditions in the present system.

The behaviour of (a) the $N_2$1+ system and then (b) the $N_2$2+ system is now discussed in further detail with particular reference to the results of chapter 9.

10.3 The N_2 1+ System in Three Part Mixtures

Individual vibrational-vibrational electronic transitions were not resolvable in the perturbation spectrum of this system, even with the use of the cooled RCA photomultiplier. However, the following observations were made:

(i) Transitions in the N_2 1+ system between about 6000 and 9000 Å always exhibited a negative perturbation in both discharge modes; c.f. refs. (10 and (49).

(ii) They did not show any evidence of switching polarity over the range of currents 10 to 40 mA. (It was not possible to observe N_2 1+ perturbation lines below 10 mA).

(iii) The approximate intensities of the bands were similar in both discharge modes.

The $B^3\Pi_g$ state of N_2 may be considered to be populated mainly by spontaneous transitions from the $C^3\Pi_u$ level (2 + transitions), and direct excitation by electrons from the ground state (27), rather than recombination from the atomic state (49). Franck Condon factors for the N_2 2+ ($C^3\Pi_u$ - $B^3\Pi_g$) system reveal that significant contributions to all vibrational levels of the $B^3\Pi_g$ state are primarily made from the first five of the $C^3\Pi_u$ vibrational populations. It would appear from experimental evidence that the integrated effect of the $V_c^1 \rightarrow V_B^{11}$ transitions ($V_c^1 > 1$) on the populations of the V_B^{11} levels of the $B^3\Pi_g$ state is larger than that of $V_c^1 \rightarrow V_B^{11}$ ($V_c^1 = 0, 1$). This is so since V_c^1 (> 1) levels are always depleted by the action of the laser field and consequently their contribution to the $B^3\Pi_g$ vibrational levels is reduced. Although under certain conditions the influence of the $V_c^1 = 0, 1$ levels will be to enhance the overall $B^3\Pi_g$ population, the effect is small. Hence subsequent

spontaneous emission from this state is always reduced by the action of the 10.6μm field.

10.4 N_2 2+ Perturbation Spectra in Three Part Mixtures

The complex behaviour of the 2+ system of N_2 makes it the most interesting of the perturbed bands in a three or four part mixture. The discussion of results will treat the cc and cv controlled modes separately and comparison of the cc results with the model presented in section 9.1 will be made.

In the voltage controlled discharge mode all transitions in the 2+ band appeared to be negative in polarity; no switch in polarity of the 0 - V or 1 - V transitions was observed, unlike the results reported in (7), over a range of currents from 5 to 40 mA. The technique used for each scan was to tune the detection system for phase shift and frequency so as to maximise the 0 - 0 transition, and then the whole 2+ system was scanned at this setting. It would appear that at all currents collisional perturbation effects were sufficiently small to be hidden by the current perturbation effects which always tended to decrease the electron impact pumping as the laser field in the discharge was increased.

The only analysis made of sidelight spectra obtained in the cv mode appears in section 10.5 below where data is used in equation 7.1 in order to obtain corrected sidelight data to compare with that obtained experimentally in the cc mode. In view of the result of this comparison, it was decided that further investigation of the cv results would not yield useful information regarding the explanation of sidelight perturbations. Due to the added complexity and overriding effects of amplified current and pressure changes in a voltage controlled discharge

the nature of any collisional perturbation to the optically excited levels of N_2 is hidden.

10.5 Comparison of Present Results with those obtained by Previous Authors

Three papers relevant to the present work are by the authors Crane et al (7), (11) and (12). They used a perturbation technique which allowed the discharge current in the absorption cell to change (equivalent to the cv mode of operation), and corrected their observed sidelight results with a formula similar to equation 7.1 (7). Because the present system was operable in both cv and cc modes, it was decided to see if such a correction was valid.

Following the method described in the latter part of 7.2 the following results in Figs. 10.2, 10.3 and 10.4 were obtained. Fig. 10.2 shows how the 0 - 0 and 0 - 1 transitions in the $N_2$2+ sidelight perturbation spectrum vary as a function of discharge current in the cc and cv modes. It is evident that the perturbation in the cc mode is usually positive but undergoes a switch in polarity at about 5 mA. In the cv mode the perturbation is negative at all currents in which the discharge could be stably operated. Fig. 10.3 shows a plot of the quantities $\left(\frac{\partial S}{\partial I}\right)_i^{calc} dI \quad (= dS_{cv} - \left(\frac{\partial S}{\partial I}\right)_I di\ )$, and $\left(\frac{\partial S}{\partial I}\right)_i^{meas} dI \quad (= dS_{cc})$ for the $N_2$2+ 0 - 0 transition. It can be seen that they are dissimilar. A similar calculation was carried out for the CO Angstrom band 0 - 3 transition and the result appears in Fig. 10.4; again the measured and calculated values of the sidelight perturbation due to collisional effects only are not the same. It must be concluded that equations of the type 7.1 do not give the relevant correction to data observed under cv discharge conditions such as to eliminate

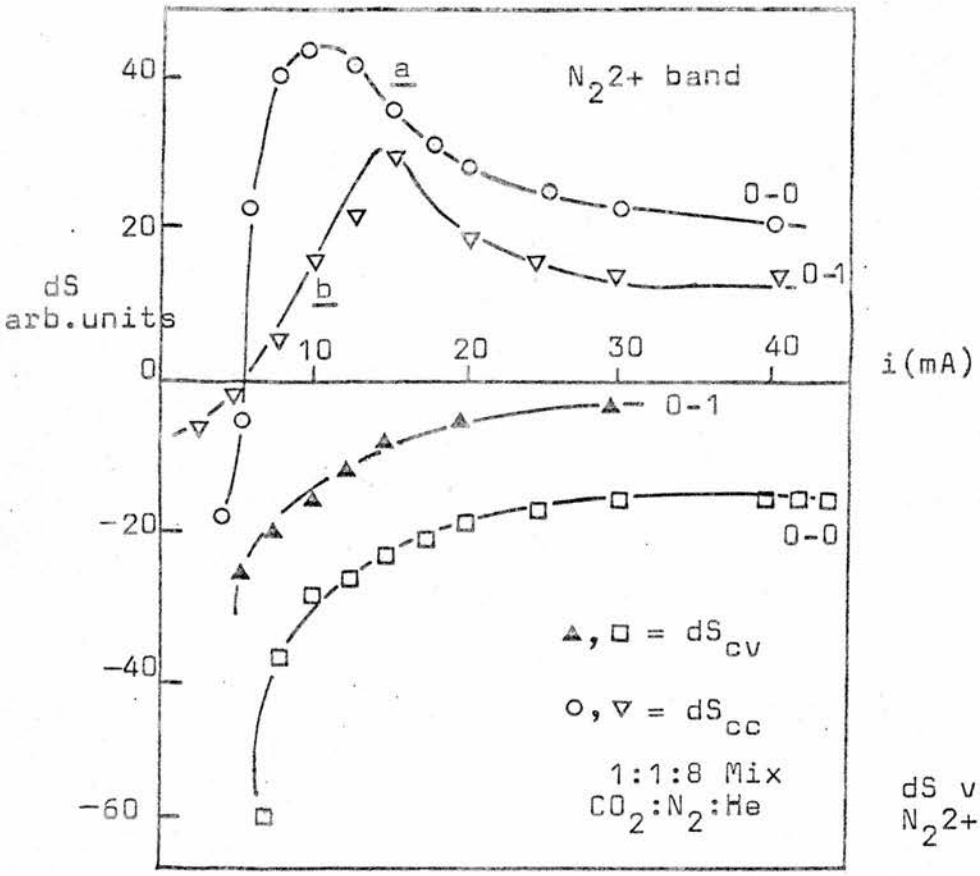

Fig. 10.2

dS versus i curves for $N_2$2+ transitions.

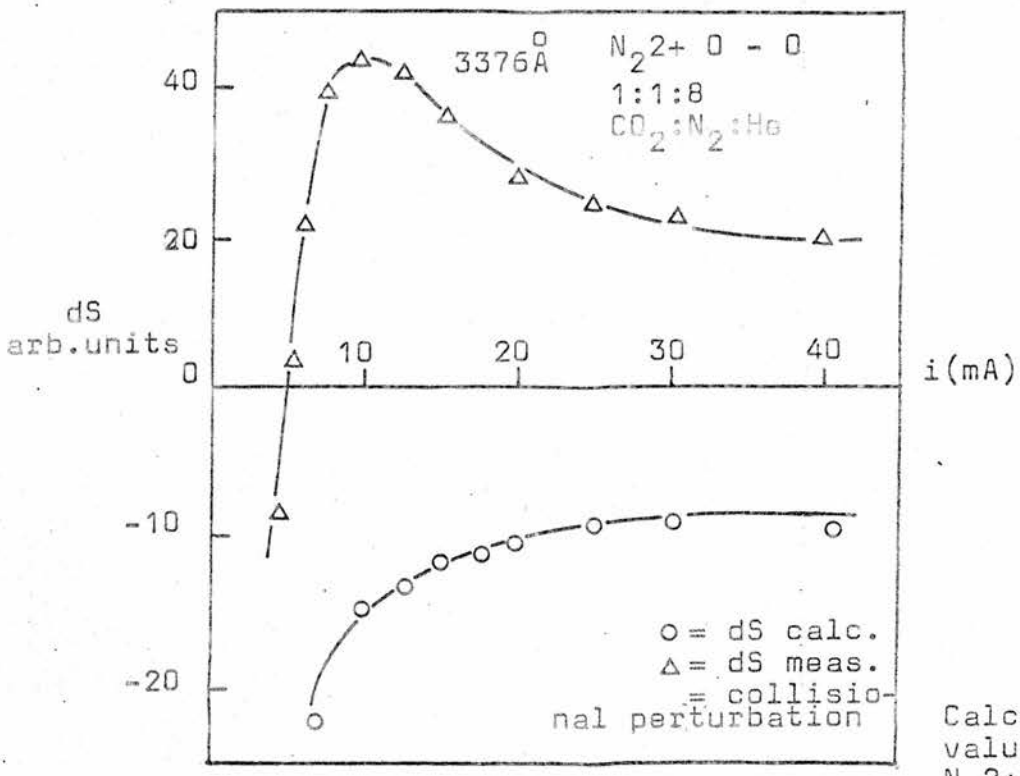

Fig. 10.3

Calculated and measured values of dS versus i for $N_2$2+ 0-0 transition.

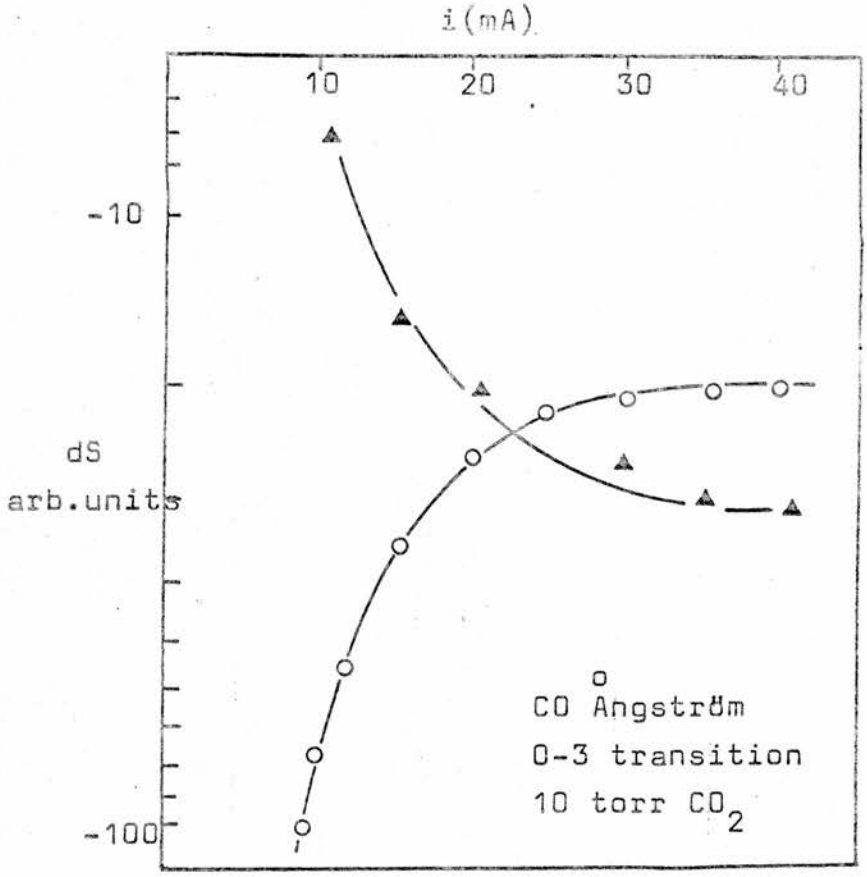

Fig. 10.4

Calculated and measured values of dS for CO Angstrom band.

$$= \left(\frac{\partial S}{\partial I}\right)_i^{calc.} dI$$

$$= dS_{cc}^{meas.}$$

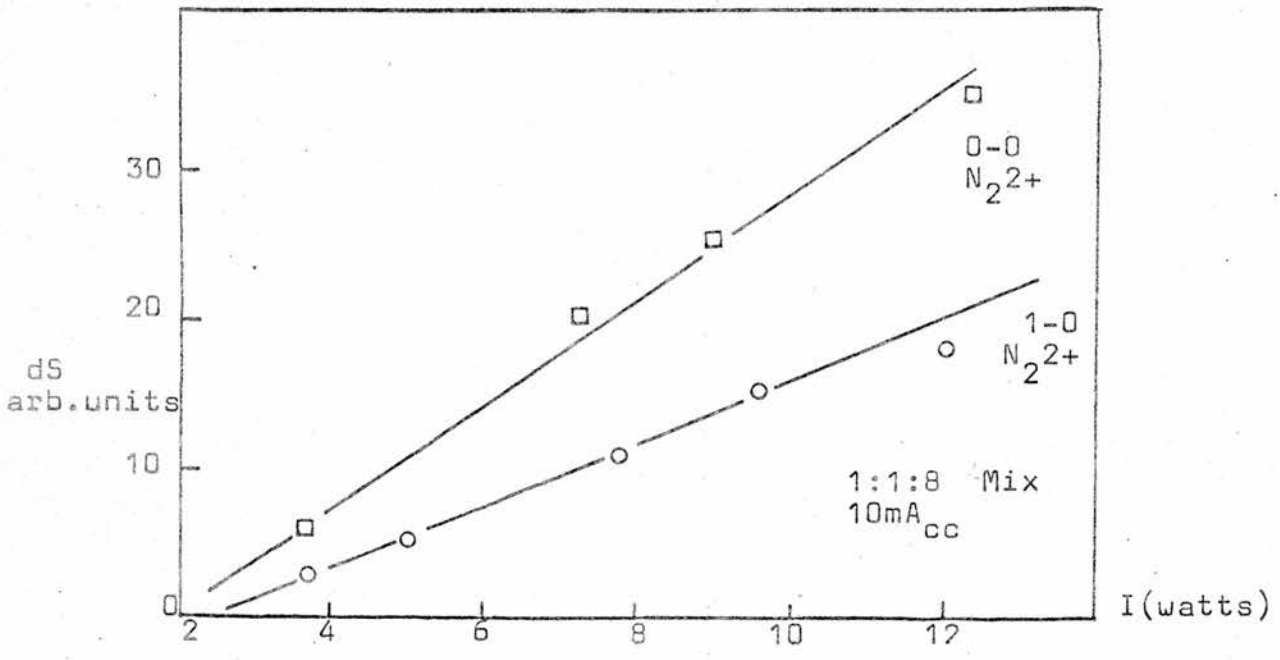

Fig. 10.5

Input power versus dS for a 1:1:8 Mix.

unwanted current effects. It is thought that this may be due to the difference in which the value of the mean electron energy (or $\frac{E}{p}$) in the discharge is changed, since this quantity has a very direct influence on the pumping of molecules to the optically excited states.

No switching in polarity of the perturbed sidelight under voltage controlled conditions was observed with any of the three or four part mixtures, Crane (7) however observed this behaviour in a flowing gas system with low helium content and obtained a curve remarkably similar to (a) in Fig. 10.2. This was in a system excited by what is described as a 'controlled dc supply' which from the nature of the text one would take to be incapable of supplying a constant current.

Although the present system does not allow large current changes it does not prevent variations in voltage occurring across the discharge cell (and hence variations in $\frac{E}{p}$ and electron energy). This point must be taken into consideration in the discussion below of $N_2 2+$ sidelight results obtained in the current controlled mode.

Section 9.2 makes the point that in a perturbation spectrum:

(a) Spontaneous emission from the 0 - V and 1 - V bands is positive.

(b) The intensity of such emission is greater at lower equilibrium vibrational temperatures.

An examination of the 0 - V and 1 - V transitions in all mixes used showed them to be positive in polarity at currents in excess of approximately 5 mA. They all exhibited similar behaviour

to the curves (a) and (b) shown in Fig. 10.2, with a pronounced maximum at 10 to 20 mA, and inversio n at around 5 mA. In this respect the curves were very similar to gain-current curves which one would expect for these mixtures. Bleekrode (28) showed that the maximum change in intensity of the band heads of the $N_2$2+ system, i.e. maximum change in $C^3\Pi u$ vibrational temperature of approximately 400^oK, occurred at the same current at which maximum output power, and therefore gain, was obtained in his laser. The inversion of the lines, however, at currents of 5 mA and less is not easily explained. The model described in chapter 9 does not predict this effect. If it were a simple change from gain to absorption in the medium at these low currents, then the model shows that negative perturbations would become positive and vice versa due to pumping of the N_2 $X^1\Sigma_g^+$ levels and consequent vibrational temperature rise. In fact all $N_2$2+ transitions are negative in these low current regions. It appears that assumptions of both constant electron number density and energy distribution is not valid. Certainly the energy distribution must be altered since the potential across the tube is changed due to 10.6μm induced impedance changes in the discharge.

Fig. 10.5 shows a plot of sidelight intensity against power input at 10.6μm for the $N_2$2+ 0 - 0 and 1 - 0 transitions at 10 mA in the cc mode; the relationship appears to be linear. The intensities of these transitions are proportional to the gain of the active medium over this range of input powers. Other transitions in the $N_2$2+ system exhibited a similar behaviour in agreement with the findings of Bletzinger (10).

10.6 Xe Perturbations

A sidelight scan of a mixture containing CO_2 : N_2 : Xe and He in the ratio 1:1:1:7 showed transitions in the Xe I spectrum at 8231Å, 8280Å and 8819Å corresponding to transitions with upper energy levels of 9.82, 9.94 and 9.72eV in the 2p state of Xe (64) and lower levels in the 1s state. These are the $2p_6$ - $1s_5$, $2p_5$ - $1s_4$, and $2p_8$ - $1s_5$ respectively.

Sidelight perturbation scans in either cc or cv modes showed perturbations to the spontaneous sidelight at these wavelengths; this has not been previously reported. The perturbation intensities were 5 to 12 times as intense as the strongest $N_2$2+ transitions although the relative perturbation intensities for all transitions was around 5%. Typical experimental results are shown in Figs. 10.6 and 10.7. The Xe sidelight perturbation intensity is a linear function of 10.6μm input power and varies with discharge current in the cc mode as shown in 10.7. The energy levels involved in the 2p state of Xe do not lie close in energy to any of the N_2 or CO electronic states which appears to rule out the possibility of collisional interactions with these different molecules. In a discharge containing Xe the $N_2$2+ 0 - V and 1 - V perturbation transitions were reduced by about a factor of 5 times in intensity for conditions similar to those in a 1:1:8 mix without added Xe. Moreover, they were negative in polarity along with the remaining $N_2$2+ transitions between 5 and 40 mA. The xenon transitions were similar in polarity to those of the $N_2$2+ and CO Angstrom band.

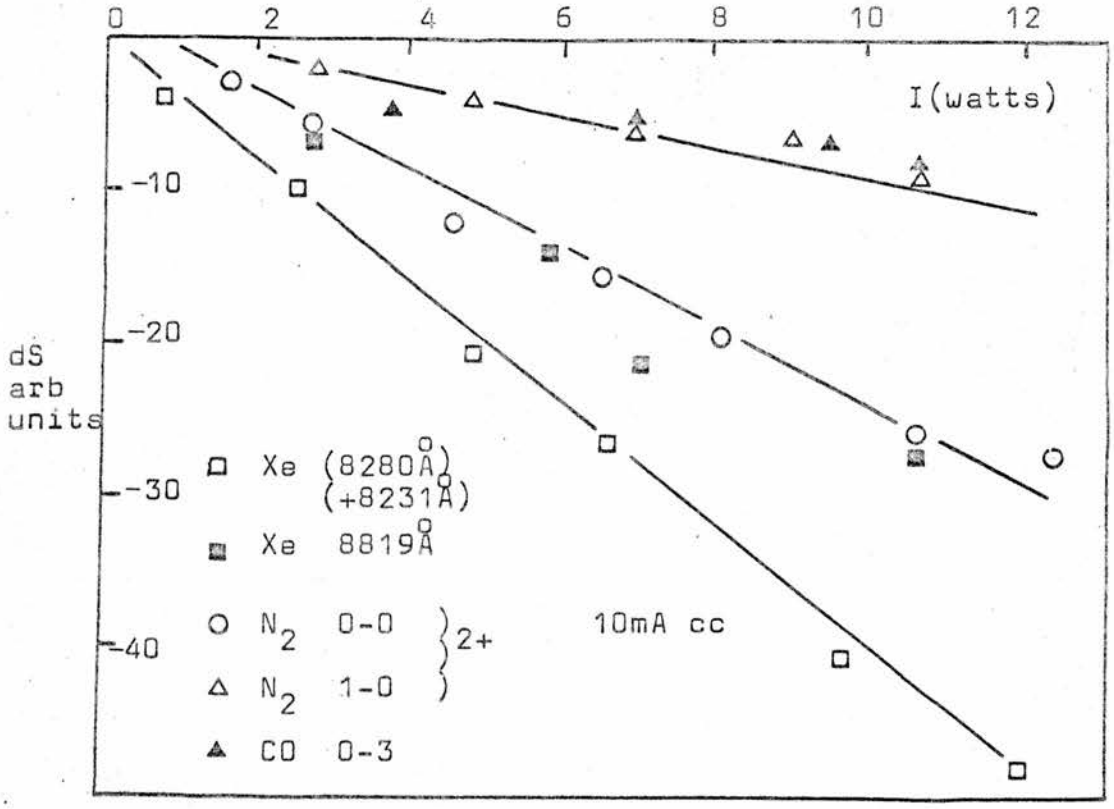

Fig. 10.6

Variation of sidelight perturbations for some transitions in a 1:1:1:7, CO_2:N_2:Xe:He mix with I.

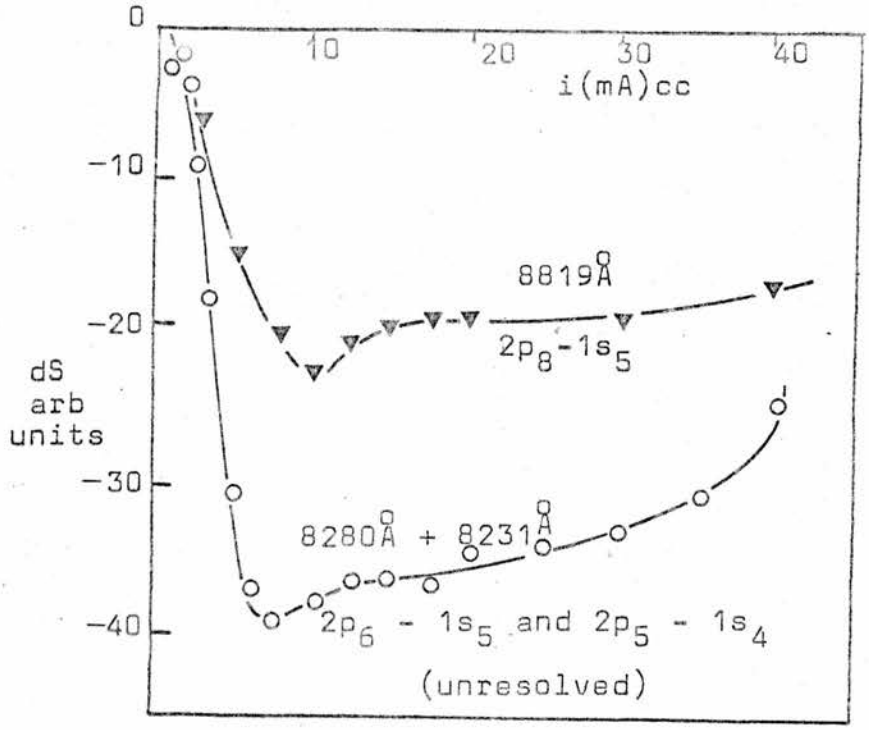

Fig. 10.7

Variation of Xe sidelight perturbations with i in a four part mix.

Xenon affects a CO_2 discharge by lowering the mean electron energy and producing a greater number of electrons (40), which would lead to an increased pumping of the ground electronic vibrational states of CO and N_2. This would account for the general increase in intensity of the transitions $V \rightarrow n$ ($V>1$), in the $N_2 2+$ perturbation spectrum. The mechanism by which Xenon transitions are perturbed, however, is by no means clear. The medium is in a gain condition and hence will have its impedance increased by the 10.6μm field. The resulting change in the value of $\frac{E}{p}$ (i.e. electron energy), may be instrumental in affecting the pumping of the Xe 2p atomic levels, or levels which feed them by radiative cascade. The omission of nitrogen in the gas mixture (i.e. 1:1:8, CO_2 : Xe : He) appeared to enhance the intensity of the Xenon perturbations by a factor of 2, its polarity was unaffected. With CO_2 missing from the active medium (i.e. 1:1:8, N_2 : Xe : He mix) no sidelight perturbation signals from any of the gas species present was observed.

10.7 Summary and Discussion

The above set of experiments constituted the main part of this work which was carried out on the sidelight properties of CO_2 laser discharges. Some additional results on vibrational temperatures appear in Appendix A.4; the following summary will be confined to the above experiments, however. It has been shown that in order to study the interaction between vibrationally excited molecules and the perturbing laser field, the massive current perturbations in the active medium must be eliminated. Two methods are possible; either the discharge is activated by a dc current controlled supply which does not

allow current changes in the plasma by more than fractions of a percent, or by the use of expressions such as equation 7.1. Neither technique is entirely satisfactory since the former unavoidably introduces changes in $\frac{E}{p}$ in the discharge which lead to a perturbation of the electron energy distribution whilst the latter relies on an initial assumption that only current and 10.6μm field intensity are factors which affect sidelight intensity.

Section 10.5 compared the above two methods of examining sidelight spectra and found them incompatible; in the particular transitions examined in the $N_2$2+ band and CO Angstrom band there was disagreement between the measured quantity dS_{cc} and the calculated quantity $(\frac{\partial S}{\partial I})_i dI$. It is not immediately apparent why this disagreement occurs but it is probably due to the difference in the $\frac{E}{p}$ changes created in the two discharge modes (cc and cv) by the perturbing field. In calculating $(\frac{\partial S}{\partial I})_i dI$ no account is taken of such a variation in the discharge condition when running in the cv mode.

The results presented above which were obtained in the cc discharge mode can be qualitatively explained purely in terms of collisional interactions in the ground electronic states of CO_2, N_2 and CO. The perturbing field may be regarded as producing a change in the population distributions in the electronic ground state vibrational levels; in the case of N_2 this change may be described in terms of a vibrational temperature change. Use was made of these concepts to predict possible population distributions in the CO $A^1\Pi$ and $N_2 C^3\Pi_u$ electronic levels for various vibrational temperatures in the $X^1\Sigma_g^+$ ground electronic states. By knowing the approximate

vibrational temperature change brought about in the $X^1\Sigma_g^+$ state of N_2 it was possible to calculate the associated relative changes in the vibrational populations of the $C^3\Pi_u$ state and hence explain the polarity of optical transitions in the $N_2$2+ system ($C^3\Pi_u$ - $B^3\Pi_g$). This explanation agreed qualitatively with experimental data obtained in the cc discharge mode, but was unable to account for the switch in polarity of the 0 - V and 1 - V transitions at low current values. The assumption of constant electronic impact pumping in both irradiated and non-irradiated conditions is thought to be a possible reason for this discrepancy, for it is at low current values where the plasma becomes unstable that it is least likely to be accurate.

It is believed that in the cc mode the intensity of the sidelight transitions in the $N_2$2+ system are related to the gain of the active medium for two reasons:

(i) The intensity of such transitions was shown (e.g. see Fig. 10.5), to be proportional to the input power of the 10.6μm field, and

(ii) Their behaviour as a function of current in the cc discharge mode closely resembled the gain curve which one would expect such an active medium to possess.

Unfortunately no measurements of gain were performed in the present system so an absolute verification of this argument cannot be made here. To illustrate the relevance of the model described in chapter 9, it is worthwhile examining quantitatively the data from a typical sidelight perturbation scan (see Fig. 10.8) in a 1:1:8 mixture containing 0.25 torr of H_2, running at 10 mA in the cc mode. The perturbation intensities of the various transitions are denoted by $dI_{V}1_{V}11$, those of a particular band

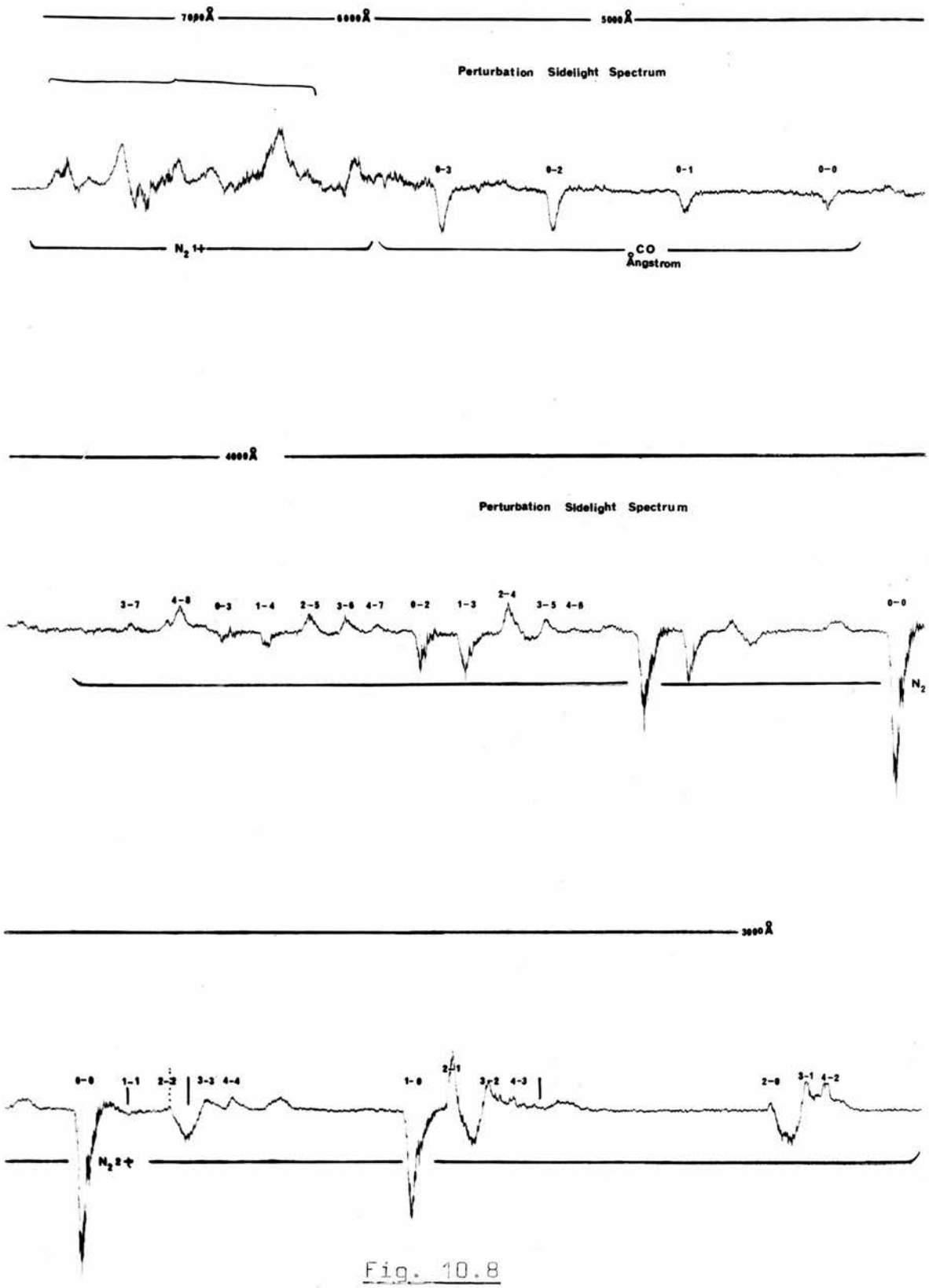

Fig. 10.8

Perturbation Sidelight Spectrum in a 1-1-0.25-7.75 CO_2 : N_2 : H_2 : He mix at 10mA cc.

as $\sum_{v^{11}=0}^{n} dI_{v^1 v^{11}}$. The intensity of a vibrational electronic transition is given by $I_{v^1 v^{11}} = N_{v^1} A_{v^1 v^{11}} E_{v^1 v^{11}}$, where $A_{v^1 v^{11}}$ is the Einstein A coefficient for the $v^1 \longrightarrow v^{11}$ dipole transition. N_{v^1} is the population of the v^1 level and $E_{v^1 v^{11}}$ is the energy separation of the $v^1 \rightarrow v^{11}$ transition. Table 7 illustrates the observed and calculated values of the sum of the intensities $\sum dI_{v^1 v^{11}}$ in a given band.

TABLE 7

Band	Intensity $\sum_{v^{11}=0}^{4} dI_{v^1 v^{11}}$		Relative Intensity $\sum dI_{0-v^{11}} / \sum dI_{v^1 - v^{11}}$	
	Meas. arb units	Calc. arb units	Meas.	Calc.
$0-v^{11}$	- 60	- 498	1.0	1.0
$1-v^{11}$	- 43	- 350	0.71	0.70
$2-v^{11}$	+ 28	+ 246	0.47	0.49
$3-v^{11}$	+ 22	+ 170	0.37	0.34
$4-v^{11}$	+ 12	+ 189	0.20	0.26

To calculate the relative intensities a value for the population density change in the v^1 levels was taken from the model assuming a non-lasing vibrational temperature of 1400°K and a lasing temperature of 1200°K. The choice of temperatures was aided by reference to Bleekrode (28) and Novgorodov et al (50). At this particular choice of gas temperature and discharge current the model predicts quite accurately the polarity and relative intensity of the $N_2$2+ bands.

The Xenon transitions were not able to be explained on the grounds of collisional interactions between the optically excited states in the Xe atoms and those in the N_2 and CO molecules

because of the lack of coincidence in these energy levels. The transitions are proportional in intensity to the 10.6μm input power and might therefore be related to the gain of the medium. However they appear to be a slowly varying function of discharge current above 10 mA (see Fig. 10.6),unlike the $N_2$2+ transitions in Fig. 10.3.

11. CONCLUSION

This final chapter provides a summary of the present work and emphasises the difficulties in interpreting the results actually obtained; it also indicates areas where further investigation might prove useful.

The discharge plasma in a multi-component gas mixture containing CO_2 is of a very complex nature. As well as collisional interactions of the various molecular species there are dissociative and associative chemical effects, and interactions between the electron gas and atoms and molecules with energies in the range of 10^{-1} up to 10 eV or greater. The plasma has a relatively low electron density but large electron-molecule collision cross-sections resulting in many highly populated vibrational energy levels. It may be described by considering three types of temperature (translational, rotational and vibrational) relating to the gas molecules, and the highly non-Maxwellian nature of the electron energy distribution. The electronic states of N_2 and CO which give rise to the optical transitions in the sidelight spectrum are known to have an insignificant role in the establishment of a population inversion in an active medium containing CO_2, N_2 and He. However, they are closely coupled to the primary laser levels as revealed by the modulation of spontaneously emitted sidelight radiation in the region 2000 to 10,000Å, when the 10.6μm radiation field intensity in the active medium is modulated. It is the mechanism of this coupling which the present work set out to explain.

Because of the high gain of the CO_2 system there is considerable interaction between the laser field and the

discharge current used to excite the medium. Immediately problems concerning the effect of massive discharge current changes on interpretation of sidelight perturbations present themselves. In order to study the direct interactions between molecules in the discharge and the irradiating field, experiments were carried out using a power supply which provided a constant current to the discharge under changing load conditions. Due to the lack of a clear explanation why the 10.6μm field produced changes in discharge current, a series of experiments was also performed to investigate this effect. The following discussion will first examine conclusions resulting from the current and pressure perturbation experiments, and will then go on to discuss the sidelight data.

11.1 Current and Pressure Perturbations

The series of experiments described in chapter 5 demonstrated the effect of pressure perturbations on the current flow through a dc excited discharge. The experiments under cc conditions showed that pressure changes could be generated in the absence of current perturbations by the interaction of the 10.6μm field and the CO_2 laser levels. Allowing the current to change in the cv mode produced amplified pressure changes which could be explained using equation 5.4, where:

$$\frac{dp}{p} = \left(\frac{\partial p}{\partial I}\right)_i dI + \left(\frac{\partial p}{\partial i}\right)_I di$$

Quantitative interpretation of $\frac{dp}{p}$ and $\frac{di}{i}$ data is difficult. Because of the geometry of the cell a correction factor must be applied to the measured values of $\frac{dp}{p}$ in order to ascertain the value of pressure changes in the active irradiated part of the discharge volume. The true current change in the discharge is amplified due to the nature of the impedance—

current characteristic as discussed in section 5.6 and the value of this amplification factor was not determined. Graphs such as 5.16 and 5.17 can therefore only illustrate the semi-quantitative nature of the dependence of $\frac{di}{i}$ on $\frac{dp}{p}$. At currents in excess of 20mA the relative pressure and current changes are approximately linearly related with slopes of between -0.3 for the xenon mix and -1.5 for the helium mix; they are smaller than the expected slope of -2 given from equation 5.10:

$$\frac{dp}{p} = \frac{1}{4} \frac{dX}{X} - \frac{1}{2} \frac{di}{i}$$

for very small values of $\frac{dX}{X}$. It is apparant that equation 5.10 does not provide a complete explanation as to the interaction of gas pressure and current change. Certainly the parameter $\frac{dX}{X}$ must have a value which is of the same order of magnitude as $\frac{di}{i}$ and $\frac{dp}{p}$ at low discharge currents. $\frac{dX}{X}$ will exhibit maximum changes in current regions where either the electron energy distribution changes markedly (e.g. at very low currents) or where there is a maximum perturbation in laser level populations (e.g. at the peak of the gain curve). It is expected that both these effects would occur at currents below 20mA for the above active media, in the non-linear region of the $\frac{di}{i}$ versus $\frac{dp}{p}$ plots. Both a change in gas pressure (or number density) and a change in the energy lost per electron molecule collision (due to a perturbation in vibrational populations or electron energy distribution), would result in a change in discharge current. Although all of these factors must be involved, it would appear from the above results that at currents beyond those where the medium exhibits maximum gain it is a change in molecular translational temperature which produces pressure changes and hence alters the electron mean free

path and thence the current. The parameter $\frac{dX}{X}$ has a relatively insignificant contribution. However, at low currents and in the region of maximum gain, the change in vibrational temperature due to the influence of the 10.6μm field results in a much greater change in $\frac{dX}{X}$ and it becomes a significant mechanism in altering the discharge current. All three quantities in equation 5.10 are then highly current dependent. The electron energy distribution in both cc and cv discharge modes is greatly altered in this latter condition which must affect the pumping of the electronic levels giving rise to optical transitions in the N_2 and CO spectra.

11.2 Sidelight Perturbations

By eliminating large current changes it was possible to study the influence of the 10.6μm field on the vibrational populations of both the ground and electronically excited states in discharges containing CO_2. A current controlled power supply enabled current changes to be kept down to fractions of a per cent. This method of obtaining data was favoured over that due to Crane et al (12), since the quantity dS_{cc} could be measured directly without the necessity of obtaining curves of current perturbations and static sidelight characteristics with their additional experimental errors. A comparison of the two methods showed a disagreement in the variation of dS_{cc} with current which could not be accounted for by experimental error alone. It is believed that the magnitude of laser field induced changes in $\frac{E}{p}$ (and hence electron energy distribution), will differ according to which mode (cc or cv) the discharge is operated in, and hence the associated change in electron impact excitation will also be different. The behaviour of the

$N_2$2+ and 1+ bands and CO Angstrom band sidelight perturbations was investigated in both current and voltage controlled discharge modes. The cc data was interpreted in a more detailed fashion by, (i) considering vibrational population distribution changes in the ground electronic states of CO and N_2 due to intermolecular energy exchange with the CO_2 laser levels, and (ii) assuming electron impact excitation from ground to optically excited levels with excitation cross-sections proportional to the appropriate Franck Condon factor. The polarity of all observed sidelight perturbations was thus able to be explained in both absorption and gain conditions, but the observed switching in polarity of the $N_2$2+ 0 - V and 1 - V transitions was not explicable solely in terms of electronic ground state vibrational population changes.

The intensity of a $N_2$2+ transition appears to be dependent on the gain of the active medium since it is proportional to 10.6μm input power (cf $(\frac{dp}{p})_{cc}$) and its variation with current resembles that of the gain curve one would expect such a medium to exhibit. Some additional gain data on the absorption cell used for these experiments would have proved useful in confirming this argument. It would also be of value to know if the maximum change in vibrational temperature coincided with the peaks in both the gain curve and in the $N_2$2+ perturbation sidelight intensity curve, Fig.10.2. Further data on vibrational temperature changes would be useful for quantitative comparison with the model described in chapter 9 to determine its range of validity. The model itself could be improved by considering the effect of a variation in electron energy distribution on the populations $N_{V_c}1$.

The perturbation to the XeI atomic transitions (2p-1s) has not been reported before. They were observed in the cc as well as cv discharge mode and do not appear to be due to atom-molecule collisions; they may be caused by a perturbation introduced to the electron energy distribution. If this is so, then such sidelight intensity changes ought to be observed in spectra of other possible gas additives such as Argon or Krypton.

11.3 Summary

This work serves to illustrate some problems involved in obtaining and interpreting data from a molecular discharge capable of exhibiting high optical gain. It is the phenomenon of tight coupling between the 10.6μm field and the vibrational populations of molecules present which introduces perturbations to the discharge current (~6%), gas pressure (~0.2%), kinetic and vibrational temperatures (1% and 15% respectively), and spontaneous sidelight (5%). Any method used to control the discharge parameters itself introduces a perturbation to the system. For example, the discharge current through the medium is held constant only as a result of increasing the voltage across it, and pressure changes are unavoidable in either discharge mode. However, by minimising the macroscopic changes in the active medium, the experimental technique used in this work makes it possible to investigate the direct interaction between the laser radiation field and molecular vibrational and electronic states. Resulting data was able to be interpreted in terms of microscopic parameters describing the molecules such as collisional relaxation processes, and also in terms of gas kinetic and vibrational temperature

changes. It should be possible to extend the technique to other molecular gas laser systems such as CO and HCN.

The dependence of sidelight properties on the gain of the active medium has been mentioned by several authors (for example 66, 67, 68) as having practical uses. Thomason (67) in a recent paper used the variation in impedance of a laser plasma tube to frequency stabilise a CO_2 laser. Stefanov (68) has used current changes to detect the presence of laser action and to optimise mirror alignment. He suggests that such a technique might be particularly suitable for devices operating in the far infra-red where suitably sensitive optical detectors were not available. It would appear possible that in a cc controlled discharge maximum gain is obtained where vibrational temperature changes (28) and therefore sidelight changes, are a maximum. Hence by monitoring the optical sidelight of a device, its output power at a different wavelength could be optimised.

A.1 SATURATION EFFECTS IN THE MEDIUM

The saturation parameter Is in the equation

$\alpha = \alpha_o(1+\frac{I}{Is})^{-\gamma}$; ($\alpha = \alpha(\lambda)$ is the gain coefficient, $\gamma = 1$ for homogeneous broadening, $\gamma = \frac{1}{2}$ for inhomogeneous broadening, and α_o = the small signal gain coefficient), is defined as the value of the radiation field intensity I in the active medium at which the gain coefficient becomes half the value of the small signal gain coefficient α_o. The work of Christensen et al (60) gives a value of Is of between 25 and 100 watts cm^{-2} at beam widths of 1.8 mm and 5 mm respectively in a sealed amplifier containing CO_2:N_2: He :H_2 (1.4: 1.7 : 7.0 : 0.2) at 10.3 torr. These figures are comparable with the irradiating intensities, I, used in the present experiments in which the laser beam width was 3 mm before entering the evacuated absorption cell, and became 8 mm after passing out of the exit window. The introduction of 10 torr of CO_2 did not noticeably change the output beam width. The upper and lower limits of the field intensity inside the cell at beam widths of 3 and 8 mm respectively are then 200 and 30 watts cm^{-2}. For inhomogeneous broadening the gain coefficient for I = 20 watts cm^{-2}, beam width = 0.5 mm will be $\alpha = \alpha_o(1-\frac{I}{2Is})$ substituting in the above values,

$$\alpha = \alpha_o \left(1 - \frac{1}{2} \cdot \frac{20}{100}\right)$$

and so $\alpha = 0.9\alpha_o$

The error in measuring $\frac{dp}{p}$ at all powers I is about 10% which may account for the lack of positive identification of the effects of gain saturation, see Figs. A.1 to A.4, because of:

(1) The lack of information describing changes in beam width inside the active medium.

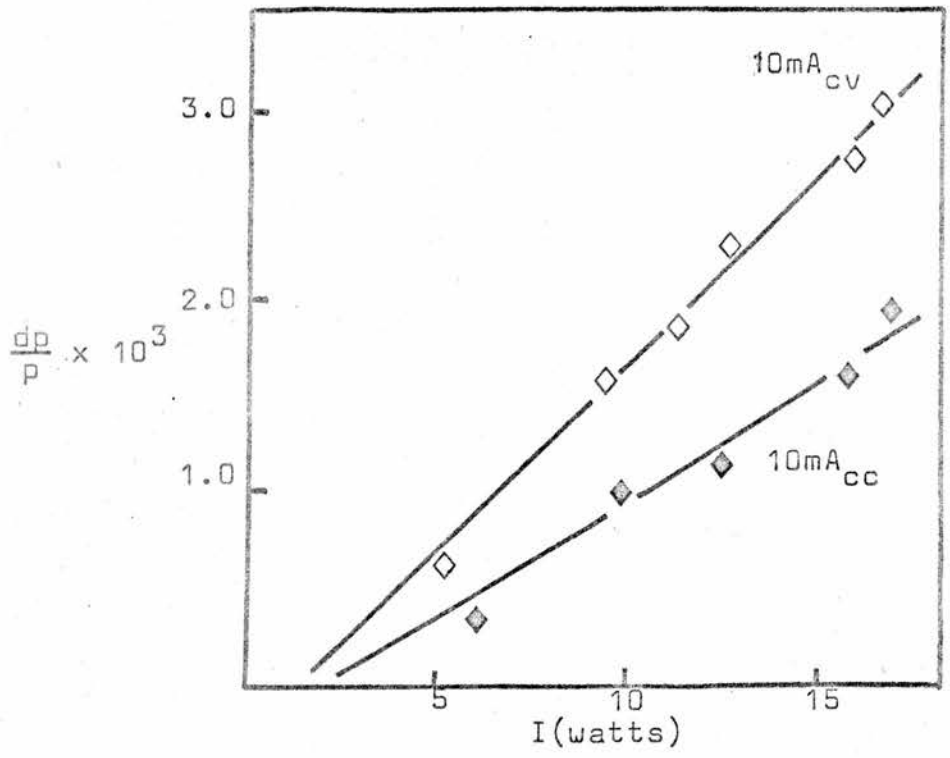

Fig. A.1
Variation of $\frac{dp}{p}$ (cv mode) with input power I. 1:1:8 (10 torr) $CO_2:N_2:He$; τ = 35 ms.

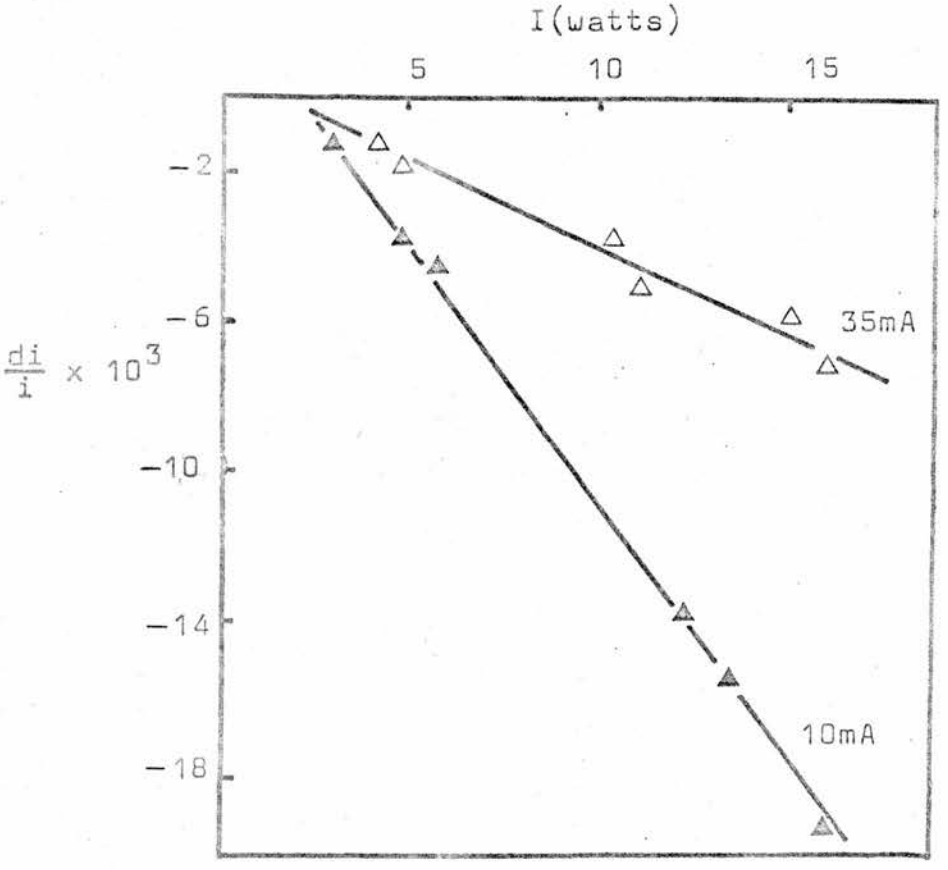

Fig. A.2
Variation of $\frac{di}{i}$ with input power I 1:1:8(10 torr) $CO_2:N_2:He$, τ = 35 ms.

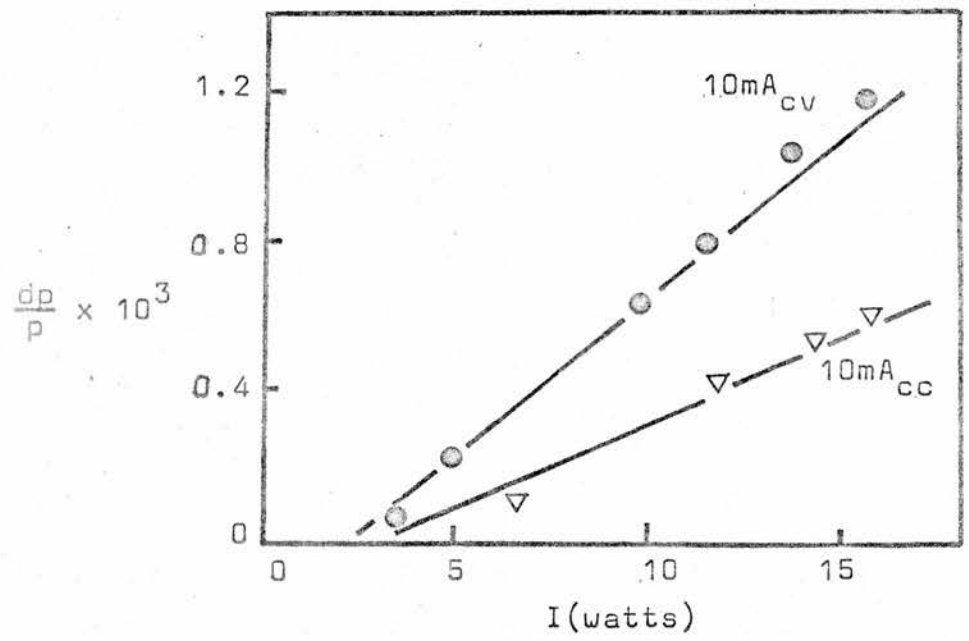

Fig. A.3

Variation of $\frac{dp}{p}$ with input power I. 1:1:1:7 (10 torr), CO_2:N_2:Xe:He. τ = 35 ms.

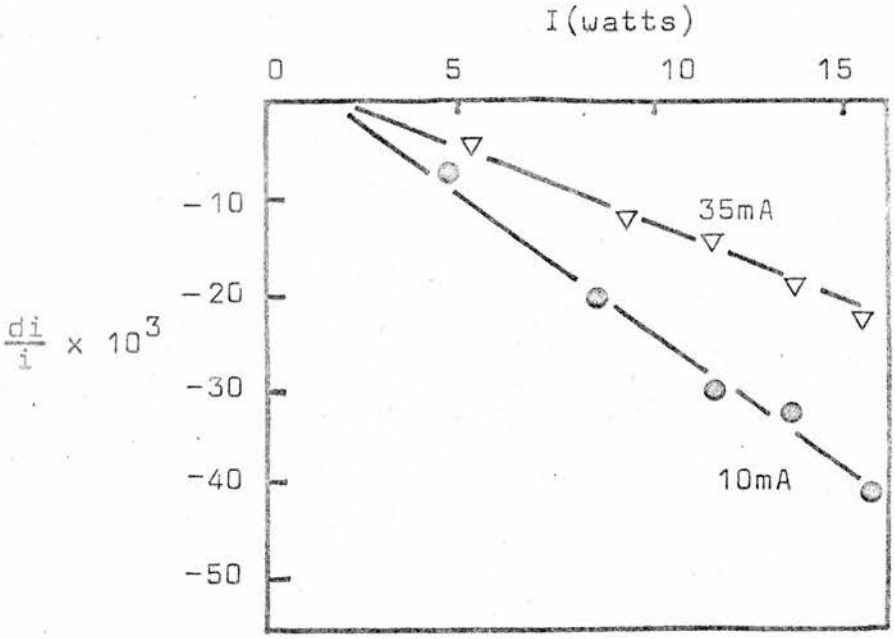

Fig. A.4

Variation of $\frac{di}{i}$ with input power I. 1:1:1:7 (10 torr) CO_2:N_2:Xe:He. τ = 35 ms.

(ii) The fact that the transition is homogeneously as well as inhomogeneously broadened.

(iii) The fact that the gain coefficient is modified due to diffusion processes and the coupling of the oscillating rotational vibrational transitions with others present, it is difficult to obtain an accurate figure for I_s; 100 watts cm^{-2} may be too small a value in the case of the present system.

A.2 CORRECTION APPLIED TO $\frac{dp}{p}$ CURVES

The gas pressure fluctuations dp, measured by the MDC manometer are not equal in magnitude to those occurring in the active irradiated volume of discharge. This is due to the fact that the laser beam only irradiates a fraction of the volume of discharge (and dead space), and the induced pressure (or number density) change taking place in this fractional volume is finally detected as a diminished change in pressure in the total volume of the cell. We must take into consideration the volume of gas available to interact both directly and indirectly with the radiation field.

The on-time of the laser field was normally $\frac{\tau_i}{2} \approx 17$ ms, and CO_2 molecules in the primary laser levels can diffuse from a non-irradiated to an irradiated volume in this period of time. The following calculations show typical diffusion path lengths for CO_2 molecules in the gas mixtures of interest. Using the formula given by Present (61) the diffusion coefficients, D, of CO_2 in a nominal 10 torr cold fill of pure CO_2 (assumed for simplicity to become 1 torr of CO_2 and 9 torr of CO at a current and pressure of 10 to 20 mA and 10 torr respectively - we neglect the oxygen partial pressure) , and in a CO_2, He mixture (no dissociation) were calculated and appear in Table A.1. The parameter $\bar{x}$ is the diffusion length, i.e. the average distance a CO_2 molecule can travel in a time of 17 ms. It is assumed that the average beam diameter in the cell is 5 mm and that the gas kinetic temperatures are $750^{o}K$ for 'pure' CO_2 and $400^{o}K$ in the helium mix.

TABLE A.1

Gas	T ^{o}K	P torr	D cm^2s^{-1}	$\bar{x}$ cm
CO_2 : CO	750	10 (1:9)	46	1.25
CO_2 : He	400	10 (1:9)	68	1.52

The table may be interpreted as follows. During the on-time of the laser field a CO_2 molecule can travel a distance of 1.25 or 1.52 cm depending on the active medium, hence the effective volume of gas which can interact with the radiation field is enclosed by an external radius r which depends on D, see Fig. A.5.

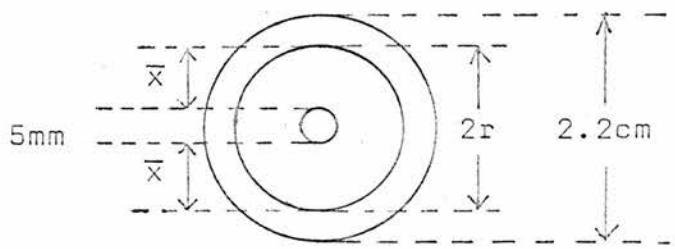

Hence r $\approx$15 mm and 18 mm in CO_2 : CO and CO_2 : He discharges respectively. Since the tube radius is 11 mm all the gas is effectively irradiated. Similarly in the non-active irradiated volumes (Fig. A.6) all of the gas volume is irradiated. For all the gas mixtures involved

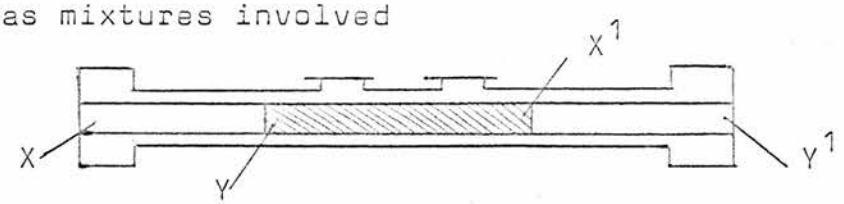

Fig. A.6

gas in these dead spaces (XY and X^1Y^1) is heated by the laser field giving a pressure change which is given approximately by the value of dp when the discharge current is zero dp^1 (i= 0). In a CO_2 : CO discharge this expansion is less than or equal to that occurring in the active discharge region

when current is flowing - see Fig. 5.7. For gas mixtures in a gain condition there is a decrease in pressure in regions XY and X^1Y^1 (due to gas expansion) and an increase in pressure in the remaining volume where there is optical gain. The correction to the measured perturbed pressure dp^1 will be of the form

$$dp(i) = dp^1(i) \frac{V_o}{V_i} + dp^1 \ (i = 0) \qquad \ldots\ldots A.1$$

where V_i is the volume of discharge irradiated and V_o is the total system volume. Table A.2 gives correction factors for the gas mixtures.

TABLE A.2.

Gas	$10^3 \times dp^1(i=0)$	V_o/V_i
CO_2 : CO	- 3.5	6.5
CO_2 : N_2 : He	+ 0.9	
+ H_2	+ 0.35	
+ Xe	+ 0.6	

A.3 FRANCK CONDON FACTORS

The Einstein A coefficient $A_{v^1 v^{11}}$ for the v^1-v^{11} band of an electric dipole band system is given by,

$$A_{v^1 v^{11}} = \frac{C\, S_{v^1 v^{11}}}{\lambda^3 v^1 v^{11}} \quad s^{-1} \qquad \ldots\ldots \text{A.2}$$

where g_u is the upper level degeneracy and the band strength $S_{v^1 v^{11}}$ is defined by,

$$S_{v^1 v^{11}} = \left| \int \psi_{v^1} \; R_e(r) \psi_{v^{11}} dr \right|^2 \qquad \ldots\ldots \text{A.3}$$

ψ_{v^1} and $\psi_{v^{11}}$ are wave functions of the v^1 and v^{11} vibrational levels; $R_e(r)$ is the electronic transition moment of the band system and is a measure of the total change in electron distribution in a transition. Equation A.3 may be rewritten as,

$$S_{v^1 v^{11}} = R_e^2(r) \left| \int \psi_{v^1} \psi_{v^{11}} dr \right|^2 = R_e^2(r)\, q_{v^1 v^{11}} \qquad \ldots\ldots\ldots \text{A.4}$$

where the vibrational overlap integral square is

$$q_{v^1 v^{11}} = \left| \int \psi_{v^1} \psi_{v^{11}} \right|^2 \qquad \ldots\ldots\ldots \text{A.5}$$

and is called the Franck Condon factor of the band.

It is assumed that $R_e(r)$ is a very slowly varying function of r and thus for each of the v^1 - v^{11} bands

$$\int \psi_{v^1} . R_e(r) . \psi_{v^{11}} dr = \bar{R}_e \int \psi_{v^1} \psi_{v^{11}} dr$$

where $\bar{R}_e(r)$ is the average of this slowly varying function over the relevant range of r .

The integrated intensity of a molecular band $I_{v^1 v^{11}}$ may be defined as,

$$I_{v^1 v^{11}} = N_{v^1} A_{v^1 v^{11}} E_{v^1 v^{11}} = N_{v^1} E^4_{v^1 v^{11}} R_e^2(r) q_{v^1 v^{11}} \qquad \ldots\ldots \text{A.6}$$

Here $q_{v^1 v^{11}}$ may vary by many orders of magnitude across the whole band system whilst other factors vary less, and hence $q_{v^1 v^{11}}$ exerts a dominating influence on the intensity distribution

of the band system. In electron excitation proceses between two states with vibrational levels V^1 and V^{11} the excitation probability between such states is nearly proportional to the Franck Condon factor for that transition. Novgorodov et al (50) took the excitation probability between vibrational levels V^{11}_x and V^1_c of the $X^1\Sigma^{1+}_g$ and $C^3\Pi_u$ states of N_2 to be proportional to the Franck Condon factors for the Tanak system $C^3\Pi_u - X^1\Sigma^{+}_g$; i.e. took $\langle v\, \sigma \rangle_{V^{11}_x\, V^1_c} \propto q_{V^1_c V^{11}_x}$. This assumption is also adopted in chapter 9 of the present work.

A.4 VIBRATIONAL TEMPERATURES

An adaptation of the technique due to Weiss et al (48) was used to determine the vibrational temperatures in the $C^3\Pi u$ state of N_2 in a three part mix (1-1-8) of CO_2, N_2 and He. Weiss et al measured the band head intensities of $N_2 2+$ transitions in the spontaneous sidelight of a CO_2 laser discharge under cw lasing and non lasing conditions. If a Boltzmann distribution of populations in the $C^3\Pi u$ state of N_2 is assumed, then the ratio of the populations in the V'th vibrational level for two temperatures T and T^1 (non-lasing and lasing respectively) is given by:

$$\frac{N_V(T)}{N_V(T^1)} = \left[\frac{E^V}{(1-E)^{-1}}\right] \cdot \left[\frac{(1-E^1)^{-1}}{(E^1)^V}\right] \qquad \ldots\ldots\ldots \text{A.6}$$

where $E = \exp(-h\nu/kT)$

Taking the intensity of a transition $V_c^1 \longrightarrow V_B^{11}$ to be proportional to the population in the $N_{V_c}1$ level we have,

$$\ln\left[\frac{I_V(T)}{I_V(T^1)}\right] = \ln\left[\frac{N_V(T)}{N_V(T^1)}\right] = V\ln\left[\frac{E}{E^1}\right] + \ln\left[\frac{1-E}{1-E^1}\right] \qquad \ldots \text{A.7}$$

Hence a log-linear plot of the ratio of the non-lasing to lasing band head intensities of the vibrational electronic transitions $(V \rightarrow n)$ in the $N_2 2+$ system against upper level vibrational quantum number V is linear and the slope and intercept determine the values of T and T^1. In the present work the quantity dI is measured for each transition $V_c^1 \longrightarrow V_B^{11}$ and we take $dI = I - I^1$

where I = spontaneous emission intensity with the discharge not irradiated

I^1 = spontaneous emission intensity with the discharge irradiated.

Hence $$\frac{I_V(T)}{I_V(T^1)} = \frac{I^1 + dI}{I^1} \qquad \ldots\ldots \text{A.8}$$

Table A.2 gives a summary of the results.

TABLE A.2

Discharge Mode	T ^{o}K	T^{1} ^{o}K	dT ^{o}K
10mA cc	4650	4500	150
10mA cv	4800	4450	350

It may be seen that the temperatures measured are higher than those obtained by Bleekrode (28) in a somewhat similar system ($2600^{o}K$). However, the temperature difference between the lasing and non-lasing conditions is in reasonable agreement ($\sim 250^{o}K$). In the present experiment it is felt that a truer indication of the effect of the laser field alone on the populations in the $C^{3}\Pi u$ state is given by temperatures obtained in the cc discharge mode.

REFERENCES

(1) Parks J.H. and Javan A. Phys.Rev. 139, 5A 1351-1358 1965.

(2) Weaver L.A. and Frieberg R.J. J.App. Phys. 37, 4, 1528-1535 1966.

(3) Khaikin A.S. Sov.Phys. J.E.T.P. 24, 1, 25-32 1967.

(4) Khaikin A.S. Sov.Phys. J.E.T.P. 27, 1, 28-33 1968.

(5) Freiberg R.J. and Weaver L.A. J.App.Phys. 38, 1, 250-262 1967.

(6) Rigden J.D. and Moeller G. J. Quant. Elec. 2, 365-369 1966.

(7) Crane R.A. and Waksberg A.L. App.Phys.Lett. 10, 9, 237-239 1967.

(8) Carswell A.I. and Wood J.I. J. App. Phys. 38, 3028-3030 1967.

(9) Garscadden A.and Adams S.L. Proc. I.E.E.E.(Lett.) 54, 427-428 1966.

(10) Bletzinger P. and Garscadden A. Proc. I.E.E.E.(Lett.) 1966.

(11) Crane R.A. Canadian J. Phys. 47, 2785 - 2788 1969.

(12) Crane R.A. and Waksberg A.L. Canadian J. Phys. 50, 3067-3069 1972.

(13) Kindl H. et al Proc. I.E.E.E.(Lett.) 56, 781-782 1968.

(14) Motorola Application Note AN.445 Fay G.V. and Freyling N.F.

(15) Houghton J.T. and Smith S.D. 'Infra-Red Physics' O.U.P. 1966.

(16) E.M.I. Brochure P001/fP70.

(17) Sherring C.W. J.Phys. E. 3, 1016-1018 1970.

(18) Jacobs H. et al J. App. Phys. 38, 8 3412-3413 1967.

(19) Kerecman A.J. et al I.E.E.E. J.Q.E. 474-476 1969.

REFERENCES (Continued)

(20) Rosenberger D. — Z.Angew Phys. 26, 3, 200-206 1969.

(21) Aoki T. et al — Jap. J. App. Phys. 10, 3, 332-338 1971.

(22) Lobov G.D. et al — Radio Eng. and Elec.Phys. 968-972 1971.

(23) Kindl H. et al — 8th I.C.P.I.G. 3.2.12. 258 1967.

(24) Gebhardt and Smith — App. Phys. Lett. 20, 3, 129 1972.

(25) Bradley Moore C. et al — J.Chem.Phys. 46, 4222-4231 1967.

(26) Tyte D.C. — Proc. Phys. Soc. 80, 1347-1353 1962.

(27) Howorth R. — J. Phys. B. 5, 402-407 1972.

(28) Bleekrode R. — I.E.E.E. J.Q.E. 5, 2, 57-60 1969.

(29) Jeunehomme J. and Duncan A.B.F. — J. Chem. Phys. 41, 6, 1692 1964.

(30) Herzberg — 'Infra-Red and Raman Spectra' Van Nostrand 1946.

(31) Smith A.L.S. — B.J.App.Phys.(J.Phys.D.), 2, 2, 1129-1134,1969.

(32) Cheo P.K. and Cooper H.G. — I.E.E.E. J.Q.E. 3,2, 79-84 1967.

(33) Deutsch T.F. — I.E.E.E. J.Q.E. 3,4, 151-155 1967.

(34) Antropov E.T. et al — I.E.E.E. J.Q.E. 4, 11, 1968.

(35) Cheo P.K. — I.E.E.E. J.Q.E. 3, 12, 683-689 1967.

(36) McQuillan A.K. et al — Can. J. Phys. 49, 1611-1619 1971.

REFERENCES (Continued)

(37) Gerry E.T. et al — App.Phys. Lett. 8, 227 1966.

(38) Clark P.O. and Wada J.Y. — I.E.E.E. J.Q.E. 4, 5, 263 1968.

(39) Bletzinger P. and Garscadden A. — I.E.E.E. J.Q.E. 59, 4, 675-679 1971.

(40) Bletzinger P. and Garscadden A. — App. Phys. Lett. 12, 9, 289-291 1968.

(41) Nighan W.L. — Phys. Rev. A2, 5, 1989-2000 1970.

(42) Bullis R.H. et al — A1AA Journal 10, 4, 407-414 1972.

(43) Sviridov A.G. et al — J.E.T.P. Lett., 6, 72 1967.

(44) Waszink J.H. and Van Vliet J.A.J.M. — J. App. Phys. 42, 9, 3374 1971.

(45) Laderman A.J. and Byron S.R. — J. App. Phys. 42, 8, 3138 1971.

(46) Sobolov N.N. and Sokovikov V.V. — Usp. Fiz. Nauk. 91, 425-454 1967.

(47) Schultz G.J. — Phys. Rev. 135, 988-994 1964.

(48) Weiss K.A. et al — J.Q.Spectrosc. Rad.Trans. 9, 885-888 1968.

(49) Bleekrode R. — I.E.E.E. J.Q.E. Lett. 297-298 1969.

(50) Novgorodov M.Z. et al — Sov. Phys. Tech.Phys. 15, 6, 977-982 1970 (Eng. Translation)

(51) Garscadden A. and Blezinger P. — 8th I.C.P.I.G. 258, 1967.

(52) Roberts T.G. et al — I.E.E.E. J.Q.E. 3, 11, 605-609 1967.

(53) Lassetre F.N. and Silverman S.M. — J. Chem. Phys. 40, 1964.

(54) Moore J.H. and Robinson D.W. — J.Chem. Phys. 18, 11, 4870-4874 1968.

(55) Tyte D.C. — Proc.Phys.Soc. 80, 1354-1363 1962.

(56) Zare R.N. et al — J. Molec. Spectrosc. 15, 117, 1965.

(57) Schultz G.J. — Phys. Rev. A 135, 4, 988, 1964.

(58) Von Engel.A. — "Ionised Gases" 2nd Edition, Oxford Clarendon Press, 1965.

(59) Gordiez et al — Phys. Lett. 25A, 173, 1967.

(60) Christensen C.P. et al — I.E.E.E. J.Q.E. 5, 6, 276-283, 1969.

(61) Present P.D. — 'The Kinetic Theory of Gases' McGraw-Hill London & New York 1958.

(62) Avivi P. et al — J. App. Phys. 44, 2, 723-724, 1973.

(63) Legay F. et al — J. Phys. (France) 25, 999, 1965.

(64) Mikaberidze A.A. et al — Sov. J.Q.E. 1, 3, 276-279, 1971.

(65) Ochkin V.N. — 11th I.C.P.I.G. 1.2.1.5., 12,1973.

(66) Skolnick M.L. — I.E.E.E. J.Q.E. 139-140, 1970.

(67) Thomason W.H. and Elbers D.C. — Rev. Sci. Instr. 46, 4, 409-412, 1975.

(68) Stefanov V.J. — J.Phys.E.Scientific Instruments 3, 1027-1078, 1970.

(69) Smith A.L.S. and Browne P.G. — J.Phys.D. 7, 1652-1659, 1974.